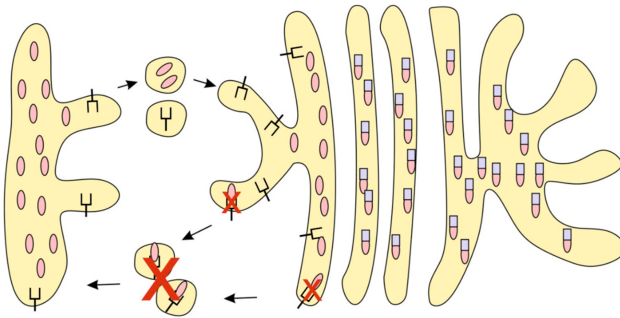


**DOMINIK FLOREK**

---

Functional characterization of accessory  
protein 7b encoded by feline coronaviruses



**INAUGURAL DISSERTATION**

submitted to the  
Faculty of Medicine in partial fulfillment  
of the requirements for the PhD-Degree  
of the Faculties of Veterinary Medicine and Medicine  
of the Justus Liebig University Giessen

**Das Werk ist in allen seinen Teilen urheberrechtlich geschützt.**

**Die rechtliche Verantwortung für den gesamten Inhalt dieses Buches liegt ausschließlich bei dem Autor dieses Werkes.**

Jede Verwertung ist ohne schriftliche Zustimmung des Autors oder des Verlages unzulässig. Das gilt insbesondere für Vervielfältigungen, Übersetzungen, Mikroverfilmungen und die Einspeicherung in und Verarbeitung durch elektronische Systeme.

1. Auflage 2017

All rights reserved. No part of this publication may be reproduced, stored in a retrieval system, or transmitted, in any form or by any means, electronic, mechanical, photocopying, recording, or otherwise, without the prior written permission of the Author or the Publishers.

1<sup>st</sup> Edition 2017

© 2017 by VVB LAUFERSWEILER VERLAG, Giessen  
Printed in Germany



*édition linguistique*  
**VVB LAUFERSWEILER VERLAG**

STAUFENBERGRING 15, D-35396 GIESSEN  
Tel: 0641-5599888 Fax: 0641-5599890  
email: [redaktion@doktorverlag.de](mailto:redaktion@doktorverlag.de)

[www.doktorverlag.de](http://www.doktorverlag.de)

# **Functional characterization of accessory protein 7b encoded by feline coronaviruses**

## **INAUGURAL DISSERTATION**

submitted to the  
Faculty of Medicine in partial fulfillment  
of the requirements for the PhD-Degree  
of the Faculties of Veterinary Medicine and Medicine  
of the Justus Liebig University Giessen

by

**Dominik Florek**  
of Tarnow (Poland)

Giessen 2017

From the Institute of Virology  
Faculty of Veterinary Medicine  
Justus Liebig University Giessen

Supervisor: Prof. Dr. Gergely Tekes

1. Reviewer and Member of the PhD

Committee:

Prof. Dr. Gergely Tekes

2. Reviewer:

Prof. Ronald Dijkman, Ph.D. (Bern)

Other members of the PhD Committee:

Prof. Dr. Friedemann Weber  
(Chairman)

Prof. Dr. John Ziebuhr

Defense Date:

27.10.2017

## **Declaration**

“I declare that I have completed this dissertation single-handedly without the unauthorized help of second party and only with the assistance acknowledged therein. I have appropriately acknowledged and referenced all text passages that are derived literally from or based on the content of published or unpublished work of others, and all information that relates to verbal communications. I have abided by the principles of good scientific conduct laid down in the character of the Justus-Liebig-University of Giessen in carrying out the investigations described in the dissertation.“

Dominik Florek



The study was supported by the Deutsche Forschungsgemeinschaft (DFG) through the Collaborative Research Centre 1021: “RNA viruses: RNA metabolism, host response and pathogenesis” (project B01).

To my father, mother, brother and Stephanie

# Table of Contents

Table of Contents .....	I
List of Figures .....	V
List of Tables .....	VII
List of Abbreviations .....	VIII
1 Introduction .....	- 1 -
1.1 Coronaviruses .....	- 1 -
1.1.1 Taxonomy .....	- 1 -
1.1.2 Morphology .....	- 4 -
1.1.3 Genome Organization .....	- 5 -
1.1.4 Replication of Coronaviruses .....	- 7 -
1.2 Feline Coronaviruses .....	- 11 -
1.3 Feline Infectious Peritonitis (FIP) .....	- 13 -
1.4 Accessory Proteins of Coronaviruses .....	- 14 -
1.4.1 Accessory Genes and Accessory Proteins of Feline Coronaviruses ....	- 17 -
1.4.1.1 Current Knowledge on Accessory Genes and Accessory Proteins of Feline Coronaviruses .....	- 17 -
1.4.1.2 FCoV Accessory Genes/Proteins Studied by Reverse Genetics ....	- 19 -
1.5 N-linked Protein Glycosylation .....	- 20 -
1.6 Aims of the Study .....	- 22 -
2 Materials & Methods .....	- 23 -
2.1 Materials .....	- 23 -
2.1.1 Cells .....	- 23 -
2.1.1.1 Eukaryotic Cells .....	- 23 -
2.1.1.2 Prokaryotic Cells .....	- 23 -
2.1.2 Viruses .....	- 23 -
2.1.3 Plasmids .....	- 24 -
2.1.4 Enzymes .....	- 24 -
2.1.5 Antibodies .....	- 24 -
2.1.6 Chemicals .....	- 25 -
2.1.7 Kits .....	- 28 -
2.1.8 Culture Media .....	- 28 -

2.1.8.1 Bacterial Culture Media .....	- 28 -
2.1.8.2 Cellular Culture Media .....	- 28 -
2.1.9 Buffers and Solutions.....	- 30 -
2.1.10 Consumables.....	- 33 -
2.1.11 Equipment.....	- 34 -
2.1.12 Synthetic DNA Oligonucleotides .....	- 36 -
2.1.12.1 Oligonucleotides for FCoV 79-1146 Genome .....	- 36 -
2.1.12.2 Other Oligonucleotides .....	- 39 -
2.2 Methods .....	- 40 -
2.2.1 Eukaryotic Cells: Techniques.....	- 40 -
2.2.1.1 General Techniques .....	- 40 -
2.2.1.2 Cell Counting.....	- 40 -
2.2.1.3 Cryopreservation and Storage of Cells.....	- 40 -
2.2.1.4 Cell Infection.....	- 41 -
2.2.1.5 Indirect Immunofluorescence Assay.....	- 41 -
2.2.1.6 Transfection of Eukaryotic Cells .....	- 42 -
2.2.1.6.1 Chemical Transfection.....	- 42 -
2.2.1.6.2 Physical Transfection (Electroporation).....	- 43 -
2.2.2 Prokaryotic Cells: Techniques .....	- 43 -
2.2.2.1 Cultivation of Bacteria.....	- 43 -
2.2.2.2 Preparation of Competent <i>E. coli</i> Cells.....	- 44 -
2.2.2.3 Transformation of Competent <i>E. coli</i> Cells .....	- 44 -
2.2.3 Molecular Techniques – DNA .....	- 44 -
2.2.3.1 Standard Techniques .....	- 44 -
2.2.3.1.1 Polymerase Chain Reaction (PCR).....	- 44 -
2.2.3.1.2 QuickChange PCR.....	- 45 -
2.2.3.1.3 Digestion with Restriction Enzymes .....	- 46 -
2.2.3.1.4 Dephosphorylation .....	- 46 -
2.2.3.1.5 Ligation.....	- 46 -
2.2.3.2 DNA Purification .....	- 47 -
2.2.3.2.1 Phenol/Chloroform Extraction with Ethanol Precipitation .....	- 47 -
2.2.3.2.2 Purification of PCR products .....	- 47 -
2.2.3.2.3 Gel Extraction.....	- 47 -
2.2.3.3 DNA Isolation.....	- 48 -
2.2.3.3.1 Plasmid DNA Isolation from Bacteria Culture.....	- 48 -

2.2.3.3.2 Vaccinia Virus DNA Isolation from Eukaryotic Cells .....	- 48 -
2.2.3.4 DNA Analysis.....	- 49 -
2.2.3.4.1 DNA Agarose Gel Electrophoresis .....	- 49 -
2.2.3.4.2 Sequencing .....	- 49 -
2.2.3.5 Plasmid Generation .....	- 50 -
2.2.4 Molecular Techniques - RNA .....	- 52 -
2.2.4.1 RNA Isolation from Eukaryotic Cells.....	- 52 -
2.2.4.2 Reverse Transcription .....	- 52 -
2.2.4.3 <i>In vitro</i> Transcription .....	- 53 -
2.2.4.4 RNA Analysis.....	- 54 -
2.2.4.4.1 RNA Agarose Gel Electrophoresis .....	- 54 -
2.2.5 Molecular Techniques for Working with Proteins .....	- 54 -
2.2.5.1 Cell Lysis .....	- 54 -
2.2.5.2 Protein Deglycosylation .....	- 54 -
2.2.5.3 Protein Analysis.....	- 55 -
2.2.5.3.1 Sodium Dodecyl Sulfate Polyacrylamide Gel Electrophoresis (SDS-PAGE) .....	- 55 -
2.2.5.3.2 Immunoprecipitation and N-terminal Edman Sequencing .....	- 56 -
2.2.5.3.3 Western Blotting.....	- 57 -
2.2.6 Techniques for Working with Viruses.....	- 58 -
2.2.6.1 Vaccinia Virus.....	- 58 -
2.2.6.1.1 Selection .....	- 58 -
2.2.6.1.2 Positive Selection.....	- 58 -
2.2.6.1.3 Negative Selection .....	- 59 -
2.2.6.1.4 Vaccinia Virus Plaque Purification Assay .....	- 60 -
2.2.6.2 FIPV and Recombinant FIPV .....	- 60 -
2.2.6.2.1 Titration of FIPVs.....	- 60 -
2.2.6.2.2 Growth Kinetics of FIPVs .....	- 61 -
2.2.7 Generation of Recombinant Viruses .....	- 61 -
2.2.7.1 Generation of Recombinant Vaccinia Viruses .....	- 61 -
2.2.7.2 Generation of Recombinant FIPVs .....	- 61 -
2.2.7.2.1 Recovery of Recombinant FIPVs .....	- 61 -
2.2.7.2.2 Plasmids, Recombinant Vaccinia Viruses and Recombinant FIPVs .....	- 62 -
3 Results.....	- 65 -

3.1 Generation of Recombinant FIPV Expressing the Non-glycosylated 7b Protein .....	- 65 -
3.1.2 Generation of Recombinant Vaccinia Virus vrFIPV-GPT- $\Delta$ 7ab .....	- 66 -
3.1.3 Generation of vrFIPV-7b(1-206/N68S) .....	- 68 -
3.1.4 Recovery of rFIPV-7b(1-206/N68S).....	- 70 -
3.1.5 Characterization of the Non-glycosylated Form of 7b Protein Using rFIPV-7b(1-206/N68S).....	- 72 -
3.2 FIPVs with Flag-tagged Forms of 7b Protein .....	- 74 -
3.2.2 Generation of rFIPV-flag-7b(1-206) .....	- 74 -
3.2.3 Detection of 7b Protein after Infection with rFIPV-flag-7b(1-206).....	- 76 -
3.2.4 Signalase Cleavage Site in 7b Protein.....	- 77 -
3.2.5 Generation of rFIPV-7b(1-17/flag/18-206) and rFIPV-7b(1-17/flag/18-206/N68S). .....	- 79 -
3.2.6 Characterization of 7b Protein in rFIPV-7b(1-17/flag/18-206)- and rFIPV-7b(1-17/flag/18-206/N68S)-infected Cells. ....	- 82 -
3.3 Subcellular Localization of 7b Protein .....	- 84 -
3.4 Impact of C-terminal Sequence of 7b Protein on Subcellular Localization ..	- 85 -
3.4.1 Generation of rFIPV-7b(1-206)-flag .....	- 85 -
3.4.2 Characterization of 7b Protein Encoded by rFIPV-7b(1-206)-flag.....	- 88 -
3.4.3 Generation of Recombinant FIPVs with Altered KTEL Motif .....	- 89 -
3.4.4 Role of the C-terminal KTEL Motif in Subcellular Localization of 7b Protein .....	- 93 -
3.5 Subcellular Localization of 7b Protein after Inhibition of Ongoing Protein Synthesis .....	- 95 -
4 Discussion .....	- 101 -
4.1 Localization of 7b Protein in FIPV-infected Cells .....	- 102 -
4.2 Role of the C-terminal Sequence in the Localization of 7b Protein .....	- 104 -
4.3 Protein Retention in the ER.....	- 106 -
5 Summary .....	- 112 -
6 Zusammenfassung .....	- 114 -
7 References .....	- 116 -
Acknowledgments .....	- 142 -

## List of Figures

Figure 1. Coronavirus morphology. ....	- 5 -
Figure 2. Schematic representation of the FCoV genome.....	- 7 -
Figure 3. Schematic representation of the proteolytic processing of pp1a and pp1ab. ....	- 8 -
Figure 4. Expression strategy of coronaviruses. ....	- 9 -
Figure 5. Schematic representation of subgenomic RNA synthesis.....	- 10 -
Figure 6. Genome organization of representatives of genera Alpha-, Beta- (lineages A-D), Gamma- and Deltacoronavirus with focus on accessory genes downstream of ORF 1a and ORF 1b. ....	- 16 -
Figure 7. Schematic representation of a semi-dry transfer sandwich.....	- 57 -
Figure 8. Prediction of N-linked glycosylation site based on amino acid sequence of 7b protein. ....	- 65 -
Figure 9. Generation and analysis of recombinant vaccinia virus vrFIPV-GPT- $\Delta$ 7ab. ....	- 67 -
Figure 10. Amplification of the FIPV genome in recombinant vaccinia virus vrFIPV-GPT- $\Delta$ 7ab. ....	- 68 -
Figure 11. Generation and analysis of recombinant vaccinia virus vrFIPV-7b(1-206/N68S). ....	- 69 -
Figure 12. Amplification of the FIPV genome in recombinant vaccinia virus vrFIPV-7b(1-206/N68S) DNA. ....	- 70 -
Figure 13. Analysis of the vrFIPV-7b(1-206/N68S) DNA and the transcribed RNA.....	- 71 -
Figure 14. Characterization of rFIPV-7b(1-206/N68S). ....	- 72 -
Figure 15. 7b protein detection in FIPV-infected cells using anti-7b monoclonal antibody 14D8 ( $\alpha$ -7b mAb). ....	- 73 -
Figure 16. Analysis of recombinant vaccinia virus vrFIPV-flag-7b(1-206). ....	- 75 -
Figure 17. Characterization of rFIPV-flag-7b(1-206). ....	- 76 -
Figure 18. Western blot analysis of N-terminal flag-tagged 7b protein in rFIPV-flag-7b(1-206)-infected CRFK cells. ....	- 77 -
Figure 19. Signal peptide prediction for FCoV 7b protein.....	- 78 -

Figure 20. Analysis of recombinant vaccinia viruses vrFIPV-7b(1-17/flag/18-206) and vrFIPV-7b(1-17/flag/18-206/N68S).....	- 80 -
Figure 21. Characterization of rFIPV-flag-7b(1-206) and rFIPV-flag-7b(1-206/N68S). .....	- 82 -
Figure 22. Detection of 7b protein in FIPV-infected cells.....	- 83 -
Figure 23. Glycosidase treatment of 7b protein.....	- 84 -
Figure 24. Analysis of recombinant vaccinia virus vrFIPV-7b(1-206)-flag. ....	- 86 -
Figure 25. Characterization of rFIPV-7b(1-206)-flag. ....	- 87 -
Figure 26. Effect of the C-terminal flag tag on subcellular localization of 7b protein. ....	- 89 -
Figure 27. Analysis of recombinant vaccinia viruses vrFIPV-7b(1-17/flag/18-202/KTEV), vrFIPV-7b(1-17/flag/18-202/KTE), vrFIPV-7b(1-17/flag/18-202/AAAA) and vrFIPV-7b(1-17/flag/18-202/KDEL). ....	- 90 -
Figure 28. Characterization of recombinant FIPVs expressing 7b protein with altered C-terminal motif.....	- 92 -
Figure 29. Influence of altered C-terminal motifs in 7b protein on subcellular localization and secretion. ....	- 94 -
Figure 30. Effect of cycloheximide treatment on localization of 7b protein with different C-terminal motifs. ....	- 97 -
Figure 31. Western blot analysis of CHX-treated versus non-treated FIPV-infected cells.....	- 98 -
Figure 32. Effect of cycloheximide treatment on localization of 7b protein with different C-terminal motifs in infected FCWF-4 and Fc3Tg cell lines.....	- 99 -
Figure 33. Retention of proteins with C-terminal KDEL/KTEL motifs in the ER..	- 107 -
Figure 34. Model for FCoV 7b Golgi retention in FCoV-infected feline cells.....	- 109 -
Figure 35. Model for FCoV 7b trafficking with C-terminal KTEV motif in FCoV-infected feline cells.....	- 110 -

## List of Tables

Table 1. Coronavirinae subfamily.....	- 3 -
Table 2. Oligonucleotides used for the PCR to analyze the integrity of FCoV cDNA (2.2.6.1.4).....	- 37 -
Table 3. FCoV 79-1146 specific oligonucleotides used for plasmid generation (2.2.3.5).....	- 39 -
Table 4. Oligonucleotides used for sequencing.....	- 39 -
Table 5. Antibodies for Indirect Immunofluorescence Assay.....	- 42 -
Table 6. PCR standard protocol.....	- 45 -
Table 7. QuickChange PCR standard protocol.....	- 45 -
Table 8. Reverse transcription standard protocol.....	- 53 -
Table 9. SDS-PAGE gel recipe.....	- 55 -
Table 10. N-terminal Edman sequencing of 7b protein.....	- 79 -

## List of Abbreviations

°C	degree Celsius
μF	microfarad
μl	microliter
A	alanine
Ab	antibody
ACE2	angiotensin-converting enzyme 2
APN	aminopeptidase N
APS	ammonium persulfate
ATCC	American Type Culture Collection
BAC	bacterial artificial chromosome
BHK	baby hamster kidney cells
bp	base pair
BSA	bovine serum albumin
CCM 34	cell culture medium 34
cDNA	complementary deoxyribonucleic acid
CEACAM1	carcinoembryonic antigen-related cell adhesion molecule 1
CHX	cycloheximide
cm	centimeter
CMC	carboxymethyl cellulose
CoV	coronavirus
CRFK	Crandell Reese feline kidney
C-terminal	carboxy terminal
C-terminus	carboxy terminal end

CV-1	monkey kidney cells
D	aspartic acid
DABCO	1,4-Diazabicyclo(2.2.2)octane
DAPI	4',6-diamidino-2-phenylindole
dATP	deoxyadenosine triphosphate
dCTP	deoxycytosine triphosphate
ddH <sub>2</sub> O	double distilled water
dGTP	deoxyguanosine triphosphate
DMEM	Dulbecco's modified Eagle's medium
DMSO	dimethyl sulfoxide
DMV	double-membrane vesicle
DNA	deoxyribonucleic acid
DNase	deoxyribonuclease
dNTP	deoxynucleotide triphosphate
DTT	dithiothreitol
dTTP	deoxythymidine triphosphate
E	glutamic acid/envelope protein
<i>E. coli</i>	<i>Escherichia coli</i>
EDTA	ethylenediaminetetraacetic acid
EP	electroporation
ER	endoplasmic reticulum
ERAD	ER-associated degradation
ERGIC	endoplasmic reticulum-Golgi intermediate compartment
Fc3Tg	feline tongue cells

FCoV	Feline Coronavirus
FCS	fetal calf serum
FCWF	felis catus whole fetus
fDC-SIGN	feline dendritic cell-specific intercellular adhesion molecule-3-grabbing nonintegrin
FECV	Feline Enteric Coronavirus
FIP	Feline infectious peritonitis
FIPV	Feline Infectious Peritonitis Virus
gpt	guanine phosphoribosyltransferase
h	hour
HE	hemagglutinin-esterase protein
ICTV	International Committee on Taxonomy of Viruses
IVT	<i>in vitro</i> transcription
K	lysine
kb	kilobase
kDa	kilodalton
L	leucine
M	membrane protein
mAb	monoclonal antibody
MEM	minimal essential media
min	minute
ml	milliliter
MOI	multiplicity of infection
MOPS	3-(N-morpholino)propanesulfonic acid

MPA	mycophenolic acid
M <sup>pro</sup>	main proteinase
N	asparagine/nucleocapsid protein
N-terminal	amino terminal
N-terminus	amino terminal end
NP-40	Nonident P40
nsp	nonstructural protein
OD	optical density
ORF	open reading frame
OST	oligosaccharyltransferase
PBS	phosphate buffered saline
PBST	phosphate buffered saline with Tween-20
PCR	polymerase chain reaction
PFU	plaque forming unit
p.i.	post infection
PL1 <sup>pro</sup> , PL2 <sup>pro</sup>	papain-like proteinase 1, 2
pp	polyprotein
rFIPV	recombinant Feline Infectious Peritonitis Virus
RFS	ribosomal frameshifting
RNA	ribonucleic acid
RT	room temperature
RTC	replication/transcription complex
RT-PCR	reverse transcription polymerase chain reaction
S	serine/spike protein

SDS	sodium dodecyl sulfate
sec, s	seconds
sg	subgenomic
T	threonine
TAE	Tris-acetate-EDTA
<i>Taq</i>	<i>Thermus aquaticus</i> -polymerase
TEMED	Tetramethylethylenediamine
6-TG	6-Thioguanine
TRS	transcription regulatory sequence
UTR	untranslated region
V	valine
w/v	mass/volume
Y	tyrosine



# 1 Introduction

## 1.1 Coronaviruses

### 1.1.1 Taxonomy

Coronaviruses (CoVs) belong to the family *Coronaviridae* that include the subfamilies *Coronavirinae* and *Torovirinae*. This virus family was established in 1975 by the International Committee on Taxonomy of Viruses (ICTV) (Tyrrell et al. 1975). The family *Coronaviridae* together with the families *Arteriviridae*, *Mesoniviridae* and *Roniviridae* form the order *Nidovirales* (Adams et al. 2013; de Groot et al. 2012b). Generation of a 3'-coterminally set of subgenomic mRNAs (sg mRNAs) during transcription is a hallmark of all members of the order *Nidovirales*. These sg mRNAs are called 'nested set' (lat. *nidus* = nest) (de Groot et al. 2012b). Although the members of the order *Nidovirales* differ in the morphology of virions, size of the genome and the number of encoded accessory proteins (Siddell et al. 2005), they share similarities based on their replicase polyproteins that contain a number of characteristic domains arranged in a conserved order (Brierley et al. 1987; Brierley 1995; Cowley et al. 2000; Snijder et al. 2016).

<b>Genus</b>	<b>Species</b>
<i>Alphacoronavirus</i>	<i>Alphacoronavirus-1</i>
	Feline coronavirus (FCoV)
	Canine coronavirus (CCoV)
	Transmissible gastroenteritis virus (TGEV)
	Porcine respiratory coronavirus (PRCoV)
	<i>Porcine epidemic diarrhea virus (PEDV)</i>

*Bat coronavirus CDPHE15 (BatCoV CDPHE15)*

*Bat coronavirus HKU10 (BatCoV HKU10)*

*Miniopterus bat coronavirus 1 (Mi-BatCoV 1)*

*Miniopterus bat coronavirus HKU8 (Mi-BatCoV HKU8)*

*Mink coronavirus 1 (MCV)*

*Rhinolophus bat coronavirus HKU2 (Rh-BatCoV HKU2)*

*Scotophilus bat coronavirus 512 (Sc-BatCoV 512)*

*Human coronavirus 229E (HCoV 229E)*

*Human coronavirus NL63 (HCoV NL63)*

---

*Betacoronavirus*

*Betacoronavirus-1*

*Bovine coronavirus (BCoV)*

*Porcine hemagglutinating encephalomyelitis virus (PHEV)*

*Equine coronavirus (ECoV)*

*Human coronavirus OC43 (HCoV OC43)*

*Hedgehog coronavirus 1 (EriCoV)*

*Middle East respiratory syndrome coronavirus (MERS-CoV)*

*Murine coronavirus*

*Mouse hepatitis virus (MHV)*

*Rat coronavirus (RCoV)*

*Severe acute respiratory syndrome-related coronavirus (SARS-CoV)*

*Human coronavirus HKU1 (HCoV HKU1)*

*Pipistrellus bat coronavirus HKU5 (Pi-BatCoV HKU5)*

*Rousettus bat coronavirus HKU9 (Ro-BatCoV HKU9)*

*Tylonycteris bat coronavirus HKU4* (Ty-BatCoV HKU4)

---

<i>Gammacoronavirus</i>	<i>Avian coronavirus</i>  Infectious bronchitis virus (IBV)  Turkey coronavirus (TCoV)  Pheasant coronavirus (PhCoV)  <i>Bottlenose dolphin coronavirus HKU22</i> (BdCoV HKU22)  <i>Beluga whale coronavirus SW1</i> (BWCoV SW1)
<i>Deltacoronavirus</i>	<i>Bulbul coronavirus HKU11</i> (BuCoV HKU11)  <i>Common moorhen coronavirus HKU21</i> (CMCoV HKU21)  <i>Munia coronavirus HKU13</i> (MunCoV HKU13)  <i>Porcine coronavirus HKU15</i> (PorCoV HKU15)  <i>Night heron coronavirus HKU19</i> (NHCoV HKU19)  <i>Thrush coronavirus HKU12</i> (ThCoV HKU12)  <i>White-eye coronavirus HKU16</i> (WECOV HKU16)  <i>Wigeon coronavirus HKU20</i> (WiCoV HKU20)

---

**Table 1. Coronavirinae subfamily.** Genera, species and abbreviations of the virus names are listed.

Based on phylogenetic analysis, the subfamily *Coronavirinae* is divided into genera *Alpha-*, *Beta-*, *Gamma-* and *Deltacoronavirus* (Table 1). Feline coronaviruses, which represent the focus of this work, together with closely related canine coronavirus (CCoV), porcine transmissible gastroenteritis virus (TGEV) and porcine respiratory coronavirus (PRCoV) belong to the species *Alphacoronavirus-1* within the genus *Alphacoronavirus*. Other members of this genus are more distantly related viruses like porcine epidemic diarrhea virus (PEDV), human coronaviruses 229E (HCoV-229E) and NL63 (HCoV-NL63). Coronaviruses detected in minks and some bat species also belong to this genus (de Groot et al. 2012a). The genus *Betacoronavirus* contains important animal viruses like bovine CoV (BCoV), equine

CoV (ECoV) and porcine hemagglutinating encephalomyelitis virus (PHEV). Human betacoronaviruses are the severe acute respiratory syndrome-coronavirus (SARS-CoV), Middle East respiratory syndrome coronavirus (MERS-CoV) and human coronavirus OC43 (HCoV OC43). Recently, a novel betacoronavirus related to MERS-CoV was isolated from European hedgehogs (Corman et al. 2014). Coronaviruses pathogenic for mice, rats and bats are also part of this genus. The genus *Gammacoronavirus* contains avian viruses like infectious bronchitis virus (IBV), turkey coronavirus (TCoV) and pheasant coronavirus (PhCoV) (Cavanagh et al. 2002). Recently, beluga whale coronavirus SW1 (BWCoV SW1) and bottlenose dolphin coronavirus HKU22 (BdCoV HKU22) were added to this genus (Mihindukulasuriya et al. 2008; Woo et al. 2014). In 2009, three avian coronaviruses, bulbul coronavirus HKU11 (BuCoV HKU11), munia coronavirus HKU13 (MunCoV HKU13) and thrush coronavirus HKU12 (ThCoV HKU12) were identified and clustered under the new coronavirus genus – *Deltacoronavirus* (Woo et al. 2009). Besides these avian coronaviruses, porcine coronavirus HKU15 (PorCoV HKU15) belongs to this genus as well.

### 1.1.2 Morphology

Coronaviruses are enveloped, pleomorphic, mostly spherical with a diameter ranging between 120 and 160 nm (Fig. 1A). Virions are surrounded by characteristic surface projections (ca. 20 nm) consisting of trimers of the spike glycoprotein (S) (Cavanagh 1983; Delmas & Laude 1990). The name 'coronavirus' is derived from the petal-shaped surface projections resembling the corona of the Sun observed in electron micrographs (Davies & Macnaughton 1979).

Beside the spike glycoprotein (180-220 kDa), the membrane (M) protein (25-30 kDa) and the envelope (E) protein (10-12 kDa) are also integrated into the envelope of the virion (Fig. 1B). The spike protein is a glycosylated transmembrane protein that is important for receptor binding and fusion of the virions with the cellular membrane (Kubo et al. 1994; McBride & Machamer 2010; Yoo et al. 1991). Furthermore, this protein is responsible for induction of neutralizing antibodies (Compton et al. 1993). The membrane protein (M) binds the nucleocapsid (N) through its C-terminal domain and is crucial for particle assembly (Escors et al. 2001; Narayanan et al. 2000;

Rottier 1995). The envelope protein (E) was shown to be involved in virion assembly and morphogenesis. Furthermore, it was identified as a virulence factor for SARS-CoV (de Groot et al. 2012a; DeDiego et al. 2011). Certain members of the genus *Betacoronavirus* contain additional surface projections (5-7 nm in length) formed by the homodimeric hemagglutinin-esterase (HE) glycoprotein (60-65 kDa). This protein mediates reversible attachment of virions to O-acetylated sialic acids (King et al. 1985; Langereis et al. 2010; Vlasak et al. 1988). The envelope of the virion surrounds the nucleocapsid, which consists of the RNA genome and the nucleocapsid (N) protein (43-63 kDa) (Fig. 1B) (Baric et al. 1988). In addition to genome encapsidation, the N protein plays an important role in transcription and translation of viral mRNAs. It also acts as type I interferon antagonist (Almazan et al. 2004; Baric et al. 1988; Ding et al. 2014; Laude & Masters 1995; Lu et al. 2011; Rose & Weiss 2009; Ye et al. 2007).

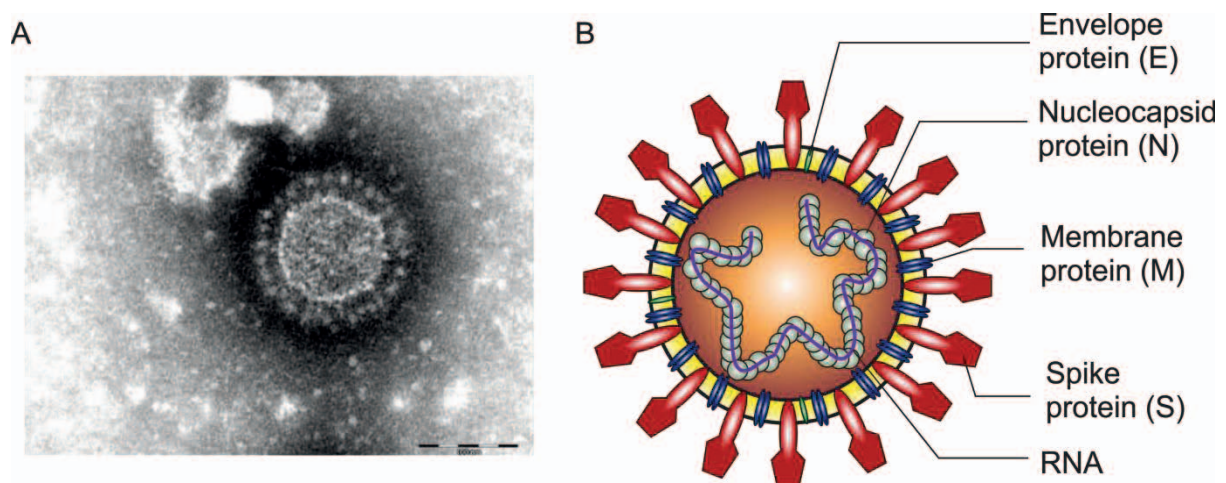


**Figure 1. Coronavirus morphology.** (A) Electron micrograph of negatively stained porcine epidemic diarrhea virus (PEDV) particle (Hanke et al. 2015). (B) Schematic representation of an *Alphacoronavirus* particle. Structural proteins and RNA are shown.

### 1.1.3 Genome Organization

Coronaviruses possess a linear, single-stranded, non-segmented RNA genome of positive polarity with a size of 27-31.5 kilobases (kb); these are the largest viral RNA genomes in nature (Gorbalenya et al. 2006). Similar to eukaryotic mRNAs, the CoV

genome is capped at the 5' end (Lai & Stohlman 1981) and polyadenylated at the 3' end (Lai & Stohlman 1978; Lomniczi 1977; Masters 2006; Schochetman et al. 1977; Wege et al. 1978). These features allow translation of the viral RNA by the cellular machinery directly after infection. As was shown before, coronaviral RNA alone is infectious and can initiate the CoV replication cycle (Almazan et al. 2000; Casais et al. 2001; Scobey et al. 2013; Tekes et al. 2008; Tekes et al. 2012; Thiel et al. 2001a; Yount et al. 2000; Yount et al. 2002; Yount et al. 2003).

The 5' end of the CoV genome comprises an untranslated region (UTR) of about 200-500 nt. The first 65-98 nucleotides comprise the so called *Leader*-sequence, which is also present at the 5' end of all viral subgenomic RNAs (Lai & Holmes 2001; Lai & Cavanagh 1997). The 3' end of the genome also contains an UTR with a size of about 200-400 nt. Both UTRs contain *cis*-active elements, which are essential for viral replication and transcription of the coronavirus genome (Chang et al. 1994; Madhugiri et al. 2014; Madhugiri et al. 2016; Masters 2007; Raman et al. 2003; Sola et al. 2011; Zust et al. 2008).

The coronavirus genome contains 6 to 14 open reading frames (ORFs). The order of the ORFs from 5' to 3' end is conserved for all CoVs: replicase gene-S-E-M-N (Fig. 2) (de Haan et al. 2002). The replicase gene occupies two thirds of the genome (ca. 20 kb) and contains ORF 1a and ORF 1b. ORF 1a encodes a polyprotein (pp) pp1a with a molecular mass of 450-500 kDa (Siddell et al. 2005). ORF 1b is translated through a -1 ribosomal frameshifting (RFS) into a 750-800 kDa pp1ab (Brierley et al. 1989; Siddell et al. 2005). The so called '*slippery*' sequence (UUUAAAC) and an RNA structure (pseudoknot) positioned downstream of this sequence are essential for the ribosomal frameshifting. In case of a -1 frameshift, the ribosome is stalled on the '*slippery*' sequence by the pseudoknot structure and it backtracks one nucleotide (Brierley et al. 1989; Brierley 1995). Both pp1a and pp1ab are cleaved by virus-encoded proteinases into 15-16 nonstructural proteins (nsps) that form the replication and transcription complexes (Snijder et al. 2016; Ziebuhr et al. 2000).

The 3'-proximal one-third of the genome codes for structural proteins S, E, M and N and accessory proteins. The number and position of the accessory genes in the CoV genome varies between species (Fig. 2) (de Groot et al. 2012a).

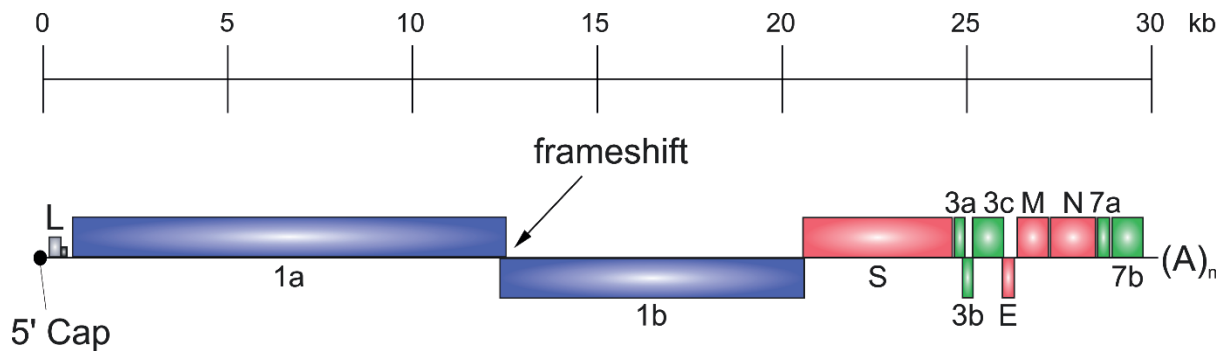


**Figure 2. Schematic representation of the FCoV genome.** ORF 1a and 1b are marked in blue, genes encoding structural proteins in red and accessory genes in green. 5' Cap structure is shown as a black dot; L, *Leader*-sequence (grey box) is followed by transcription regulatory sequence (TRS, black box); ribosomal frameshift is depicted with an arrow; (A)<sub>n</sub>, poly-(A) tail; kb, kilobase.

### 1.1.4 Replication of Coronaviruses

Coronaviruses bind through the S protein to the appropriate receptor of the host cell. Different CoVs use distinct receptors for this purpose. Serotype II FCoV, serotype II CCoV, TGEV, PRCoV, PEDV and HCoV-229E bind to aminopeptidase N (APN or CD13) (Delmas et al. 1992; Hohdatsu et al. 1998; Kolb et al. 1998; Li et al. 2007; Tresnan et al. 1996; Yeager et al. 1992). For serotype I and II FCoVs, C-type lectin dendritic cell-specific intercellular adhesion molecule-3-grabbing nonintegrin (fDC-SIGN) has been identified as a co-receptor (Regan & Whittaker 2008; Regan et al. 2010; Van Hamme et al. 2011). Further cellular receptors used by coronaviruses include angiotensin-converting enzyme 2 (ACE2) for human pathogens HCoV-NL63 and SARS-CoV (Hofmann et al. 2005; Li et al. 2003), murine carcinoembryonic antigen-related cell adhesion molecule 1 (CEACAM1 or CD66a) for MHV (Dveksler et al. 1991; Dveksler et al. 1993; Taguchi & Hirai-Yuki 2012). Some betacoronaviruses like BCoV and HCoV-OC43 bind to sialic acids (Krempl et al. 1995; Schwegmann-Wessels & Herrler 2006). Binding of the S protein to cellular receptors triggers a conformation change of the spike protein and fusion of the viral and the cellular membranes resulting in internalization of the viral genome as shown e.g. for MHV (Nash & Buchmeier 1997). Other CoVs like FCoV, TGEV, HCoV-229E and IBV infect cells through receptor-mediated endocytosis. Internalized virions fuse with the endosomal membrane followed by release of the nucleocapsid into the

cytoplasm of the host cell (Blau & Holmes 2001; Chu et al. 2006; Hansen et al. 1998; Van Hamme et al. 2007).

The positive strand RNA genome of CoVs serves as mRNA in infected cells and is directly translated in the cytoplasm. Translation gives rise to pp1a and, through a -1 ribosomal frameshifting, pp1ab. Both of these polyproteins are co- and post-translationally processed into usually 16 nonstructural proteins (nsps) by a set of virus-encoded proteinases (Fig. 3) (Ziebuhr et al. 2000). ORF 1a encodes 3 proteinases: two papain-like proteinases (PL1<sup>pro</sup> and PL2<sup>pro</sup>) and the main proteinase (3C-like protease, M<sup>pro</sup>). PL1<sup>pro</sup> and PL2<sup>pro</sup> are responsible for processing the N-terminal end of the pp1a/pp1ab. For these proteinases, three cleavage sites were identified (Ziebuhr et al. 2001). The C-terminal end of pp1a/1ab is processed by M<sup>pro</sup> at 11 identified cleavage sites (Snijder et al. 2016; Ziebuhr et al. 1995; Ziebuhr & Siddell 1999; Ziebuhr et al. 2000). Together with cellular proteins, the nonstructural proteins form the replication/transcription complex (RTC), which is associated with double-membrane vesicles (DMVs). The RTC is responsible for replication and transcription of viral genome (Gosert et al. 2002; Harcourt et al. 2004; Prentice et al. 2004; Sawicki et al. 2005; Snijder et al. 2006; Thiel et al. 2001b).

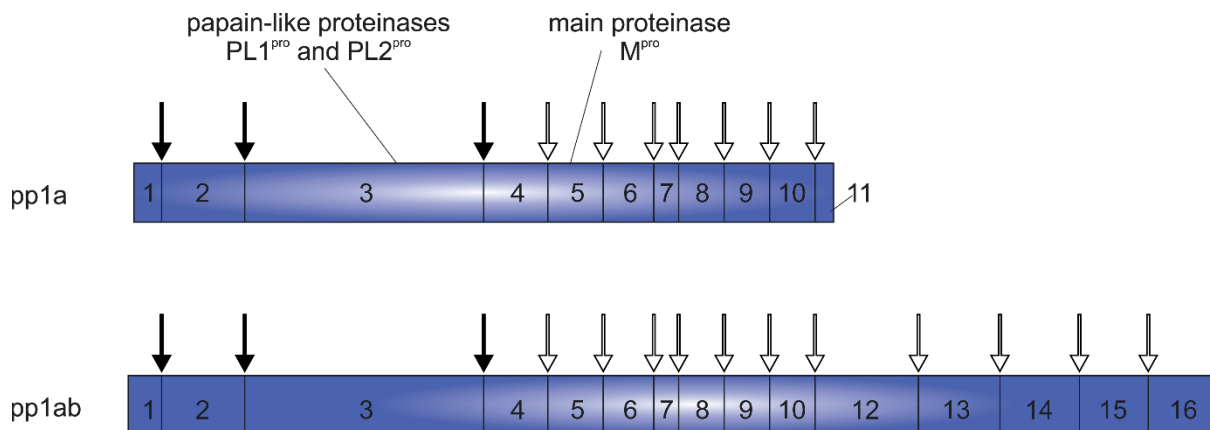


**Figure 3. Schematic representation of the proteolytic processing of pp1a and pp1ab.** Cleavage sites for the papain-like proteinases (PL1<sup>pro</sup> and PL2<sup>pro</sup>) are shown with black arrows and cleavage sites for the main proteinase (M<sup>pro</sup>) with white arrows. Nonstructural proteins (nsp1-16) are indicated. Modified after Snijder et al. (2016).

Replication of the coronavirus genome starts with negative strand RNA synthesis. The negative strand RNA serves as a template for generation of positive strand genomic RNAs. These RNAs are either translated into pp1a/pp1ab or packed into nucleocapsids (Weiss & Navas-Martin 2005).

Structural and accessory proteins are expressed from a *nested-set* of 3' co-terminal subgenomic mRNAs (sg mRNAs) (Siddell et al. 2005). All of these sg mRNAs possess an identical 3' end, which corresponds to the 3' end of the genomic RNA. At the 5' end sg mRNAs possess the *Leader*-sequence followed by a various number of ORFs (Fig. 4). Usually, only the first ORF of a sg mRNA is translated. Accordingly, coronavirus sg mRNAs are structurally polycistronic, but functionally monocistronic (Lai & Cavanagh 1997).

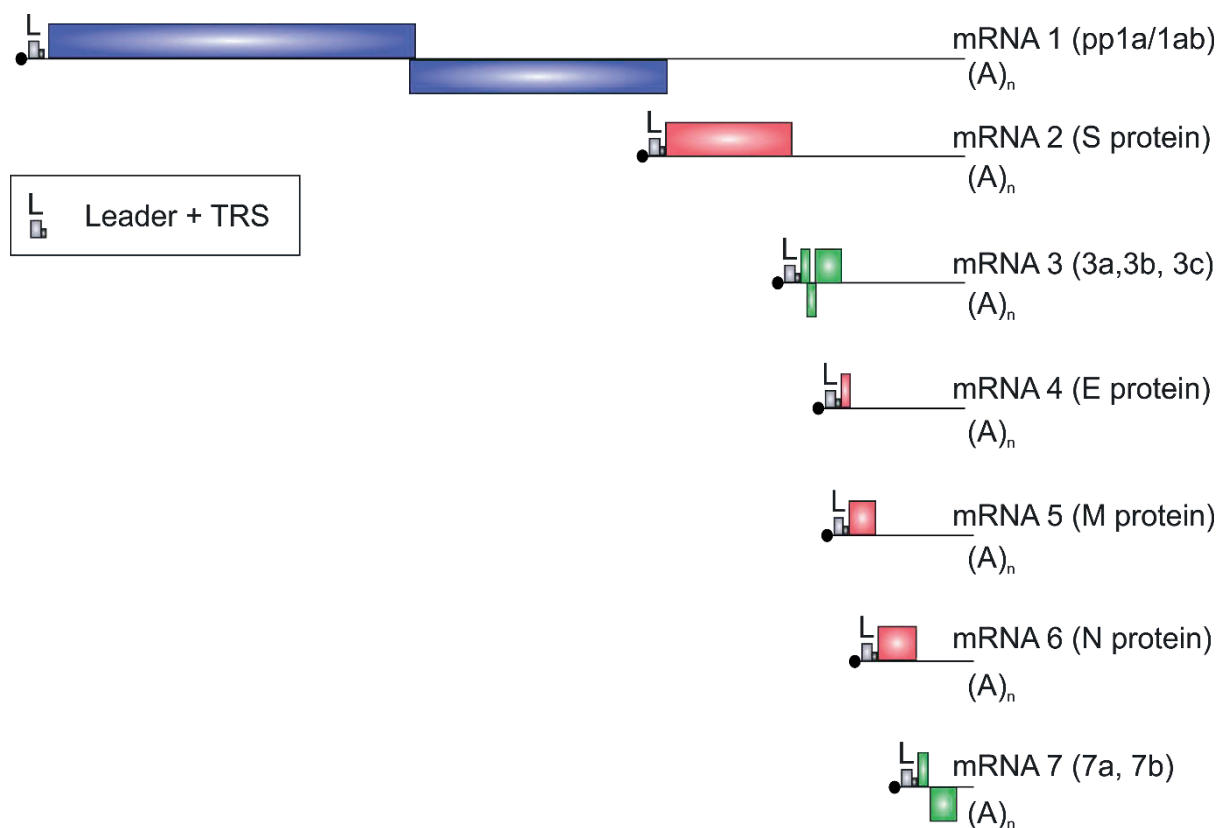


**Figure 4. Expression strategy of coronaviruses.** ORFs are shown with boxes. Black line downstream of the first ORF represents the non-translated region of the mRNA. 5' Cap structure is demonstrated with a black dot; L, *Leader*-sequence (grey box) is followed by transcription regulatory sequence (TRS, black box); (A)<sub>n</sub>, poly-(A) tail. Modified after Tekes (2008).

Subgenomic mRNAs are generated through discontinuous transcription during negative strand synthesis (Pasternak et al. 2001; Sawicki & Sawicki 1995). The so called transcription regulatory sequence (TRS) plays an essential role in this process. TRS is located in the coronavirus genome at the 3' end of the *Leader*-sequence (*Leader*-TRS) and upstream of each ORF (*Body*-TRS) (Lai & Holmes 2001). The synthesis of negative strand sg mRNAs starts at the 3' end of the genomic RNA. After the synthesis of the negative strand *Body*-TRS, the newly synthesized subgenomic RNA (- sgRNA) dissociates from the genomic RNA and translocates to the 5' end of the genome, where it binds through base pairing to the *Leader*-TRS. Then, the negative strand synthesis is continued and completed by adding the complement of the *Leader*-sequence. The synthesized - sgRNA serves as template for the generation of plus strand sg mRNAs, which are used for the translation of structural and accessory genes (Pasternak et al. 2001; Sawicki & Sawicki 1995). Schematic model of subgenomic mRNA synthesis is demonstrated in Figure 5.

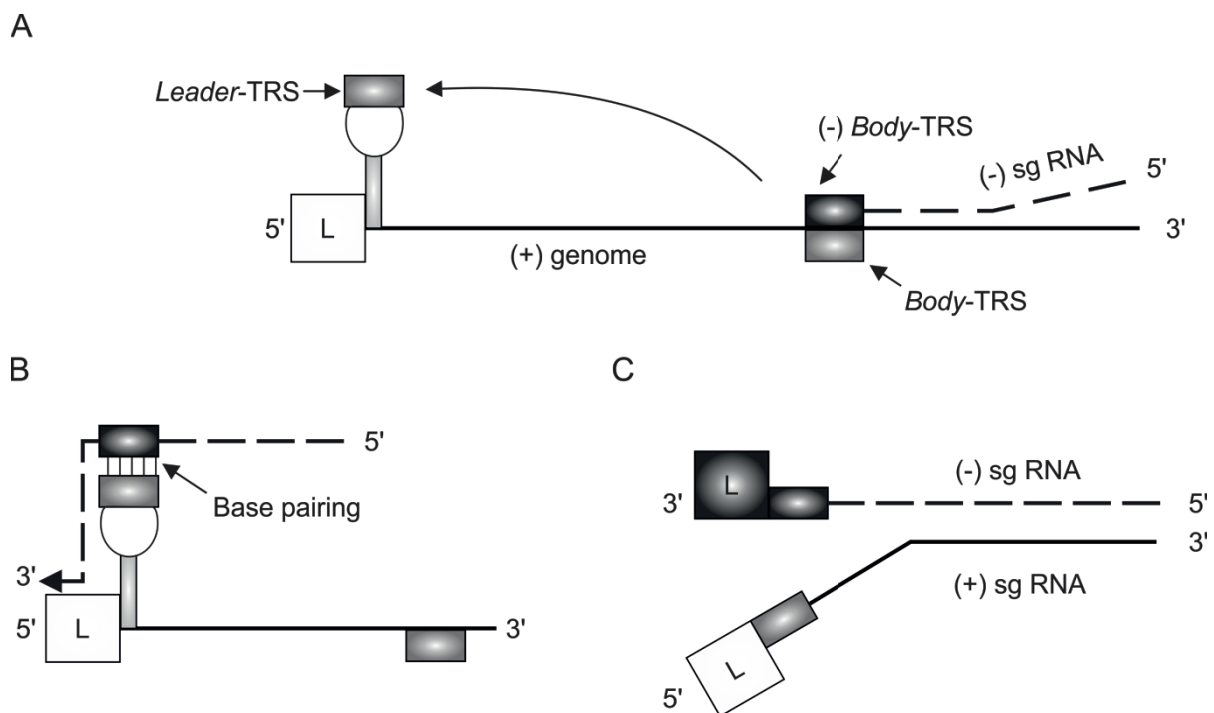


**Figure 5. Schematic representation of subgenomic RNA synthesis.** (A) Synthesis of negative strand sgRNA starts at the 3' end of the genome and pauses at *Body*-TRS. (B) Newly synthesized - sgRNA is translocated to the 5' end of the genome and binds through base pairing to the *Leader*-

TRS. Negative strand synthesis is continued until the complement of the *Leader*-sequence is added. (C) - sgRNA serves as a template for sg mRNAs synthesis. Modified after Tekes (2008).

Viral structural proteins synthesized from sg mRNAs are assembled in the endoplasmic reticulum-Golgi intermediate compartment (ERGIC) into new virions (Klumperman et al. 1994; Tooze et al. 1984) that are transported in vesicles to the plasma membrane and exocytosed (Lai & Holmes 2001; Siddell et al. 1983).

## 1.2 Feline Coronaviruses

Feline coronaviruses (FCoVs) are spread worldwide; they infect domestic as well as wild members of the family *Felidae* (Heeney et al. 1990; Hofmann-Lehmann et al. 1996; Munson et al. 2004; O'Brien et al. 1985; Paul-Murphy et al. 1994; Pedersen 2009). In single-cat households, seropositivity of FCoV reaches 10-50%, while in multi-cat households and animal shelters 80-90% of the cats are seropositive (Herrewegh et al. 1995; Pedersen et al. 1981; Pedersen & Black 1983). Most animals get infected in their first few weeks after birth, when the protection by maternal antibodies declines (Addie et al. 2009; Pedersen et al. 1981). Infected animals usually develop a persistent infection that can last from few months to few years (Addie & Jarrett 2001; Addie et al. 2003; Foley et al. 1997; Gunn-Moore et al. 1998; Herrewegh et al. 1995; Herrewegh et al. 1997).

Feline coronaviruses are divided into two serotypes (I and II) (Heeney et al. 1990; Hohdatsu et al. 1991a; Kennedy et al. 2003). Serotype I FCoVs are responsible for up to 95% of the natural infections (Addie et al. 2003; Hohdatsu et al. 1992; Kennedy et al. 2002; Kummrow et al. 2005). Serotype II FCoVs are less common in Europe or USA, but are more often found in Asia, where they can cause up to 25% of infections (Amer et al. 2012; An et al. 2011; Sharif et al. 2010). Serotype II FCoVs evolved through a double homologous recombination between serotype I FCoVs and canine coronavirus serotype II (CCoV). As a result of the recombination, serotype II FCoVs contain the S gene and surrounding regions of the CCoV in the backbone of a serotype I FCoV (Decaro & Buonavoglia 2008; Haijema et al. 2007; Herrewegh et al. 1998; Lin et al. 2013; Lorusso et al. 2008; Motokawa et al. 1996; Terada et al. 2014; Vennema 1999). According to the different origin of S genes in serotype I and II FCoVs, the *in vitro* growth characteristics of the two serotypes differ. While serotype

II FCoV s grow in cell culture, serotype I viruses do not grow *in vitro* (de Haan et al. 2005; Dye & Siddell 2005; Haijema et al. 2003; Haijema et al. 2004; Rottier et al. 2005; Tekes et al. 2012).

Based on pathogenicity, FCoVs are classified into two biotypes (Vennema 1999). Feline enteric coronavirus (FECV) leads usually to a persistent asymptomatic infection, while feline infectious peritonitis virus (FIPV) causes a lethal, immunopathological disease called feline infectious peritonitis (FIP) (Pedersen 2009; Poland et al. 1996). The horizontal transfer of FECVs occurs through fecal-oral route (Garner et al. 2008; Kipar et al. 2006; Pedersen 2009; Pedersen 2014). In contrast, FIPVs are usually not transmitted from cat to cat (Pedersen et al. 2012).

Two theories have been proposed to explain the emergence of FIPVs. The widely accepted '*internal mutation*' theory suggests that FIPV originates from FECV by acquiring mutations in persistently infected cats (Chang et al. 2011; Haijema et al. 2007; Pedersen 2009; Poland et al. 1996; Vennema et al. 1998). This hypothesis relies on sequence analyses of FECVs and FIPVs; sequences originating from one region are more similar to each other than FECVs or FIPVs sequences from geographically distant regions (Chang et al. 2011; Pedersen 2009; Vennema et al. 1998). The '*circulating virulent-avirulent FCoV*' hypothesis is based on sequence analyses of the M and 7b genes (Brown et al. 2009); they suggested the coexistence of virulent and avirulent FCoV strains in cat populations. According to this theory, cats are exposed to both virulent and avirulent strains and after infection with a virulent strain a susceptible cat develops FIP (Brown et al. 2009). It is important to note that this theory has not received any further backing. Subsequent studies have actually supported the '*internal mutation*' theory. So far, mutations responsible for the biotype switch have not been identified. However, alterations in the S gene and/or accessory genes 3c, 7a and 7b have been suggested to be involved in FIPV development (Bank-Wolf et al. 2014; Chang et al. 2010; Chang et al. 2012; Dedeurwaerder et al. 2013; Herrewegh et al. 1995; Kennedy et al. 2001; Licitra et al. 2013; Pedersen et al. 2012; Rottier et al. 2005; Takano et al. 2011; Vennema et al. 1998).

One remarkable difference between FCoV biotypes concerns the host cell tropism. FECVs primarily infect epithelial cells of the gut (Chang et al. 2010; Herrewegh et al.

1997; Kipar et al. 2010; Pedersen et al. 1981; Vogel et al. 2010), while FIPVs efficiently replicate in monocytes and macrophages. Upon FIPV infection, monocytes get activated and heavily express cytokines, adhesion molecules and enzymes that contribute to increased vascular permeability; this leads to extravasation of monocytes into tissues and effusion in body cavities (Dewerchin et al. 2005; Goitsuka et al. 1990; Kipar et al. 2005; Kipar & Meli 2014; Olyslaegers et al. 2013; Regan et al. 2009; Rottier et al. 2005; Stoddart & Scott 1989; Takano et al. 2011; Weiss et al. 1988).

### **1.3 Feline Infectious Peritonitis (FIP)**

Feline infectious peritonitis is a lethal disease caused by FIPV that was first described in 1963 (Holzworth 1963). In 1968, electron micrographs of virus particles originating from a cat that succumbed to FIP led to the suggestion that feline infectious peritonitis is caused by a coronavirus. This hypothesis was confirmed in 1976 (O'Reilly et al. 1979; Pedersen 1976; Ward 1970; Zook et al. 1968).

FIP is one of the most important lethal infectious diseases of cats. Although FECV infections are very common, FIPV develops only in approximately 5% of the persistently infected cats (Chang et al. 2011; Haijema et al. 2007; Pedersen 2009). Feline infectious peritonitis affects cats often at an age between 6 months and 2 years. The incidence of FIP decreases with increasing age (Foley et al. 1997; Pedersen 2009). Two clinical forms of FIP can be distinguished. The more common effusive form (wet) is characterized by the presence of protein-rich effusions in the abdominal and pleural cavities. The non-effusive form (dry) is defined by granulomatous lesions in different organs (Drechsler et al. 2011; Hartmann 2005; Kipar & Meli 2014; Montali & Strandberg 1972; Pedersen 2009; Pedersen 2014). The development of the different forms of FIP is assumed to be dependent on the host immune response (Pedersen 2009; Pedersen 2014).

The incubation time of naturally occurring FIP is difficult to determine. To elucidate it, experimental FIPV infections of cats have been performed. The experiments revealed an incubation time of 2-14 days for the wet form and several weeks for the dry form (Kiss et al. 2004; Pedersen et al. 1981; Pedersen & Black 1983; Pedersen

1984; Tekes et al. 2012). After infection, cats developed fever, lack of appetite and weight loss.

Currently, one FIPV vaccine is commercially available, namely Felocell FIP from Zoetis. This vaccine contains live, temperature sensitive recombinant serotype II FCoV strain DF2 for intranasal application (Christianson et al. 1989; Gerber et al. 1990a). This virus replicates in the upper respiratory tract and induces immunoglobulin A production that confers immunity in the upper respiratory tract (Gerber et al. 1990b). However, the efficacy of this vaccine is still debated.

An efficient therapy against FIP is currently not available. Recently an inhibitor of coronavirus 3C-like protease has been shown to reverse the progression of FIP under experimental conditions (Kim et al. 2016). Further experiments are required to assess this approach in natural FIP cases.

## 1.4 Accessory Proteins of Coronaviruses

The 3'-proximal one-third of the coronavirus genome codes for structural and accessory proteins (Fig. 2). Accessory proteins of CoVs are dispensable for virus growth *in vitro*, but they are relevant for virus replication and virulence *in vivo* (Casais et al. 2005; de Haan et al. 2002; Haijema et al. 2004; Hodgson et al. 2006; Ontiveros et al. 2001; Shen et al. 2003; Yount et al. 2005). The number of accessory genes in the coronavirus genomes varies among different species and sublineages from only one in *Alphacoronavirus* HCoV-NL63 (Pyrce et al. 2004) up to 9 in *Gammacoronavirus* BdCoV HKU22 (Woo et al. 2014). Homologs of these genes exist only in closely related Coronaviruses (Lai & Cavanagh 1997).

In alphacoronaviruses, accessory genes are present at two positions: (i) between S and E genes, and (ii) downstream of the N gene. FCoVs, as well as closely related CCoVs possess three ORFs (3a, 3b, 3c). TGEV contains two (3a and 3b) and other viruses, such as PEDV, HCoV-229E and HCoV-NL63 only one ORF (ORF 3). Recently, a new ORF named ORF 3 was discovered in this region for CCoV (Lorusso et al. 2008). Downstream of the N gene, FCoVs and CCoVs contain two ORFs (7a and 7b), while TGEV has only one (ORF 7) (Fig. 6A) (de Groot et al. 2012a).

In betacoronaviruses, accessory genes are located (i) downstream of the replicase gene, (ii) between S and E genes, (iii) between M and N genes, and (iv) downstream of the N gene. Additionally, an internal ORF within the N gene is present in SARS-CoV (ORF 9b), MERS-CoV (ORF 8b), HCoV-OC43 (ORF N2), HCoV-HKU1 (ORF N2), BCoV (ORF I) and MHV (ORF I) (Liu et al. 2014). The presence of accessory gene 2a and the hemagglutinin-esterase gene (HE) downstream of the replicase gene is characteristic for lineage A of betacoronaviruses and can be found in BCoV, MHV or HCoV OC43. ORF 4 and ORF 5a of this lineage are located between S and E genes and an internal ORF within the N gene is present (Fig. 6B). In betacoronavirus lineage B, accessory genes are located between M and N gene. In this region, SARS-CoV contains ORFs 6, 7a, 7b, 8a and 8b. Additionally, the SARS-CoV genome contains two ORFs (ORF 3a and 3b) between S and E gene and one within the N gene (ORF 9b) (Fig. 6C) (Liu et al. 2014). Betacoronaviruses of lineage C, like MERS-CoV, possess ORFs 3, 4a, 4b and 5 between S and E genes. In addition, this virus contains one internal ORF (ORF 8b) within the N gene (Fig. 6D). Ro-BatCoV HKU9 is a representative of betacoronavirus lineage D. This is the only member, in which two ORFs (ORF 7a and 7b) were identified downstream of the N gene. Additionally, it contains one ORF (ORF 3) downstream of the S gene (Fig. 6E) (Liu et al. 2014).

The gammacoronavirus IBV contains two ORFs (ORF 3a and 3b) between S and E genes and two others (ORF 5a and 5b) downstream of the M gene (Liu & Inglis 1991; Liu & Inglis 1992a; Liu & Inglis 1992b). Recently, a putative open reading frame was identified upstream of the ORF 5a and named ORF 4b (Fig. 6F) (Bentley et al. 2013). TCoV genome encompasses additional ORFs downstream of the M gene (ORF 4c) and downstream of the N gene (ORF 6b) (Brown et al. 2016). Gammacoronaviruses isolated from aquatic mammals, BWCoV SW1 and BdCoV HKU22, contain 8 or 9 accessory genes downstream of the M gene, respectively (Woo et al. 2014).

Members of the genus *Deltacoronavirus* possess one ORF (ORF 6) between M and N genes and up to four (ORF 7a-d) downstream of the nucleocapsid gene. Some viruses from this genus, like PorCoV HKU15 and WECov HKU16, contain an additional ORF (ORF 7) that is present within the N gene (Fig. 6G) (Fang et al. 2016; Woo et al. 2012).

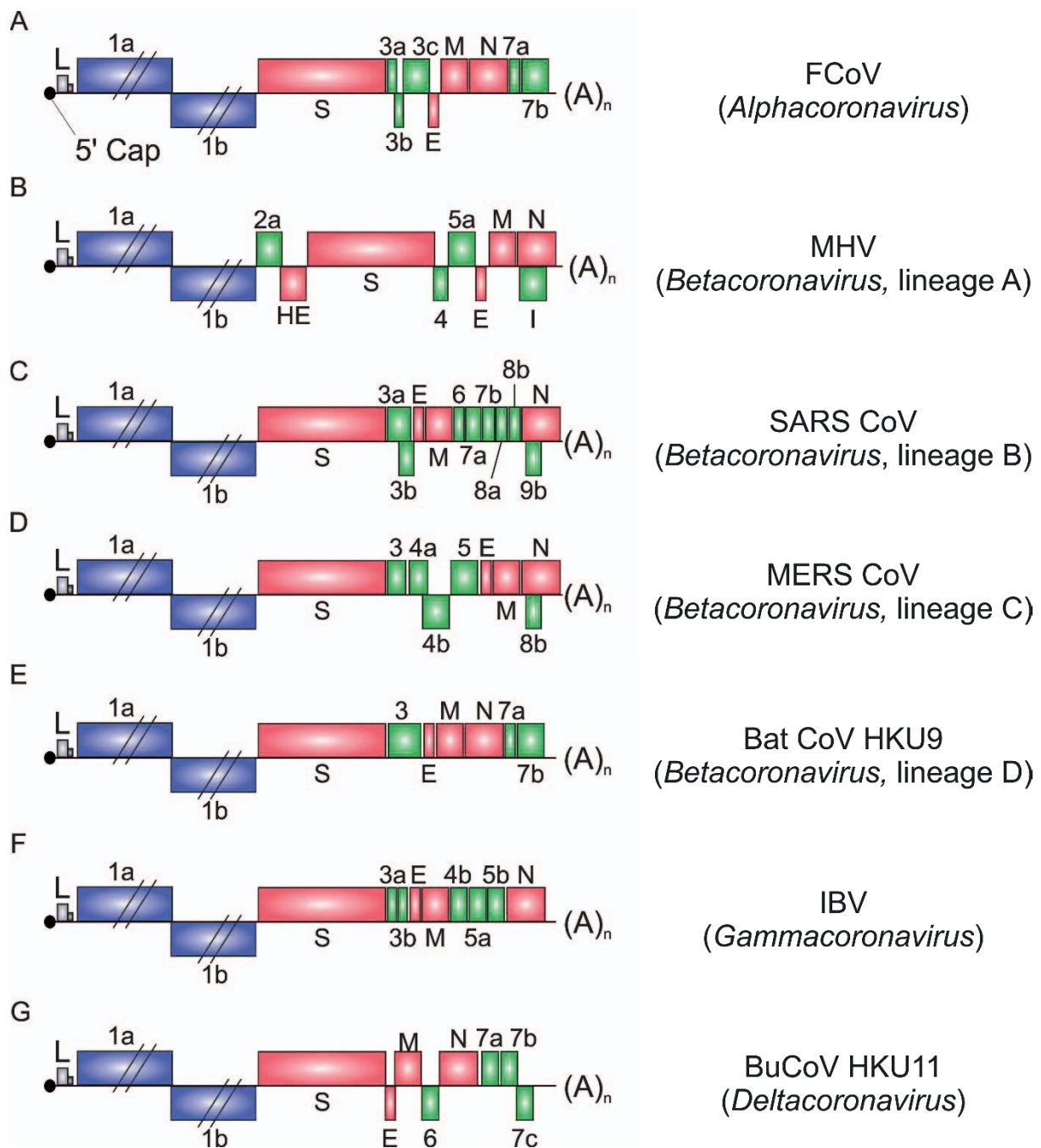


**Figure 6. Genome organization of representatives of genera Alpha-, Beta- (lineages A-D), Gamma- and Deltacoronavirus with focus on accessory genes downstream of ORF 1a and ORF 1b. (A)** FCoV, Feline coronavirus (NC\_002306), **(B)** MHV, Mouse hepatitis virus (AC\_000192), **(C)** SARS CoV, Severe acute respiratory syndrome coronavirus (NC\_004718), **(D)** MERS CoV, Middle-East respiratory syndrome coronavirus (NC\_019843), **(E)** Bat CoV HKU9, Rousettus bat coronavirus HKU9 (NC\_009021), **(F)** IBV, Infectious bronchitis virus (NC\_001451), **(G)** BuCoV HKU11, Bulbul coronavirus HKU11 (FJ376619). ORF 1a and 1b are marked in blue, ORFs encoding structural proteins in red and accessory genes in green. 5' Cap structure is shown as a black dot; L,

*Leader*-sequence (grey box) is followed by transcription regulatory sequence (TRS, black box); (A)<sub>n</sub>, poly-(A) tail. Modified after Liu et al.(2014) and Woo et al.(2012).

## **1.4.1 Accessory Genes and Accessory Proteins of Feline Coronaviruses**

The feline coronavirus genome contains five accessory genes: 3a, 3b, 3c between S and E genes and 7a, 7b downstream of the nucleocapsid gene (Lai & Cavanagh 1997).

### **1.4.1.1 Current Knowledge on Accessory Genes and Accessory Proteins of Feline Coronaviruses**

Based on sequence comparisons, FCoV ORF 3a is homologous to CCoV ORF 3a and TGEV ORF 3a (Narayanan et al. 2008a). FCoV ORF 3a encodes a 72-amino acid (aa)-long protein without any known function. This protein is supposedly expressed from subgenomic mRNA 3 (sg mRNA 3) (Dye & Siddell 2005; Tekes et al. 2008). However, the expression of this protein in FCoV-infected cells has not been demonstrated yet.

The only known homolog of FCoV ORF 3b is CCoV ORF 3b (Narayanan et al. 2008a). In the FCoV genome ORF 3b overlaps with ORF 3a and is suggested to encode a 9 kDa protein of unknown function. It is believed that 3b protein is translated by a noncanonical mechanism from sg mRNA 3. Thus far, expression of the 3b protein in FCoV-infected cells has not been shown.

FCoV ORF 3c is homologous to CCoV ORF 3c, TGEV ORF 3b and ORF 3 of all other alphacoronaviruses (Narayanan et al. 2008a). It is predicted to encode a 238 aa-long membrane protein with three transmembrane domains. The predicted topology of 3c protein resembles the topology of the M protein and SARS-CoV 3a protein (Narayanan et al. 2008b; Oostra et al. 2006). Similar to 3a and 3b, the expression of the 3c protein in FCoV-infected cells has not been demonstrated so far. It is also not known, whether 3c is expressed from the sg mRNA 3, like 3a and 3b proteins, or from a different, so far unidentified sg mRNA. The existence of a

separate sg mRNA for 3c protein is plausible, since a TRS or a highly similar sequence is present upstream of the 3c start codon in most FCoV isolates. Sequence comparison of FECVs and FIPVs revealed that over 80% of FIPVs contain mutations in this gene leading to a truncated 3c, whereas FECVs possess an intact one. Accordingly, it has been suggested that 3c protein is essential for viral replication in the gut, but dispensable for replication in monocytes (Chang et al. 2010). Homologs of FCoV 3c protein conserved in PEDV and HCoV-229E were reported to be incorporated into virions and function as ion channels (Wang et al. 2012; Zhang et al. 2014).

FCoV ORF 7a is homologous to CCoV ORF 7a and TGEV ORF 7 (Narayanan et al. 2008a). 7a protein is expected to be translated from sg mRNA 7 to generate a 101 aa-long protein (9 kDa) with an N-terminal signal sequence and a C-terminal transmembrane domain (Haijema et al. 2007). However, the expression of 7a in FCoV-infected cells has not been shown so far. 7a protein fused at the C-terminus with a GFP tag expressed from a plasmid construct was shown to co-localize with the endoplasmic reticulum (ER) and Golgi apparatus (Dedeurwaerder et al. 2014). This construct was then used to express 7a-GFP fusion protein in cells infected with recombinant FCoV where ORF 7 was deleted. These experiments led to the conclusion that 7a protein functions as a counteragent of IFN- $\alpha$  induced antiviral responses (Dedeurwaerder et al. 2014).

FCoV ORF 7b is homologous only to CCoV ORF 7b. It is the only FCoV encoded accessory protein, for which expression was demonstrated in infected cells. Furthermore, FCoV 7b-specific antibodies have been detected in sera obtained from infected cats indicating that 7b protein is produced *in vivo* (Herrewegh et al. 1995; Kennedy et al. 2008; Lemmermeyer et al. 2016; Vennema et al. 1992). Herrewegh et al. (1995) reported that deletions in FCoV ORF 7b occur during passages of the virus *in vitro*. These mutations are probably due to cell culture adaptation and lead to loss of virulence *in vivo*. 7b is expressed from sg mRNA 7, but the exact translation mechanism of this ORF remains to be determined. Most of the present knowledge on 7b protein originates from a study conducted in the early 1990s (Vennema et al. 1992). The authors identified the 7b protein in FCoV-infected cells using sera from infected cats. Furthermore, they expressed 7b protein from a plasmid in vaccinia virus-infected HeLa cells. These experiments showed that 7b is a secreted

glycoprotein (26 kDa). Localization of 7b protein in the ER was supported by treatment with Endoglycosidase H, which is able to cleave off high-mannose oligosaccharides present on the proteins in the ER, but not the complex glycan structures that are formed in the Golgi apparatus. The authors also suggested that the C-terminal KTEL motif acts as a KDEL-like endoplasmic reticulum (ER) retention signal that slows down 7b protein secretion. Vennema et al. (1992) showed that mutation of KTEL to KTEV in 7b protein led to enhanced secretion of the protein, while substitution of the KTEL with KDEL motif resulted in complete ER retention with no detectable secretion.

#### **1.4.1.2 FCoV Accessory Genes/Proteins Studied by Reverse Genetics**

Using reverse genetics, ORF 3, ORF 7 or both ORFs were deleted from the highly virulent serotype II FIPV strain 79-1146. Although the growth characteristics of the recombinant viruses were indistinguishable from that of the parental virus *in vitro*, they were unable to induce FIP *in vivo*. These results suggest that the accessory proteins are dispensable for viral replication *in vitro*, but important for the virulence *in vivo* (Haijema et al. 2004).

Another study was performed using the same recombinant viruses to infect peripheral blood monocytes (Dedeurwaerder et al. 2013). It was shown that only the parental virus (serotype II FIPV strain 79-1146) and the virus with deleted ORF 3 led to replication in monocytes, but not viruses with deleted ORF 7 or both ORFs. Accordingly, it was suggested that ORF 7 is necessary for FIPV replication in monocytes (Dedeurwaerder et al. 2013).

Influence of ORF 3 on viral replication *in vivo* was studied using the serotype II FIPV strain DF2 (Balint et al. 2012; Balint et al. 2014a; Balint et al. 2014b). In this strain, a deletion in ORF 3 results in truncated ORFs 3a and 3c and complete loss of ORF 3b. Using a reverse genetic system based on a bacterial artificial chromosome (BAC), ORF 3 was restored. Both the parental and the recombinant virus with restored ORF 3 showed similar growth characteristics in established cell lines. However, replication of the parental virus in peripheral blood monocytes was significantly higher

compared to the recombinant virus with complete ORF 3, suggesting that the deletion in ORF 3 promotes efficient virus replication in monocytes. Furthermore, the authors proposed that an intact ORF 3 is essential for the virus replication in the intestine, but is dispensable for the replication in monocytes (Balint et al. 2014a; Balint et al. 2014b).

## 1.5 N-linked Protein Glycosylation

Glycosylation is a common post-translational modification, in which sugar moieties are added to proteins and lipids in reactions catalyzed by glycosyltransferases (Lodish et al. 2000; Varki et al. 2009). Glycosylation plays various structural and functional roles in cells and viruses (Varki et al. 2009). It was shown that glycosylation of viral proteins can influence infectivity (Luo et al. 2015; Stern & Sefton 1982), pathogenicity of viruses (de Brogniez et al. 2015; Kariwa et al. 2013) and is important for viral assembly (Zai et al. 2013). Moreover, masking of epitopes through glycosylation was described as a common strategy for viruses to avoid immune recognition (Alvarado-Facundo et al. 2016; Nelson et al. 2016; Rizzo et al. 2016; Skehel et al. 1984; Townsley et al. 2015).

The number of attached monosaccharide units can vary from only one to formation of complex, highly branched structures called glycans (McDonald et al. 2016). Glycosylation occurs in the lumen of the endoplasmic reticulum (ER) as well as in the lumina of the *cis*-, *medial*- and *trans*-Golgi cisternae (Lodish et al. 2000). Since the localization of different enzymes involved in glycosylation varies between these compartments, the presence of certain sugar moieties on a glycosylated protein indicates its subcellular localization (Lodish et al. 2000; McDonald et al. 2016; Nilsson et al. 2009; Stanley 2011). Five classes of glycosylation were identified so far: N-linked glycosylation, O-linked glycosylation, glypiation, C-mannosylation and phosphoglycosylation.

N-linked glycosylation is the most common type of glycosylation and more than 50% of all eukaryotic proteins are N-glycosylated (Schwarz & Aebi 2011; Spiro 2002). During this process, glycans are covalently bound to the carboxamido nitrogen on asparagine residues. Enzymes involved in these processes are conserved across

species (Trombetta 2003). N-glycosylated proteins can possess large and extensively branched glycans that undergo four separate processing events. The initial two steps (glycan precursor assembly and its attachment to a target protein) occur identically for all proteins, while protein-specific differences manifest during subsequent trimming and glycan maturation (Trombetta 2003).

The glycan precursor that is attached co-translationally to a target protein consists of 14 sugar residues. These sugar moieties are added consecutively onto dolichol, a polyisoprenoid lipid carrier embedded in the ER membrane. Following addition of the first 7 residues to dolichol in the cytoplasm, the entire complex is transported into the lumen of the ER, where the glycan precursor is completed (Burda & Aebi 1999; Dean 1999). In the ER, oligosaccharyltransferase (OST) recognizes the Asn-X-Ser/Thr motif in the protein and attaches the glycan precursor to the carboxamido nitrogen on the asparagine residue. In the recognized motif, X can be any amino acid except for proline (Marshall 1972).

Trimming of the oligosaccharides is achieved by hydrolysis and occurs both in the ER and Golgi apparatus. Glycan trimming in the ER is used to monitor proper protein folding. The properly folded glycoprotein is then transported to the Golgi where it undergoes further maturation (Ellgaard & Helenius 2003; Roth 2002). In case of incorrect folding, the protein is transported out of the ER, deglycosylated and delivered to ER-associated degradation (ERAD) (Ermonval et al. 2001; Frenkel et al. 2003; Hosokawa et al. 2003; Kitzmuller et al. 2003).

Glycan processing in the Golgi involves trimming and addition of sugars by specific enzymes in different cisternae of the Golgi (Nilsson et al. 2009). Two different final glycan structures exist. While high-mannose oligosaccharides consist of multiple mannose residues, complex oligosaccharides contain multiple sugar types (*N*-acetylglucosamine, galactose, *N*-acetylneuraminic acid and fucose). Some glycoproteins have hybrid oligosaccharides with a combination of both structures (Stanley 2011).

Since the steps of glycosylation occur in different cellular compartments, the subcellular localization of glycoproteins can be investigated by applying various glycosidases. While PNGase F completely removes complex glycan structure from proteins, Endo H is unable to cleave off these structures that are formed beyond the

*cis*-Golgi. Thus, the conversion of a glycoprotein from the Endo H-sensitive to the Endo H-resistant form is a hallmark of arrival in the *medial*-Golgi compartment (Balch & Keller 1986).

## 1.6 Aims of the Study

Feline coronaviruses (FCoVs) are important pathogens that infect members of the family *Felidae* worldwide. Based on pathogenesis, FCoVs are divided into two biotypes. FECV causes mild symptoms, while FIPV leads to a lethal disease (FIP). There is accumulating evidence that accessory genes/proteins of FCoVs play an important role in virulence and may be important for establishment of persistent infection. However, lack of proper immunological tools thus far, limited the characterization of FCoV-encoded accessory proteins.

The FCoV-encoded accessory protein 7b was shown to be expressed in FCoV-infected tissue culture cells as well as in infected cats.

To study the expression and subcellular localization of 7b protein, a recombinant serotype II FIPV strain 79-1146 (rFIPV) expressing the non-glycosylated form of 7b protein was generated by use of a vaccinia virus-based reverse genetic system. In rFIPV-infected CRFK cells, 7b protein was characterized by Western blot and confocal microscopy using anti-7b monoclonal antibody.

Next, the mature, glycosylated form of 7b protein was studied in feline cells using a set of rFIPVs expressing flag-tagged 7b protein generated by vaccinia virus-based reverse genetics. Expression and subcellular localization of the flag-tagged, glycosylated form of 7b protein in FIPV-infected cells was analyzed with Western blot and confocal microscopy using anti-flag mAb.

Finally, we aimed to investigate the influence of the C-terminal KTEL motif of 7b protein on its subcellular localization/trafficking in infected feline cells.

## 2 Materials & Methods

### 2.1 Materials

#### 2.1.1 Cells

##### 2.1.1.1 Eukaryotic Cells

BHK-21 (Baby Hamster Kidney)	ATCC number: CCL-10
BHK-FIPV-N: (BHK cells expressing N protein of FIPV79-1146 - Tet-On system)	Institute of Virology, Giessen
CRFK (Crandell Reese feline kidney)	Institute of Virology, Giessen
CV-1 (monkey kidney cells)	ATCC number: CCL-70
D980R	gift from G. L. Smith, Imperial College, London, UK
Fc3Tg (Feline tongue)	Institute of Virology, Giessen
FCWF-4 (felis catus whole fetus)	Institute of Virology, Giessen

##### 2.1.1.2 Prokaryotic Cells

<i>E. coli</i> strain HB101 K-12	Institute of Virology, Giessen
----------------------------------	--------------------------------

#### 2.1.2 Viruses

FCoV 79-1146	gift from R.J. de Groot, Utrecht
vrFIPV	Institute of Virology, Giessen

### 2.1.3 Plasmids

pGPT-1	(Hertzig et al. 2004)
pGEM-T	Promega

### 2.1.4 Enzymes

Endo H	New England Biolabs (NEB)
Phusion DNA polymerase	Thermo Scientific
PNGase F	New England Biolabs (NEB)
Proteinase K	Roche
Restriction enzymes	New England Biolabs (NEB)
Expand Reverse transcriptase	Roche
RNase-free RQ1 DNase	Promega
<i>Taq</i> DNA polymerase	GeneCraft Germany
T4 DNA ligase	New England Biolabs (NEB)
Trypsin	Invitrogen

### 2.1.5 Antibodies

#### Primary antibodies:

anti-7b 14D8 mAb	mouse monoclonal antibody detecting 7b protein of FCoVs, Institute of Virology, Giessen
anti-Flag <sup>®</sup> M2	mouse monoclonal antibody detecting flag tag (DYKDDDDK), Sigma
anti-Giantin	rabbit polyclonal antibody detecting Golgi protein Giantin, Abcam

anti-PDI rabbit polyclonal antibody detecting ER Protein Disulfide Isomerase, Sigma

**Secondary antibodies:**

Goat anti-mouse IgG-PO	Horseradish Peroxidase-conjugated, Dianova
Goat anti-mouse IgG Alexa Fluor® 488	Invitrogen
Goat anti-rabbit IgG Alexa Fluor® 594	Invitrogen

**2.1.6 Chemicals**

Acrylamide, bisacrylamid solution 40%	Carl Roth
Agarose	Carl Roth
Alkaline phosphatase	Roche
6-aminocaproic acid	Sigma-Aldrich
Ampicillin	Serva
APS (Ammonium persulfate)	Sigma-Aldrich
Bacto Agar	Becton Dickinson
BSA (Bovine serum albumin)	Roche
Chloroform	Carl Roth
CMC (Carboxymethyl cellulose)	Sigma-Aldrich
Cycloheximide (CHX)	Sigma-Aldrich
Developer solution for X-ray films	Devomed
DMSO (Dimethyl sulfoxide)	Carl Roth
dNTPs (Deoxynucleoside triphosphate)	Invitrogen
EDTA (Ethylenediaminetetraaceticacid)	Carl Roth
Ethanol	Carl Roth

Ethidium bromide	Fluka
FCS (fetal calf serum)	Biochrom
Fixer solution for X-ray films	Devomed
Formaldehyde (37%)	Carl Roth
GeneRuler 1 Kb Plus	Thermo Scientific
Glycerin (87%)	Carl Roth
G418-Sulfate	Calbiochem
Hypoxanthine	Sigma-Aldrich
Isopropanol	Carl Roth
Lithium chloride precipitation solution	Ambion
Lipofectamine 2000	Invitrogen
$\beta$ -mercaptoethanol	Sigma-Aldrich
MOPS	Fluka
Mowiol 4-88	Sigma-Aldrich
Mycophenolic acid (MPA)	Sigma Aldrich
NaCl (sodium chloride)	Carl Roth
NP-40 (Nonident <sup>®</sup> P40)	Fluka
Page Ruler Prestained Protein Ladder	Thermo Scientific
PCR 10x buffer	GeneCraft Germany
Pefablock SC	Sigma-Aldrich
Penicillin/Streptomycin	Sigma-Aldrich
Phenol	Carl Roth
Ponceau S solution	Sigma-Aldrich
Powdered milk	Frema

Protein G-Sepharose™4 Fast Flow	GE Healthcare
Puromycin	Alexis Biochemicals
RNA cap analog	New England Biolabs (NEB)
RNA Gel Loading Dye	Ambion
RNaseOUT	Invitrogen
RNA storage solution	Ambion
Roti® Block A (10X)	Carl Roth
Roti® Block K (10X)	Carl Roth
Roti®ImmunoBlock	Carl Roth
Saccharose	Carl Roth
SDS (sodium dodecyl sulfate)	AppliChem
Sodium deoxycholate	Fluka
TEMED (Tetramethylethylenediamine)	Fluka
6-Thioguanine	Sigma-Aldrich
Tricine	Carl Roth
Tris	Carl Roth
Triton X-100	Sigma-Aldrich
Trypan blue	Serva
Tween-20	Sigma-Aldrich
Western Lightning Plus-ECL, Enhanced Chemiluminescence Substrate	Perkin Elmer
Xanthine	Sigma-Aldrich

## 2.1.7 Kits

Expand Reverse Transcriptase Kit	Roche
GenElute™ Gel Extraction Kit	Sigma-Aldrich
GenElute™ PCR Clean-up Kit	Sigma-Aldrich
GenElute™ Plasmid Miniprep Kit	Sigma-Aldrich
pGEM-T Vector System	Promega
peqGOLD Total RNA Kit	PEQLAB
RiboMax™ Large Scale RNA Production Systems	Promega

## 2.1.8 Culture Media

### 2.1.8.1 Bacterial Culture Media

LB-Medium

10g NaCl, 10g Tryptone, 5g Yeast extract for 1l H<sub>2</sub>O, pH 7.5

LB-Plates

1.5 % Bacto Agar in LB-Medium, 100 µg/ml Ampicillin

### 2.1.8.2 Cellular Culture Media

CCM 34 (prepared by the medium kitchen of the Institute of Virology, Giessen)	4.5 g/l DMEM powder, 0.0178 g/l L-Alanine, 0.7 g/l Glycine, 0.075 g/l L-Glutamic acid, 0.025 g/l Proline, 0.1 mg/l Biotin, 0.025 g/l Hypoxanthine, 3.7 g/l NaHCO <sub>3</sub> , sterile filtered, storage at 4 °C
---	---

Minimal Essential Medium (MEM) Eagle	Sigma
Negative selection medium	MEM, 1 µg/ml 6-TG, 10% FCS (v/v), 50.000 UI/ml Penicillin G, 50 mg/ml Streptomycin sulfate
Opti-MEM I	Gibco
Positive selection medium	MEM, 250 µg/ml Xanthine, 25 µg/ml MPA, 15 µg/ml Hypoxanthine, 10% FCS (v/v), 50.000 UI/ml Penicillin G, 50 mg/ml Streptomycin sulfate
Cell culture media for	
BHK-21	CCM34 450 ml + FCS 50 ml + Penicillin/Streptomycin 1ml
BHK-FIPV-N	CCM34 450 ml + FCS 50 ml + Penicillin/Streptomycin 1ml + G418 (100 µg/ml) + Puromycin (2µg/ml)
CRFK	CCM34 450 ml + FCS 50 ml + Penicillin/Streptomycin 1ml
CV-1	MEM 500 ml + FCS 50 ml + Penicillin/Streptomycin 1ml
D980R	MEM 500 ml + FCS 50 ml + Penicillin/Streptomycin 1ml
Fc3Tg	CCM34 450 ml + FCS 50 ml + Penicillin/Streptomycin 1ml
FCWF-4	CCM34 450 ml + FCS 50 ml + Penicillin/Streptomycin 1ml
Supplements for cell culture	
Penicillin/Streptomycin 500X	50.000 UI/ml Penicillin G, 50 mg/ml Streptomycin sulfate



DNA loading buffer	2.5 ml Orange G 1%, 3.5 ml Glycerin (87%), 4.0 ml H <sub>2</sub> O, 4 °C
DNase buffer (10X)	400 mM Tris, 100 mM MgSO <sub>4</sub> , 10 mM CaCl <sub>2</sub> , pH 8.0, sterile filtered
dNTP mix (25 mM) for PCR	25 mM of dATP, dCTP, dGTP, dTTP; - 20 °C
Jagow gel buffer	3 M Tris/HCl, 0.3% SDS (w/v), pH 8.45
MOPS buffer (10X)	200 mM MOPS, 50 mM sodium acetate (anhydrous), 10 mM EDTA, pH 7.0; sterile filtered and autoclaved, 4 °C
Mowiol mounting media for immunofluorescence	6 g Glycerin and 2.4 g Mowiol 4-88 were dissolved in 6 ml ddH <sub>2</sub> O, 12 ml of Tris/HCl (200 mM), pH 8.5 was added and centrifuged at 5000 × g for 15 min. 0.1 g 1,4-Diazabicyclo(2.2.2)octane (DABCO) per 1 ml medium was added before use; -20 °C

PBS	0.8 g/l NaCl, 0.2 g/l KCl, 0.2 g/l $\text{KH}_2\text{PO}_4 \times \text{H}_2\text{O}$ , 1.15 g/l $\text{Na}_2\text{HPO}_4 \times \text{H}_2\text{O}$ dissolved in ddH <sub>2</sub> O, autoclaved and stored at 4 °C
PBST	PBS with 0.1% Tween-20, 4 °C
Permeabilization solution	1% (v/v) Triton-X100 in PBS, 4 °C
Proteinase K buffer (2X)	400 mM NaCl, 200 mM Tris/HCl, 10 mM EDTA, 0.5% SDS (w/v), pH 7.5; sterile filtered
PVDF transfer buffers	
Anode buffer I	300 mM Tris
Anode buffer II	25 mM Tris
Cathode buffer	6-aminocaproic acid 40 mM
Radioimmunoprecipitation assay (RIPA) buffer	150 mM NaCl, 1% NP-40, 0.5% sodium deoxycholate (w/v), 0.1% SDS (w/v), 50 mM Tris, pH 8.0, 4 °C
SDS-PAGE sample loading buffer (4X)	8% SDS (w/v), 40% Glycerin (v/v), 0.01% Bromophenol blue (w/v), -20 °C

TFB-I	30 mM KOAc, 100 mM RbCl, 10 mM CaCl <sub>2</sub> , 50 mM MnCl <sub>2</sub> , 15 % Glycerin (v/v), pH 5.8 established with acetic acid, sterile filtered
TFB-II	10 mM MOPS, 10 mM RbCl, 75 mM CaCl <sub>2</sub> , 15 % Glycerin (v/v), pH 6.5 established with KOH, sterile filtered
Tris-acetate-EDTA (TAE) buffer for agarose gel electrophoresis (50X) 1l	242 g Tris, 57.1 ml glacial acetic acid, 5 mM EDTA, pH 8.0
Trypan blue Solution	0.25% Trypan blue (w/v), 0.15 M NaCl
Western blot transfer buffers	
Anode buffer (1X)	20% Methanol (v/v), 10 % Roti <sup>®</sup> Blot A (10X)
Cathode buffer (1X)	20% Methanol (v/v), 10 % Roti <sup>®</sup> Blot K (10X)

### 2.1.10 Consumables

Cell culture plates and dishes	Nunc, Thermo Scientific, Greiner Bio-One
Cell lifter	Corning Incorporated
Centrifuge tubes (15 and 50 ml)	Greiner Bio-One
Cryotubes	Thermo Scientific
Electroporation cuvettes	VWR

Filter paper	Whatman
Glass cover slips	MAGV
Glass pipettes	MAGV
MagNa Lyser Green Beads	Roche
Microscope slide	Carl Roth
Nitrile gloves	VWR
Nitrocellulose membrane	GE Healthcare
Pipette tips	Nerbe
Plastic pipettes (10 and 25 ml)	Thermo Scientific
PVDF membrane	Carl Roth
Reaction tubes	Eppendorf
Syringe filters (0.2 µm pore size)	Thermo Scientific
Ultracentrifuge tubes	Beckman Coulter
X-ray films	Advansta

### **2.1.11 Equipment**

Bacterial culture shaker K15/500	Noctua
Cell culture incubator (model C200)	Labotect
Class II biological safety cabinet MSC-Advantage	Thermo Scientific
Electrophoresis power cell	Biometra
Freezer (-20 °C)	Liebherr
Freezer (-80 °C) Hera Freeze	Thermo Scientific
Freezing container	Nalgene

Fridge	Liebherr
Gel documentation system <i>Rainbow</i>	Intas
Gene Pulser Electroporator	Bio-Rad
Heat block	workshop of the Institute of Virology, Giessen
Laser scanning confocal microscope TCS SP5	Leica
Light microscope DM-IL	Leica
Liquid nitrogen tank RS Series	Tec-Lab
MagNa Lyser homogenizer	Roche
NanoVue nucleic acid concentration measuring device	GE Healthcare
Neubauer Improved cell counting chamber	Marienfeld
PCR thermal cycler (model 2720)	Applied Biosystems
pH-meter	Hanna Instruments
Pipetboy	Integra Biosciences
Semi dry transfer system	Bio-Rad
Single channel pipettes	Brand
Sonopuls HD200 probe sonicator	Bandelin
Sonorex RK 52 ultrasonic bath	Bandelin
Tabletop centrifuge Fresco 21	Thermo Scientific
<i>The Sturdier</i> SDS-PAGE gel system	Hoefer Scientific Instruments
Ultracentrifuge model L8-60M	Beckman Coulter
Vacuum pump	Saskia
Water bath	Memmert

## 2.1.12 Synthetic DNA Oligonucleotides

### 2.1.12.1 Oligonucleotides for FCoV 79-1146 Genome

The numbers in the oligonucleotide name (Oligo) refer to its position in the FCoV 79-1146 genome, GenBank Accession number NC002306. Oligonucleotides used for PCR to analyze the integrity of FCoV cDNA integrated into vaccinia virus genome (2.2.6.1.4) are listed in Table 2. The rest of FCoV 79-1146-specific oligonucleotides are listed in Table 3.

PCR fragment number	Oligo	Nucleotide sequence (5' → 3')	Orient.
1	79-25-F	ACTTTTAAAGTAAAGTGAGTGTAGC	+
	79-3300-R	ACACTTGCATCAGAATCGCTTTTGTC	-
2	79-3505-F	GAGCAACTTTCCTCAGTAGAAAAAAA AGATGAAGTCTCTGC	+
	79-6500-R	TTAAGTGCGAGAAGTGCCTTAAAAA	-
3	79-6300-F	ATGGAATAGAGTTATACAATTGTCG	+
	79-9020-R	AACACCACTAGGCTGTGCCATTTTCT CAATCCGG	-
4	79-9020-F	CCGGATTGAGAAAATGGCACAGCCT AGTGGTGTT	+
	79-11300-R	AAACTATGCATAGCTGAAACTATTT	-
5	79-11200-F	TTTGAGCGAGAAGCTTCCGTGCAAA	+

	79-13750-R	CTCTGTTGTAGCGGTAATAATTGAAG	-
6	79-13750-F- XhoI	CTCGAGCCGCTACAACAGAGTCACA GTA CTTG	+
	79-16800-R- BsmBI	CGTCTCTGTAGATAACATAATCATACT TCACTACCCTGC	-
7	79-16800-F- BsmBI	CGTCTCTCTACACACAGACTTCCGAT ACACAGC	+
	79-18500-R	GGAGTGCTTTGCTATTAACAAAACCG TGCC	-
8	79-18100-F- BamHI	GGATCCGGAAGTCAATGTAGACAT GTACCCAGAG	+
	79-21850-R- NotI	GCGGCCGCCAACTTGTACTAATGCT TCAGTATACGATG	-
9	79-21300-F	GTTCCACTTTTGTAGTGGCAGGTT	+
	79-23900-R	CATTAAGTGCTGTAAGTCTACCTGT	-
10	79-23100-F	TTGAACAAGCACTTGCAATGGGTGC	+
	79-26075-R- SacI	GAGCTCTTAATAACATTTAGCAATGC TATTG	-
11	79-24303-F- XhoI	CTCGAGGGGTGTGATGTGTTGTTTG TCAAC	+
	79-27150-R	GATCCTTGTTTCGAGGGTAATGGGGT TG TAG	-
12	79-26990-F- SacII	CCGCGGGTAACATATGGTGTAACTA AACTTTC	+
	79-29355-R- SacI	GTATCACTATCAAAGGAAAATTTT	-

**Table 2. Oligonucleotides used for the PCR to analyze the integrity of FCoV cDNA (2.2.6.1.4).**

Orient., orientation of the oligonucleotide.

Oligo	Nucleotide sequence (5' → 3')	Orient.
79-27650-F-XhoI	CTCGAGGAGAACGTAGTGATTCCAAACCTA G	+
79-28130-R-EcoRI	GAATTCCAATCATCTCAACGTGTGTGTCATC A	-
79-28300-F	TGTAAATTGTTTGCAGCTTTTGAAA	+
79-28457-F-BsmBI	CGTCTCAAATAACATCATGATTGTTGTAATCC TTGTGTGT	+
79-28462-R-BsmBI	CGTCTCAATCATGATGTTAAAATAATGCACC CAACAATG	-
79-28485-R	CGTCTCTGTCATCCTTGTAATCAGCTTTAATT CCATTAGCCAAAAAGATA	-
79-28534-F	CGTCTCATGACGACGATAAGACTGCTGTGC AAAATGACCTTC	+
79-28653-F-QC-N68S	CGAAGGTTTCTCATGCACATGGCC	+
79-28653-R-QC-N68S	GGCCATGTGCATGAGAAACCTTCG	-
79-29049-R-7bF	CGTCTCTGTCATCCTTGTAATCTAACTCAGTT TTATGATGTTGGTTGAT	-
79-29068-F-AAEL	AACCAACATCATGCAGCTGAGTTATAAGGCA ACCCGA	+
79-29068-R-AAEL	TTGCCTTATAACTCAGCTGCATGATGTTGGT TGATTTTG	-
79-29071-F-KDEL	AACCAACATCATAAAGATGAGTTATAAGGCA ACCC	+
79-29071-R-KDEL	GTTGCCTTATAACTCATCTTTATGATGTTGGT TGATT	-
79-29074-F-AAAA	ACATCATGCAGCTGCTGCATAAGGCAACCC	+

	GATGTCT	
79-29074-R-AAAA	GGGTTGCCTTATGCAGCAGCTGCATGATGTT GGTTGAT	-
79-29077-F-KTE	CATCATAAACTGAGTAAGGCAACCCGATGT CTA	+
79-29077-R-KTE	CATCGGGTTGCCTTACTCAGTTTTATGATGT TGG	-
79-29077-F-KTEV	CATAAACTGAGGTTTAAGGCAACCCGATGT CTA	+
79-29077-R-KTEV	CGGGTTGCCTTAAACCTCAGTTTTATGATGT TG	-
79-29082-F-7bF	CGTCTCATGACGACGATAAGTAAGGCAACC CGATGTCTAAACTGGTC	+
79-29085-F-SacII	CCGCGGCAACCCGATGTCTAAACTGGTCT TT	+

**Table 3. FCoV 79-1146 specific oligonucleotides used for plasmid generation (2.2.3.5).** Orient., orientation of the oligonucleotide.

### 2.1.12.2 Other Oligonucleotides

Oligo	Nucleotide sequence (5' → 3')	Orient.
M13	TGTAAAACGACGGCCAG	+
M13r	CAGGAAACAGCTATGAC	-
GPT-250s	GAAGGCGATGGCGAAGGCTTCATCG	+
GPT-300as	AGTGCGCTTTTGGATACATTTACAG	-
VVL1	CTTAACGATGTTCTTCGCAGATG	-

**Table 4. Oligonucleotides used for sequencing.** Orient., orientation of the oligonucleotide.

## **2.2 Methods**

### **2.2.1 Eukaryotic Cells: Techniques**

#### **2.2.1.1 General Techniques**

All cell culture techniques were performed under sterile conditions in class II biological safety cabinet. Cells were grown on cell culture dishes with the diameter of 10 or 15 cm at 37 °C, 5% CO<sub>2</sub> in an incubator with humidity of around 96%. Cell lines were maintained in cell culture media as described above (section 2.1.8.2). Passaging cells encompassed removal of the media, washing step with 2-3 ml Trypsin and 2-5 min incubation with Trypsin in the cell culture incubator. After the cells have detached from the surface of the culture dish, they were resuspended in fresh culture media and a portion of them was seeded on a new dish.

#### **2.2.1.2 Cell Counting**

In order to determine the number of viable cells in a culture, the cells were first trypsinized (2.2.1.1) and then diluted 5X with the Trypan blue solution. Diluted cells were applied to the Neubauer Improved cell counting chamber, counted under the light microscope and the final cell number was determined from the equation:

$$n \times 5 \times 10000 = \text{number of cells/ml}$$

*n* is the average number of cells counted in 4 big squares of the chamber.

#### **2.2.1.3 Cryopreservation and Storage of Cells**

All available cell lines were cryopreserved for longer storage. Cells were first trypsinized (2.2.1.1) and centrifuged at 1400 rpm, 4 °C for 5 min. Cell pellet was resuspended in 3 ml FCS with 10% DMSO and aliquoted to 3 cryotubes. Cryotubes were then transferred to a freezing container and stored in a -80 °C freezer for two days. Subsequently, frozen cells were stored in a liquid nitrogen tank.

#### 2.2.1.4 Cell Infection

Determined number of cells (2.2.1.2) was seeded prior to virus infection. After the cells have attached, the medium was removed and cells were washed with FCS-free medium. Virus suspension with a defined MOI (*multiplicity of infection*) was used for the infection. MOI is described with a following equation:

$$\text{MOI} = \frac{\text{ml virus suspension} \times \text{virus titer/ml}}{\text{number of seeded cells}}$$

FCS-free medium was used to dilute the virus suspension to obtain the desired MOI. Cells were incubated in a cell culture incubator at 37 °C for 1 h. Following incubation, the virus suspension was removed, cells were washed with FCS-free medium and overlaid with fresh medium.

#### 2.2.1.5 Indirect Immunofluorescence Assay

Indirect immunofluorescence assay was used to determine the localization of 7b protein in serotype II FIPV strain 79-1146 infected cells. Microscope cover slips were disinfected with 70 % ethanol and washed twice with PBS. CRFK, FCWF-4 or Fc3Tg cells were counted (2.2.1.2) and seeded ( $1.2 \times 10^5$  cells/well) on the cover slips located in a 24-well cell culture plate. After the cells have attached to the cover slips (ca. 8 h), they were infected with a virus at an MOI of 1 (MOI=1) (2.2.1.4). 16 h p.i. (CRFK) or 10 h p.i. (FCWF-4, Fc3Tg) cells were fixed with 2 % paraformaldehyde for 20 minutes at room temperature (RT). In experiments, where the ongoing protein synthesis was blocked, cycloheximide (CHX, 100 µg/ml final concentration) was added 2 hours before the cells were fixed. Following fixation, cells were washed 3 times with PBS and permeabilized using 1 % Triton-X100 in PBS for 5 minutes. After 3 washing steps with PBS, residual binding sites were blocked with 10% Roti<sup>®</sup>ImmunoBlock (10X) in PBS for 10 minutes at RT. Cells were incubated with primary antibodies for 1 h at RT. Dilutions of the applied primary antibodies are described in Table 5. Following washing 3 times with PBS, cells were incubated with secondary antibodies (Table 5) for 1 h at RT. DNA was stained with 4',6-diamidino-2-phenylindole (DAPI, 66 µg/ml final concentration). Cells were then washed 3 times with PBS, cover slips were mounted with Mowiol medium and sealed using nail

polish. The preparations were visualized with Laser Scanning Confocal Microscope (Leica TCS SP5).

<b>Primary antibodies</b>	<b>Dilution*</b>
anti-7b 14D8 mAb	1:3
anti-Flag <sup>®</sup> M2	1:30.000
anti-PDI	1:500
anti-Giantin	1:200
<b>Secondary antibodies</b>	<b>Dilution*</b>
Goat anti-mouse IgG Alexa Fluor <sup>®</sup> 488	1:1000
Goat anti-rabbit IgG Alexa Fluor <sup>®</sup> 594	1:1000

**Table 5: Antibodies for Indirect Immunofluorescence Assay.** \*Antibodies were diluted in Antibody dilution buffer (2.1.9)

## 2.2.1.6 Transfection of Eukaryotic Cells

### 2.2.1.6.1 Chemical Transfection

CV-1 cells were seeded on a 6-well plate ( $5 \times 10^5$  cells/well) and on the next day infected with an appropriate vaccinia virus (MOI = 1). 1 h after the infection, two tubes containing 250  $\mu$ l of Opti-MEM were prepared. 10  $\mu$ l of Lipofectamine 2000 was added to one tube and 4  $\mu$ g of plasmid DNA to the other. Following 5 min incubation at room temperature, plasmid DNA solution was added to the tube with Lipofectamine 2000 and incubated for 30 min. Virus suspension was removed from the cells 2 h p.i., cells were washed and overlaid with 1.5 ml Opti-MEM. The DNA-Lipofectamine 2000 transfection mixture was added dropwise to the cells. Following 5-6 h incubation in cell culture incubator, the transfection medium was removed and cells were overlaid with fresh MEM medium. 2-3 days after the infection/transfection,

the cells were harvested, centrifuged at 3000 rpm, 4 °C for 3 min and resuspended in 700 µl of MEM medium. Following three cycles of freezing in liquid nitrogen and thawing in an ultrasonic bath, the virus stock was used for positive or negative selection to generate recombinant vaccinia viruses (see section 2.2.6.1.2 and 2.2.6.1.3).

### **2.2.1.6.2 Physical Transfection (Electroporation)**

Electroporation (EP) was used to introduce *in vitro* transcribed rFIPV-RNA (2.2.4.3) into BHK-FIPV-N cells. BHK-FIPV-N cells were cultured on a dish (10cm diameter) and were induced with Doxycycline (1 µg/ml final concentration) 20 hours prior EP. Next day, the cells were trypsinized (2.2.1.1) and centrifuged at 1200 rpm, 4 °C for 4 min. Medium was discarded and the cell pellet was resuspended in 10 ml PBS. Following second centrifugation step, the cell pellet (ca.  $10^7$  cells) was resuspended in 800 µl PBS and transferred into a pre-cooled electroporation cuvette. 10-20 µg of rFIPV-RNA was added to the cells. Electroporation was achieved with 2 pulses at 1.5 kV, with 200 Ω resistance and 25 µF capacitance using BioRad Gene Pulser Electroporator. Electroporated cells were transferred into a 10 cm culture dish with fresh CCM34 medium.  $10^7$  FCWF-4 cells were mixed to the BHK-FIPV-N cells and incubated for 2 days (cocultivation).

## **2.2.2 Prokaryotic Cells: Techniques**

### **2.2.2.1 Cultivation of Bacteria**

*Escherichia coli* (*E.coli*) strain HB101 K12 cells were cultivated overnight at 37 °C in LB-medium on a horizontal shaker. For selection of bacteria containing plasmid with Ampicillin resistance cassette, Ampicillin (100 µg/ml) was added to the LB-medium.

### **2.2.2.2 Preparation of Competent *E. coli* Cells**

2.5 ml LB-medium was inoculated with a single colony of *E. coli* strain HB101 K12 grown on an LB-plate. Following overnight incubation at 37 °C, the overnight culture was diluted 1:100 in LB-medium containing 20 mM MgSO<sub>4</sub> (250 ml) and grown until the optical density of the suspension measured at 590 nm (OD<sub>590</sub>) reached 0.4-0.6. The culture was centrifuged at 5000 rpm, 4 °C for 5 minutes. The cell pellet was resuspended in 100 ml ice-cold TFB-I buffer and incubated on ice for 5 min. Following second centrifugation, the cell pellet was resuspended in 10 ml TFB-II buffer and incubated on ice for 30 min. The cell suspension was then aliquoted (100 µl/tube) and stored at -80 °C freezer.

### **2.2.2.3 Transformation of Competent *E. coli* Cells**

Plasmid DNA was added to 50 µl of the competent *E. coli* HB101 K12 cell suspension (2.2.2.2) and the mixture was incubated on ice for 20 min. The cells were then submitted to heat shock at 42 °C for 45 sec. Following incubation on ice for 3 minutes, 250 µl of LB-medium was added and the cell suspension was incubated at 37 °C on a horizontal shaker for 30-60 min. Cells were then centrifuged at 5000 rpm for 3 minutes and resuspended in 100 µl of the supernatant. Transformed cell suspension was plated on an LB-plate and incubated overnight at 37 °C.

## **2.2.3 Molecular Techniques – DNA**

### **2.2.3.1 Standard Techniques**

#### **2.2.3.1.1 Polymerase Chain Reaction (PCR)**

The following protocol was used to generate PCR products for cloning (2.2.3.5) and for characterization of recombinant viruses (2.2.7.1):

Reagent	Amount [ $\mu$ l]	PCR cycles	
PCR buffer (10X)	5.0	Primary denaturation	94 °C, 3 min
Forward primer (50 mM)	0.5	35 cycles of:	
Reverse primer (50 mM)	0.5	Denaturation	94 °C, 30 s
dNTP mix	0.5	Annealing	50-60 °C, 30 s
<i>Taq</i> polymerase	0.5	Elongation	72 °C, 1 min/kb
ddH <sub>2</sub> O	40.5		
DNA template	2.5	Elongation	72 °C, 10 min

**Table 6. PCR standard protocol.**

### 2.2.3.1.2 QuickChange PCR

The protocol below was used to introduce mutations into existing plasmid sequences.

Reagent	Amount [ $\mu$ l]	PCR cycles	
PCR HF buffer (5X)	10.0	Primary denaturation	94 °C, 3 min
Forward primer (50 mM)	1	18 cycles of:	
Reverse primer (50 mM)	1	Denaturation	94 °C, 30 s
dNTP mix	1	Annealing	56-63 °C, 45 s
<i>Phusion</i> polymerase	0.5	Elongation	68 °C, 40 s/kb
ddH <sub>2</sub> O	36		
Plasmid DNA	0.5	Elongation	68 °C, 10 min

**Table 7. QuickChange PCR standard protocol.**

### **2.2.3.1.3 Digestion with Restriction Enzymes**

Restriction enzymes were used to control the result of a ligation (2.2.3.1.5) and to generate plasmids (2.2.3.5).

pGEM-T-based plasmids purified with Miniprep Kit (2.2.3.3.1) were controlled by digesting with *EagI* restriction enzyme. For this purpose 200 ng of plasmid was incubated with 5U of *EagI* at 37 °C for 1 hour. The cleaved DNA was resolved by electrophoresis (2.2.3.4.1) using a 1% agarose gel.

For the generation of plasmids, an insert from one plasmid was subcloned into another plasmid. To achieve that, both plasmids (4 µg each) were digested with the same set of restriction enzymes as recommended by the supplier.

### **2.2.3.1.4 Dephosphorylation**

In order to prevent self-ligation of digested plasmids, the vectors were dephosphorylated. For this purpose, vectors after digestion with restriction enzymes (2.2.3.1.3) were incubated with 5 U of alkaline phosphatase (Roche) at 37 °C for 30 min.

### **2.2.3.1.5 Ligation**

Purified PCR products (2.2.3.2.2) were cloned into pGEM-T vector using pGEM-T Vector System Kit (Promega). This procedure utilizes adenines added by the *Taq* polymerase at the 3' end of the PCR products. Linearised vector with complementary thymines was ligated with the PCR product in the presence of T4 DNA ligase.

Ligation of products after restriction enzyme cleavage was performed in 10 µl final volume. Vector- and insert-DNA was mixed in 1:3 molar ratio. 1 µl of 10X T4 DNA ligase buffer and 0.5 µl T4 DNA ligase were added to the DNA mixture and the reaction was filled up to 10µl with ddH<sub>2</sub>O. Ligation was performed at 4 °C overnight.

## **2.2.3.2 DNA Purification**

### **2.2.3.2.1 Phenol/Chloroform Extraction with Ethanol Precipitation**

To extract the DNA from aqueous solution, same volume of Phenol was added. After mixing the two phases, the mixture was centrifuged at 13.000 rpm, 4 °C for 4 minutes. The upper phase was pipetted into a new tube and mixed with an equal volume of Chloroform. Following centrifugation, upper phase was removed and mixed with 2.5 volume of 100 % ice-cold ethanol. Following 10 min incubation on ice, precipitated DNA was centrifuged at 13.000 rpm, 4 °C for 10 minutes and the supernatant was removed. The DNA pellet was washed with 200 µl 70 % ethanol and centrifuged for another 5 minutes. After repeating the washing step, DNA was resolved in 40 µl ddH<sub>2</sub>O.

### **2.2.3.2.2 Purification of PCR products**

Purification of PCR products was performed using GenElute™ PCR Clean-up Kit (Sigma-Aldrich) according to the manufacturer's recommendations.

### **2.2.3.2.3 Gel Extraction**

DNA resolved with agarose gel electrophoresis (2.2.3.4.1) was visualized using a UV table. DNA bands of interest were excised from the gel using a sterile scalpel and were purified using GenElute™ Gel Extraction Kit (Sigma-Aldrich) according to the manufacturer's recommendations.

### **2.2.3.3 DNA Isolation**

#### **2.2.3.3.1 Plasmid DNA Isolation from Bacteria Culture**

The plasmid DNA isolation from bacterial culture was performed using GenElute™ Plasmid Miniprep Kit (Sigma-Aldrich) according to the manufacturer's recommendations.

#### **2.2.3.3.2 Vaccinia Virus DNA Isolation from Eukaryotic Cells**

##### **2.2.3.3.2.1 Analytical Scale**

This method was used to isolate recombinant vaccinia virus DNA for further characterization. Infected CV-1 cells in a 6-well plate were scrapped off using a reversed pipette tip and centrifuged at 3000 rpm, RT for 3 minutes. The cell pellet was resuspended in 200 µl H<sub>2</sub>O. After addition of 200 µl Proteinase K buffer (2X) and 4 µl of Proteinase K (10 mg/ml), the solution was mixed and incubated at 55 °C for 2 hours. The DNA precipitation was performed as described in section 2.2.3.2.1.

##### **2.2.3.3.2.2 Preparative Scale**

Vaccinia virus DNA from infected BHK-21 cells was isolated in large scale for *in vitro* transcription (2.2.4.3). Infected BHK-21 cells from 8 cell culture dishes (15 cm diameter) were removed using a cell lifter and centrifuged at 3000 rpm, 4 °C for 5 minutes. Supernatant was removed and cell pellet was resuspended in 4 ml ice cold Buffer A (1X). Cell suspension was aliquoted into MagNaLyser Green Beads tubes and homogenized at 5000 rpm for 20 sec with MagNaLyser (Roche). After homogenization, tubes were centrifuged (3000 rpm, 3min, 4 °C) and supernatant was pipetted into fresh reaction tubes (1ml/tube). After addition of 100 µl Trypsin solution to each tube, the cell lysate was incubated at 37 °C for 30 min. During the

incubation, 18 g of saccharose was dissolved in 50 ml H<sub>2</sub>O. 25 ml of the saccharose was transferred into a 50 ml canonical tube and gently overlaid with the trypsin-digested cell lysate. Following centrifugation at 13000 rpm, 4 °C for 80 minutes, the supernatant was discarded and the virus pellet was resuspended in 700 µl Buffer A (1X). After addition of 80 µl DNase buffer (10X) and 8 µl *RQ1 DNase* (RNase-free), the virus suspension was incubated at 37 °C for 30 min. The DNase was inactivated by incubation at 65 °C for 20 min with additional 40 µl EDTA (10 mM). Virus suspension was divided into 4 aliquots (200 µl each). To each of the aliquots 200 µl Proteinase K Buffer (2X) and 4 µl Proteinase K was added and incubated at 55 °C for 2 hours. The DNA precipitation was performed as described in section 2.2.3.2.1.

#### **2.2.3.4 DNA Analysis**

##### **2.2.3.4.1 DNA Agarose Gel Electrophoresis**

Agarose gel electrophoresis of DNA was used to analyze and isolate DNA. 1% agarose was prepared by mixing the agarose powder with Tris-acetate-EDTA buffer (TAE 1X) and boiled. Samples were mixed with DNA loading buffer in 4:1 ratio and transferred into the wells of the gel. GeneRuler 1 Kb Plus (Thermo Scientific) was used as a molecular marker. The electrophoresis was performed in ethidium bromide-stained 1X TAE buffer at 100 V for 45 minutes. After the electrophoresis, DNA bands were visualized with a UV table and documented using a camera.

##### **2.2.3.4.2 Sequencing**

Plasmid DNA or DNA purified after PCR (2.2.3.2.2) was mixed with appropriate sequencing primer and sent to Seqlab-Microsynth (Lindau, Germany) for sequencing. pGEM-T based plasmids were sequenced using M13 and M13r primers (2.1.12.2). The obtained results were analyzed using BioEdit software version 7.2.5.

### 2.2.3.5 Plasmid Generation

cDNA obtained after reverse transcription of serotype II FIPV strain 79-1146 RNA (2.2.4.2) was used as a template for generation of plasmids. pGPT-1- $\Delta$ 7ab plasmid contains sequence corresponding to nt 27651 to 29355 of the type II FIPV strain 79-1146 genome, where 7ab genes (nt 28152 to 29082) are substituted with *E. coli* guanosine-phosphoribosyltransferase gene (*gpt*). To construct pGPT-1- $\Delta$ 7ab, pGPT-1 plasmid was used (Hertzog et al. 2004). In the first cloning step, sequence corresponding to nucleotides (nt) 27651 to 28151 of the type II FIPV strain 79-1146 genome was amplified with PCR (primer pair 79-27650-F-XhoI and 79-28130-R-EcoRI) (2.2.3.1.1), purified (2.2.3.2.2) and cloned into pGEM-T vector (Promega) (2.2.3.1.5). The generated plasmid and plasmid pGPT-1 were both treated with *EcoRI* and *XhoI* restriction enzymes (2.2.3.1.3). pGPT-1 vector was additionally dephosphorylated (2.2.3.1.4). Treated samples were resolved on an agarose gel (2.2.3.4.1), purified (2.2.3.2.3) and the type II FIPV strain 79-1146 sequence was ligated downstream of the *gpt* gene in the pGPT vector (2.2.3.1.5). In the second cloning step, obtained plasmid was used to incorporate the FIPV sequence (corresponding to nt 29083 to 29355 of type II FIPV strain 79-1146) upstream of the *gpt* gene in a similar way (primer pair 79-29085-F-SacII and 79-29355-R-SacI). In this step, *SacII* and *SacI* restriction enzymes were used. The resulting plasmid (pGPT-1- $\Delta$ 7ab) was used for the generation of vrFIPV-GPT- $\Delta$ 7ab (2.2.6.1).

Plasmids pDF1 – pDF9 are based on the pGEM-T vector (Promega). Plasmid pDF1 contains sequence corresponding to nt 27651 to 29355 of the type II FIPV strain 79-1146 genome, where nt 28663 to 28665 were changed from AAT to TCA to replace asparagine with serine at aa position 68 in 7b protein. To generate this plasmid, sequence corresponding to nt 27651 to 29355 of the type II FIPV strain 79-1146 genome was amplified with PCR and cloned into pGEM-T vector (primer pair 79-27650-F-XhoI and 79-29355-R-SacI). The substitution of nt 28663 to 28665 from AAT to TCA was achieved with QuickChange PCR (primers 79-28653-F-QC-N68S and 79-28653-R-QC-N68S) (2.2.3.1.2).

Plasmid pDF2 contains sequence corresponding to nt 27651 to 29355 of type II FIPV strain 79-1146, where additional flag tag sequence upstream of 7b gene (nt 28465) was inserted. To generate this plasmid, two sequences were amplified with PCR and

cloned into pGEM-T vector. Insert I corresponds to nt 27651 to 28464 (primer pair 79-27650-F-XhoI and 79-28462-R-BsmBI) and insert II to 28465 to 29355 (primer pair 79-28462-F-BsmBI and 79-29355-R-SacI) of type II FIPV strain 79-1146. Both plasmids were then digested with *BsmBI* and *NotI* enzymes and resolved on an agarose gel. Following purification of DNA fragments from the gel, insert II was ligated into pGEM-T containing insert I. Plasmids pDF3 and pDF4 were generated with a similar approach. Plasmid pDF3 contains sequence corresponding to nt 27651 to 29355 of type II FIPV strain 79-1146, where additional flag tag sequence was introduced downstream of nt 28512 of 7b gene. Nucleotide sequences 27651 to 28512 (primer pair 79-27650-F-XhoI and 79-28485-R) and 28513 to 29355 (primer pair 79-28534-F and 79-29355-R-SacI) were amplified by PCR for this purpose. Plasmid pDF4 contains nt 27651 to 29355 of type II FIPV strain 79-1146, with an additional flag tag sequence inserted downstream of 7b gene (nt 29079). Sequences corresponding to nt 27651 to 29079 (primer pair 79-27650-F-XhoI and 79-29049-R-7bF) and nt 29080 to 29355 (primer pair 79-29082-F-7bF and 79-29355-R-SacI) of type II FIPV strain 79-1146 were amplified with PCR to construct this plasmid.

Plasmids pDF5 – pDF9 were generated by performing QuickChange PCR on plasmid pDF3. The sequence of plasmid pDF5 is identical with pDF3, but in pDF5 nt 28663 to 28665 were changed from AAT to TCA to replace asparagine with serine at aa position 68 in 7b protein. Primers 79-28653-F-QC-N68S and 79-28653-R-QC-N68S were used for the QuickChange PCR. Plasmid pDF6 sequence is identical with pDF3, but in pDF6 leucine, corresponding to aa position 206 of 7b protein, was substituted with valine. This was achieved by altering nt 29077 to 29079 from TTA to GTT using 79-29077-F-KTEV and 79-29077-R-KTEV primers in QuickChange PCR. The sequence of pDF7 is identical with pDF3, but in pDF7 nucleotides corresponding to aa position 206 of 7b protein (29077 to 29079) are deleted. Primers 79-29077-F-KTE and 79-29077-R-KTE were used for this purpose. Plasmid pDF8 sequence is identical with that of pDF3, but in pDF8 nt 29071 to 29073 were altered from ACT to GAT to substitute threonine with aspartic acid at position corresponding to aa 204 in 7b protein. To achieve that, primers 79-29071-F-KDEL and 79-29071-R-KDEL were used. The sequence of pDF9 is identical with pDF3, but in pDF9 nt 29068 to 29079 were replaced with GCAGCTGCTGCA to exchange KTEL with AAAA at position corresponding to aa 203-206 of 7b protein. Two rounds of QuickChange PCR were

needed to obtain pDF9. First, with primers 79-29068-F-AAEL and 79-29068-R-AAEL and second, on the obtained plasmid, with primers 79-29074-F-AAAA and 79-29074-R-AAAA. Generated plasmids pDF1 – pDF9 were used to generate *gpt* negative recombinant vaccinia viruses (2.2.6.1.3).

## 2.2.4 Molecular Techniques - RNA

### 2.2.4.1 RNA Isolation from Eukaryotic Cells

FIPV-infected FCWF-4 cells were harvested and centrifuged at 1400 rpm, 4 °C for 4 min. Total RNA was isolated from the cell pellet using peqGOLD Total RNA Kit (PEQLAB) according to manufacturer's recommendations. Isolated RNA was stored at -80 °C.

### 2.2.4.2 Reverse Transcription

RNA was transcribed into DNA using the Expand Reverse Transcriptase Kit (Roche). The following protocol was applied:

Reagent	Amount [µl]	Reaction conditions	
1 µg isolated RNA	1-3		
Reverse primer (50 mM)	0.5		
ddH <sub>2</sub> O	To 10.5	Denaturation	65 °C, 10 min
		Cool on ice	4 °C
5X Expand Reverse Transcriptase buffer	4		
DTT (100 mM)	2		
dNTP mix	2		

RNaseOUT	0.5	Elongation	43 °C, 60 min
Exapnd Reverse Transcriptase 50 U/μl	1		
Total volume	20	Cool on ice	4 °C

**Table 8. Reverse transcription standard protocol.**

Obtained cDNA was then used as a template for PCR (2.2.3.1.1).

### 2.2.4.3 *In vitro* Transcription

For the *in vitro* transcription (IVT), RiboMax™ Large Scale RNA Production Systems kit (Promega) was used. Recombinant vaccinia virus DNA isolated in preparative scale (2.2.3.3.2.2) was digested with *ClaI* restriction enzyme for 3 hours at 37 °C and purified with Phenol/Chloroform procedure (2.2.3.2.1). Digested DNA was then used for the *in vitro* transcription:

10 μl	T7 Transcription 5X buffer
5 μl	RNA cap analog
0.7 μl	rGTP (100 mM)
3.75 μl	rATP, rCTP, rUTP (100 mM)
5 μl	T7 enzyme mix
1 μl	RNaseOUT
17 μl	DNA after <i>ClaI</i> digestion

The mixture was incubated at 30 °C for 2 h. After incubation, 2 μl of *RQ1 DNase* were added and the reaction tube incubated at 37 °C for 30 min. Following addition of 26 μl Lithium Chloride Precipitation Solution (Ambion), the RNA was precipitated at -20 °C for 30 minutes. Precipitated RNA was then centrifuged at 13000 rpm, 4 °C for 25 minutes, washed with 200 μl 70% ethanol and centrifuged again for 4 minutes. RNA pellet was resolved in 24 μl of RNA Storage Solution (Ambion). 2 μl RNA was

used for RNA electrophoresis (2.2.4.4.1) and the rest was electroporated into BHK-FIPV-N cells (2.2.1.6.2).

## **2.2.4.4 RNA Analysis**

### **2.2.4.4.1 RNA Agarose Gel Electrophoresis**

Agarose gel electrophoresis was used to assess the quality of the *in vitro* transcribed-RNA (2.2.4.3). 0.63 g agarose was mixed with 45.5 ml MOPS buffer (1X) and boiled. After cooling down the gel solution to 50 °C, 4.5 ml of 37% formaldehyde (Carl Roth) was added. 2 µl *in vitro* transcribed-RNA was mixed with 5 µl RNA Gel Loading Dye (2X) and denatured at 65 °C for 10 min. After addition of 1 µl ethidium bromide (10mg/ml), the sample was loaded on a gel and resolved in 1X MOPS buffer at 90 V for 45 min. After electrophoresis, RNA bands were visualized with a UV table and documented using a camera.

## **2.2.5 Molecular Techniques for Working with Proteins**

### **2.2.5.1 Cell Lysis**

Cells were lysed in order to release proteins for further analysis. To achieve that, medium was removed from the cell culture dish, cells were washed with PBS and overlaid with RIPA buffer (80 µl per well in a 24-well plate). After 5 min incubation on ice, the lysate was collected in a reaction tube and sonicated twice for 2 sec. Aliquots of the lysate were stored at -20 °C.

### **2.2.5.2 Protein Deglycosylation**

Cell lysates were treated either with Endo H (NEB) or PNGase F (NEB) according to manufacturer's recommendations to remove sugar rests from glycosylated proteins.

### 2.2.5.3 Protein Analysis

#### 2.2.5.3.1 Sodium Dodecyl Sulfate Polyacrylamide Gel Electrophoresis (SDS-PAGE)

SDS-PAGE (Laemmli 1970) was used to resolve proteins on a polyacrylamide gel for further analysis with Western blot (2.2.5.3.3) or for N-terminal Edman Sequencing (2.2.5.3.2). Tris-Tricine buffer system was used for this purpose (Schagger & von Jagow 1987). It allows the separation of small proteins between 1 and 100 kDa. It is a double-phase gel system, where proteins are first concentrated in the 4% stacking gel and then resolved in 10 % resolving gel. The gel recipe is presented in Table 9.

Reagent	Resolving gel (10%)	Stacking gel (4%)
Acrylamide, bisacrylamid solution 40% (29:1)	9.0 ml	1.4 ml
Glycerin (87%)	2 ml	-
Jagow gel buffer	12.0 ml	3.5 ml
ddH <sub>2</sub> O	12.9 ml	9.0 ml
APS (10%)	175 µl	116 µl
TEMED	15 µl	12 µl

**Table 9. SDS-PAGE gel recipe.** Gels were cast in *The Sturdier* SDS-PAGE system (Hoefler Scientific Instruments).

Cell lysate or cell culture supernatant was mixed with SDS-PAGE sample loading buffer (4X) in a 4:1 ratio. Additionally,  $\beta$ -mercaptoethanol was added (5% total sample volume) and the sample denatured at 95 °C for 5 min. After loading on the gel, the samples were concentrated in the stacking gel at 60 V. Once the samples

have entered the resolving gel, the voltage was increased to 80 V overnight. Afterwards, samples were transferred onto a membrane.

### **2.2.5.3.2 Immunoprecipitation and N-terminal Edman Sequencing**

To determine the exact signalase cleavage site in 7b protein, immunoprecipitated 7b protein sample was subjected to N-terminal Edman sequencing. To achieve that, rFIPV-7b(1-206/N68S) infected CRFK cells (MOI = 1) from a 10 cm culture dish were lysed with 1 ml RIPA buffer (2.2.5.1). The lysate was pipetted into a reaction tube, incubated at 4 °C for 30 min on a rotary shaker and centrifuged at 13000 rpm, 4 °C for 30 min. Supernatant was incubated with 300 µl anti-7b mAb 14D8 for 1 hour at 4 °C on the rotary shaker. 300 µl of Protein G-Sepharose™ 4 Fast Flow beads was centrifuged at 10000 rpm, 4 °C for 1 min. The supernatant was removed, the beads were washed with 500 µl RIPA buffer and centrifuged twice. Washed beads were added to the lysate-antibody mixture and incubated for 1h at 4 °C on a rotary shaker. Excess protein was removed from the sample by washing 3 times with RIPA buffer. Washed beads were denatured with sample loading buffer (4X) and resolved using SDS-PAGE (2.2.5.3.1).

After electrophoresis, the gel was incubated for 5 min in PVDF cathode transfer buffer. The PVDF membrane was activated in methanol for 2 minutes. The gel and the activated PVDF membrane were prepared for the semi-dry transfer as described in Figure 7. The transfer was performed at 15 V for 60 min using semi-dry transfer system (Bio-Rad).

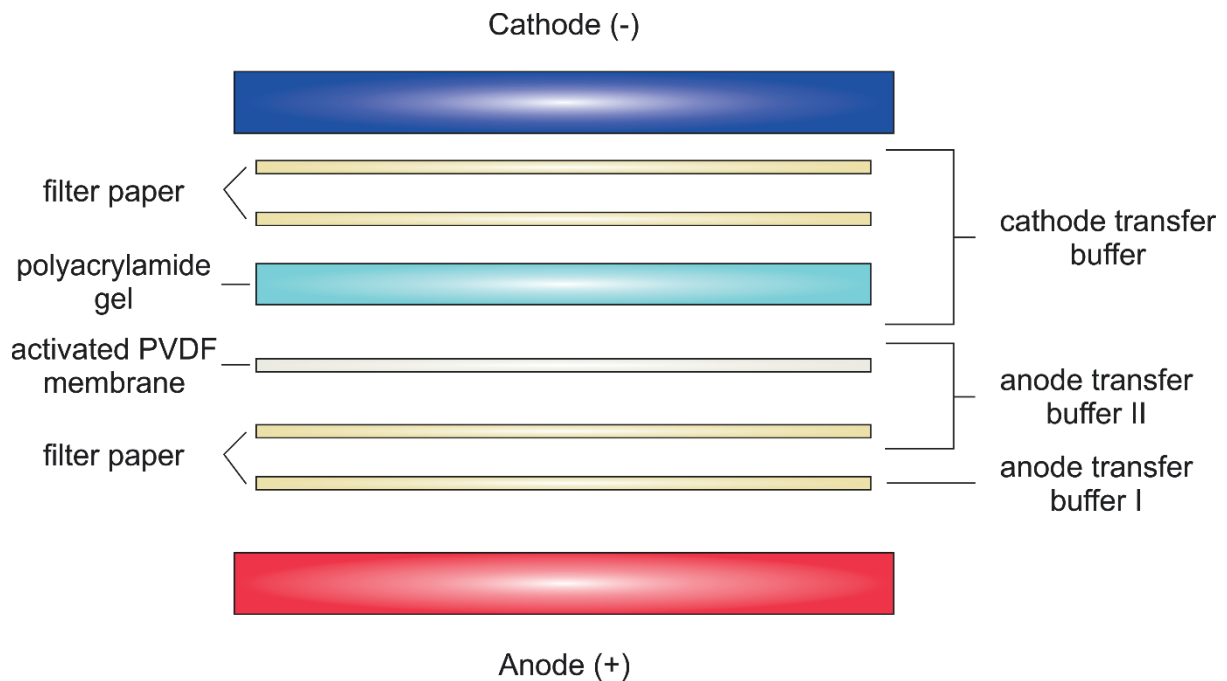


**Figure 7. Schematic representation of a semi-dry transfer sandwich.** Buffers, in which the respective components were equilibrated are listed on the right.

Transferred proteins were visualized on a PVDF membrane using Ponceau S solution (Sigma-Aldrich) and destained with ddH<sub>2</sub>O. The band corresponding to non-glycosylated 7b protein (24 kDa) was excised and subjected to N-terminal Edman sequencing (Protein Analytik, Giessen).

### 2.2.5.3.3 Western Blotting

Western blot was used to detect 7b protein expressed in FIPV-infected cells. To achieve that, cell lysate or cell culture supernatant from FIPV-infected CFRK cells (MOI = 0.1) was mixed with sample loading buffer (4X), denatured and resolved using SDS-PAGE procedure (2.2.5.3.1). Proteins were then transferred onto a nitrocellulose membrane. Samples in the polyacrylamide gel and Whatman filter paper were equilibrated in the Western blot transfer cathode buffer, whereas nitrocellulose membrane and another filter in Western blot transfer anode buffer. For the assembly of the transfer sandwich, first a filter from the anode buffer was placed in the transfer chamber, then membrane, gel and at the end the filter paper from the

cathode buffer. The transfer was performed at 15 V for 60 min using semi-dry transfer system (Bio-Rad).

After transfer, the nitrocellulose membrane was blocked with 5% milk in PBST for 1 hour at room temperature. Following blocking, the membrane was washed twice with PBST for 5 min at RT and incubated with primary antibody diluted in PBST for 1 hour at RT. In order to detect 7b protein, two antibodies were used. Either anti-7b mAb 14D8 diluted 1:35, which recognizes the non-glycosylated form of 7b protein or anti-Flag<sup>®</sup> M2 (Sigma-Aldrich) diluted 1:100000, which detects a flag tag. After incubation with the primary antibody, the membrane was washed three times with PBST and incubated with Goat anti-mouse IgG-PO (1:20000 dilution) for 1 hour at RT. Following washing three times with PBST, the membrane was incubated with Western Lightning Plus-ECL Enhanced Chemiluminescence Substrate (Perkin Elmer) for 2 min at RT. The chemiluminescent signal from bound antibodies was recorded on X-ray films (Advansta).

## **2.2.6 Techniques for Working with Viruses**

### **2.2.6.1 Vaccinia Virus**

#### **2.2.6.1.1 Selection**

To obtain recombinant vaccinia viruses, a *gpt* gene (guanine phosphoribosyltransferase) originating from *E. coli* was applied as a selection marker (Eriksson et al. 2008; Hertzog et al. 2004; Kerr & Smith 1991; Tekes et al. 2008; Tekes et al. 2010; Tekes et al. 2012).

#### **2.2.6.1.2 Positive Selection**

The previously generated recombinant vaccinia virus vrFIPV was used (Tekes et al. 2012) for positive selection. This virus contains the type II FIPV strain 79-1146 full-

length genome as a cDNA. To obtain vrFIPV-GPT- $\Delta$ 7ab, CV-1 cells were infected with vrFIPV and transfected (2.2.1.6.1) with plasmid pGPT-1- $\Delta$ 7ab (2.2.3.5). During vaccinia virus replication recombination takes place between homologous parts of the vaccinia virus and the plasmid. Thus, this event leads to the integration of *gpt* gene into the vaccinia virus genome and loss of a part of the FIPV genome. The site of the recombination is directed by FIPV sequences located downstream and upstream of the *gpt* gene in the plasmid.

CV-1 cells were seeded on a 6-well plate. Next day, the medium was changed to positive selection medium (2.1.8.2). 4-6 hours after replacement of the medium, cells were infected with a virus stock obtained after the infection/transfection (2.2.1.6.1) and incubated in a cell culture incubator for 48 h. 24 h p.i. the medium was replaced with fresh positive selection medium. 48 h p.i. plaques were marked and picked in 150  $\mu$ l of medium. Infected cells harvested this way were first subjected to three cycles of freezing in liquid nitrogen and thawing in an ultrasonic bath, before they were used for infection of new CV-1 cells. After 3-4 rounds of positive selection, DNA of recombinant vaccinia virus was isolated (2.2.3.3.2.1) and analyzed with PCR (2.2.3.1.1).

### **2.2.6.1.3 Negative Selection**

To generate recombinant vaccinia viruses that contain altered forms of FIPV 7b gene, vrFIPV-GPT- $\Delta$ 7ab (2.2.6.1.2) was used for negative selection. CV-1 cells infected with this virus were transfected (2.2.1.6.1) with plasmids pDF1 – pDF9, respectively (2.2.3.5). Double homologous recombination leads to substitution of the *gpt* gene by FIPV sequence in the vaccinia virus genome.

D980R cells were seeded on a 6-well plate and on the next day, the medium was changed to the negative selection medium (2.1.8.2). 4-6 h after replacement of the medium, the cells were infected with the recombinant vaccinia virus and incubated in cell culture incubator for 48 h. 48 h p.i. plaques were harvested in 150  $\mu$ l medium. Following three steps of freezing in liquid nitrogen and thawing in an ultrasonic bath, 10-15  $\mu$ l of the sample was used for the next selection round. After 3-4 rounds,

recombinant vaccinia virus DNA was isolated (2.2.3.3.2.1) and analyzed with PCR (2.2.3.1.1).

#### **2.2.6.1.4 Vaccinia Virus Plaque Purification Assay**

To further purify a recombinant vaccinia virus, plaque purification assay was used. In this approach, recombinant vaccinia virus was used to infect CV-1 cells. 48 h p.i. plaques were harvested in 150 µl medium. After three rounds of freezing in liquid nitrogen and thawing in an ultrasonic bath, infected cells were used to infect fresh CV-1 cells. Following 3 rounds of plaque purification, recombinant vaccinia virus DNA was isolated (2.2.3.3.2.1) and the integrity of FIPV cDNA was analyzed with PCR (2.2.3.1.1). Oligonucleotides used for the PCR are listed in Table 2 (2.1.12.1). Vaccinia virus plaque purification assay was used for all recombinant vaccinia viruses before vaccinia virus DNA was isolated in preparative scale (2.2.3.3.2.2).

### **2.2.6.2 FIPV and Recombinant FIPV**

#### **2.2.6.2.1 Titration of FIPVs**

To estimate the titer of FIPVs, FCWF-4 cells were first seeded on a 24-well plate. Next day, 10X serial dilutions of the virus stock in FCS-free CCM34 medium were prepared. The medium was removed from the cells, cells were washed with FCS-free medium and overlaid with 250 µl of the appropriate virus suspension. After 1 h incubation, 1 ml CCM34 media with 1% carboxymethyl cellulose (CMC) was added to the cells to prevent the spread of virions through the media. After 20 h incubation, the plaques were counted and the titer was estimated using following equation:

$$n \times f \times 4 = PFU/ml$$

$n$  is the number of plaques counted in one well and  $f$  is the dilution factor. The result is given in plaque forming units (PFU) per milliliter.

### **2.2.6.2.2 Growth Kinetics of FIPVs**

To analyze the growth kinetics of FIPVs, FCWF-4 cells were seeded on a 6-well plate and infected with a virus at an MOI of 0.01. The cell culture supernatant was harvested (6, 12, 18 and 24 hours post infection) and titrated (2.2.6.2.1).

## **2.2.7 Generation of Recombinant Viruses**

### **2.2.7.1 Generation of Recombinant Vaccinia Viruses**

To generate recombinant vaccinia viruses, vrFIPV was used in positive selection (2.2.6.1.2) with plasmid pGPT-1- $\Delta$ 7ab (2.2.3.5). The resulting vrFIPV-GPT- $\Delta$ 7ab was first analyzed with PCR (2.2.3.1.1) and plaque purified (2.2.6.1.4). After confirming the FIPV cDNA integrity, vrFIPV-GPT- $\Delta$ 7ab was used for negative selection (2.2.6.1.3) with plasmids pDF1 – pDF9, respectively. The obtained recombinant vaccinia viruses were plaque purified and characterized with PCR. DNA of generated viruses was isolated in preparative scale (2.2.3.3.2.2), digested with *Clal* enzyme and used for *in vitro* transcription (2.2.4.3) to recover recombinant FIPVs (2.2.7.2.1).

### **2.2.7.2 Generation of Recombinant FIPVs**

#### **2.2.7.2.1 Recovery of Recombinant FIPVs**

To recover recombinant FIPVs, *in vitro*-transcribed RNA (2.2.4.3) was electroporated into BHK-FIPV-N cells that were co-cultured with FCWF-4 cells (2.2.1.6.2). After 2 days incubation, the co-culture was harvested and centrifuged at 1500 rpm, 4 °C for 4 min. 2 ml of the supernatant were used to infect fresh FCWF-4 cells on a 10 cm dish. The rest of the co-culture supernatant was stored at -80 °C. Infected FCWF-4 cells were harvested and used for RNA isolation (2.2.4.1) and RT-PCR (2.2.4.2) to confirm the sequence of the recombinant virus. Supernatant was aliquoted, stored at -80 °C and used to determine the virus titer (2.2.6.2.1). Recombinant FIPVs (rFIPVs)

were used to infect cells for indirect immunofluorescence assay (2.2.1.5), immunoprecipitation and N-terminal Edman sequencing (2.2.5.3.2) and Western blot (2.2.5.3.3).

### **2.2.7.2.2 Plasmids, Recombinant Vaccinia Viruses and Recombinant FIPVs**

#### **(a)**

Name of the vaccinia clone used: vrFIPV  
Name of the plasmid: pGPT-1- $\Delta$ 7ab  
Name of the generated vaccinia virus: vrFIPV-GPT- $\Delta$ 7ab

vrFIPV-GPT- $\Delta$ 7ab contains type II FIPV strain 79-1146 cDNA, where 7ab gene was substituted with the *gpt* gene. This recombinant vaccinia virus was used to generate all below mentioned recombinant viruses.

#### **(b)**

Name of the plasmid: pDF1  
Name of the generated vaccinia virus: vrFIPV-7b(1-206/N68S)  
Name of the generated rFIPV: rFIPV-7b(1-206/N68S)

In rFIPV-7b(1-206/N68S) nt 28663 to 28665 were changed from AAT to TCA which leads to substitution of asparagine with serine in 7b protein at aa position 68.

#### **(c)**

Name of the plasmid: pDF2  
Name of the generated vaccinia virus: vrFIPV-flag-7b(1-206)  
Name of the generated rFIPV: rFIPV-flag-7b(1-206)

In rFIPV-flag-7b(1-206) an additional flag tag sequence preceding 7b gene (downstream of nt 28464) was inserted.

**(d)**

Name of the plasmid: pDF3  
Name of the generated vaccinia virus: vrFIPV-7b(1-17/flag/18-206)  
Name of the generated rFIPV: rFIPV-7b(1-17/flag/18-206)

rFIPV-7b(1-17/flag/18-206) contains an additional flag tag sequence introduced downstream of nt 28512, which corresponds to aa position 17 of 7b protein.

**(e)**

Name of the plasmid: pDF4  
Name of the generated vaccinia virus: vrFIPV-7b(1-206)-flag  
Name of the generated rFIPV: rFIPV-7b(1-206)-flag

In rFIPV-7b(1-206)-flag an additional flag tag sequence was inserted downstream of nt 29079 that corresponds to the C-terminal end of 7b protein.

**(f)**

Name of the plasmid: pDF5  
Name of the generated vaccinia virus: vrFIPV-7b(1-17/flag/18-206/N68S)  
Name of the generated rFIPV: rFIPV-7b(1-17/flag/18-206/N68S)

rFIPV-7b(1-17/flag/18-206/N68S) contains a flag tag sequence downstream of nt 28512 that corresponds to aa 17 of 7b protein. Additionally, nt 28663 to 28665 were changed from AAT to TCA which leads to substitution of asparagine with serine in 7b protein at aa position 68.

**(g)**

Name of the plasmid: pDF6  
Name of the generated vaccinia virus: vrFIPV-7b(1-17/flag/18-202/KTEV)  
Name of the generated rFIPV: rFIPV-7b(1-17/flag/18-202/KTEV)

In rFIPV-7b(1-17/flag/18-202/KTEV) an additional flag tag sequence was inserted downstream of nt 28512 that corresponds to aa 17 of 7b protein. Moreover, nt 29077

to 29079 were altered from TTA to GTT, substituting leucine with valine in 7b protein at aa position 206.

**(h)**

Name of the plasmid: pDF7  
Name of the generated vaccinia virus: vrFIPV-7b(1-17/flag/18-202/KTE)  
Name of the generated rFIPV: rFIPV-7b(1-17/flag/18-202/KTE)

rFIPV-7b(1-17/flag/18-202/KTE) contains a flag tag sequence downstream of nt 28512 that corresponds to aa 17 of 7b protein and a deletion of nt 29077 to 29079, resulting in removal of aa 206 in 7b protein

**(i)**

Name of the plasmid: pDF8  
Name of the generated vaccinia virus: vrFIPV-7b(1-17/flag/18-202/KDEL)  
Name of the generated rFIPV: rFIPV-7b(1-17/flag/18-202/KDEL)

InrFIPV-7b(1-17/flag/18-202/KDEL) a flag tag was inserted downstream of nt 28512 corresponding to aa 17 of 7b protein. Additionally, nt 29071 to 29073 were altered from ACT to GAT to substitute threonine with aspartic acid in 7b protein at aa position 204.

**(j)**

Name of the plasmid: pDF9  
Name of the generated vaccinia virus: vrFIPV-7b(1-17/flag/18-202/AAAA)  
Name of the generated rFIPV: rFIPV-7b(1-17/flag/18-202/AAAA)

rFIPV-7b(1-17/flag/18-202/AAAA) contains a flag tag downstream of nt 28512 that corresponds to aa 17 of 7b protein. Furthermore, nt 29068 to 29079 were changed to GCAGCTGCTGCA to replace the C-terminal KTEL sequence (aa 203-206) of 7b protein with 4 alanine residues (AAAA).

### 3 Results

#### 3.1 Generation of Recombinant FIPV Expressing the Non-glycosylated 7b Protein

In order to study expression and localization of serotype II FIPV strain 79-1146 7b protein in infected feline cells, monoclonal antibodies (mAbs) against 7b protein were previously generated at the Institute of Virology, JLU, Giessen (Lemmermeyer et al. 2016). Detailed characterization of the mAbs revealed that they recognized only the non-glycosylated precursor of 7b protein. Since 7b represents a glycoprotein (Fig. 8), certain aspects, like expression, subcellular localization or secretion of the authentic protein, could not be studied using these antibodies. To overcome this limitation, a recombinant FIPV expressing the non-glycosylated form of 7b protein was generated.

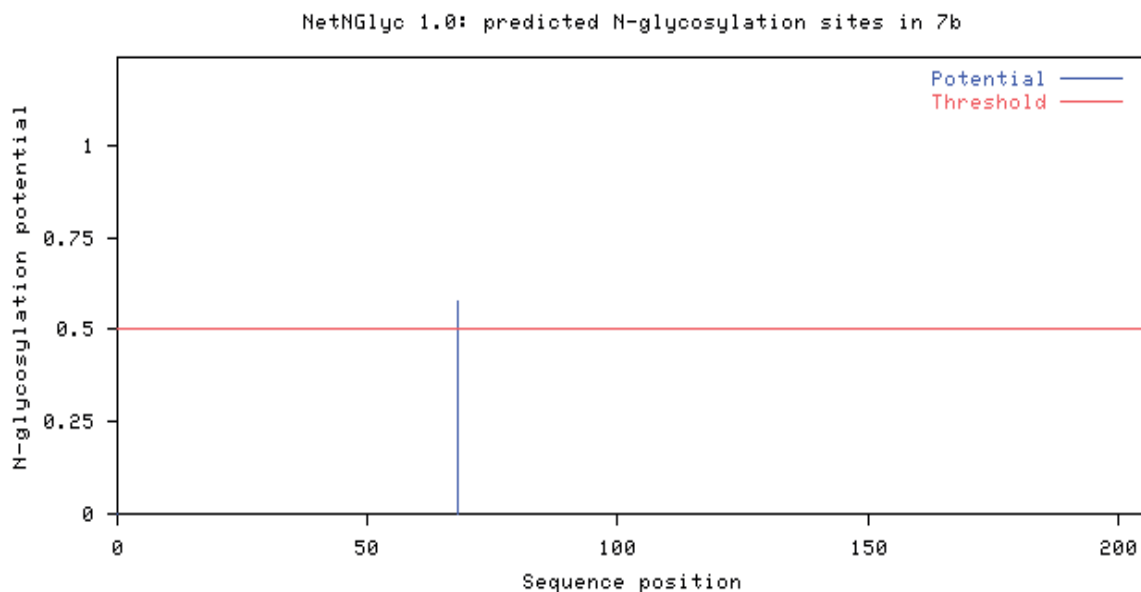


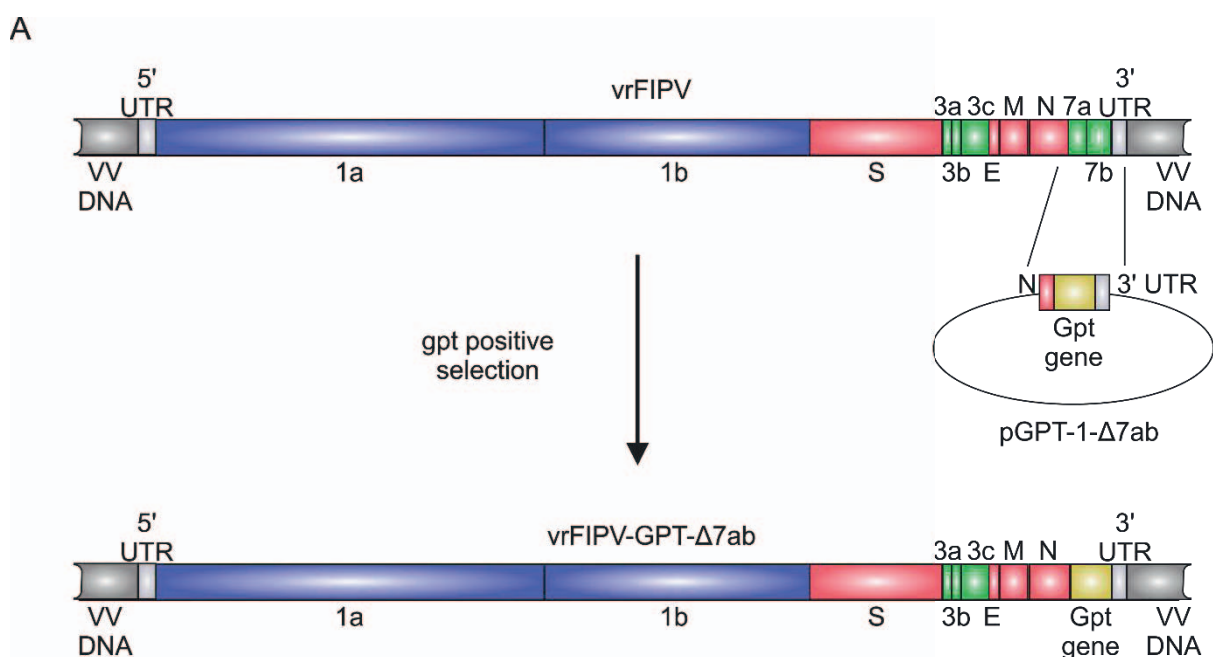
**Figure 8. Prediction of N-linked glycosylation site based on amino acid sequence of 7b protein.** NetNGlyc 1.0 online analyzer predicted one N-glycosylation site at amino acid position 68 in 7b protein.

Comparison of available 7b protein sequences revealed that some FCoV field isolates contain serine instead of asparagine at amino acid position 68 in 7b protein. To enable the detection of non-glycosylated 7b protein in FIPV-infected cells by the

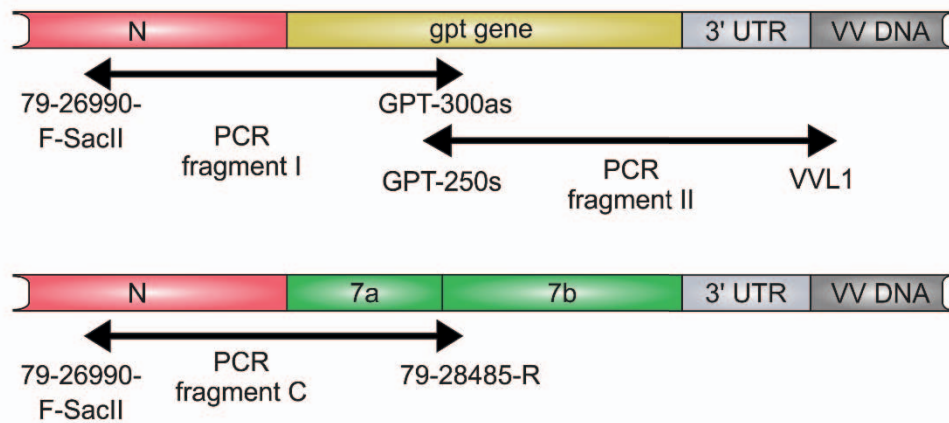
mAbs, a recombinant virus that expresses 7b protein without the only glycosylation site was generated using vaccinia virus-based reverse genetic system (see below).

### 3.1.2 Generation of Recombinant Vaccinia Virus vrFIPV-GPT- $\Delta$ 7ab

To allow the modification of 7b gene, recombinant vaccinia virus vrFIPV-GPT- $\Delta$ 7ab was generated. For this purpose, a recombinant vaccinia virus containing the type II FIPV strain 79-1146 full-length genome as cDNA (vrFIPV) (Tekes et al. 2012) was used to infect CV-1 cells. Infected cells were then transfected with plasmid pGPT-1- $\Delta$ 7ab (2.2.3.5 and 2.2.1.6.1). During incubation, vaccinia virus-mediated homologous recombination takes place between the vaccinia virus- and the plasmid-DNA leading to the replacement of part of the FIPV sequence by the guanine phosphoribosyltransferase (*gpt*) gene that served as a selection marker. In order to investigate the proper integration of the *gpt*-gene into the vrFIPV genome after *gpt* positive selection (2.2.6.1.2) (Fig. 9A), vrFIPV-GPT- $\Delta$ 7ab DNA was isolated from infected CV-1 cells (2.2.3.3.2.1). The recombination sites were amplified with PCR (2.2.3.1.1) (Fig. 9B and C). PCR fragment C was used as a control to show that the obtained recombinant vaccinia virus was not contaminated with the parental vrFIPV.



B



C

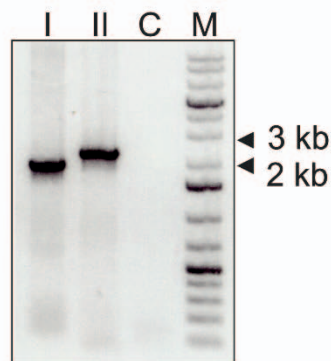


**Figure 9. Generation and analysis of recombinant vaccinia virus vrFIPV-GPT- $\Delta$ 7ab.** (A) Schematic representation of the positive selection of vrFIPV-GPT- $\Delta$ 7ab. (B) Positions of the PCR fragments as well as applied primers are presented. (C) PCR analysis of vrFIPV-GPT- $\Delta$ 7ab recombinant vaccinia virus DNA. PCR products were resolved in ethidium bromide-stained 1% agarose gel. The size of selected marker bands is shown on the right. I, PCR fragment I; II, PCR fragment II; C, PCR fragment C; M, DNA marker.

After sequence analysis of the recombination sites, vrFIPV-GPT- $\Delta$ 7ab was plaque purified (2.2.6.1.4). Furthermore, the entire FIPV genome was amplified by 12 PCR products to demonstrate its integrity (Fig. 10). The characterized vrFIPV-GPT- $\Delta$ 7ab served as a starting material for negative selection to generate all viruses used in this thesis expressing altered forms of 7b protein (see below).

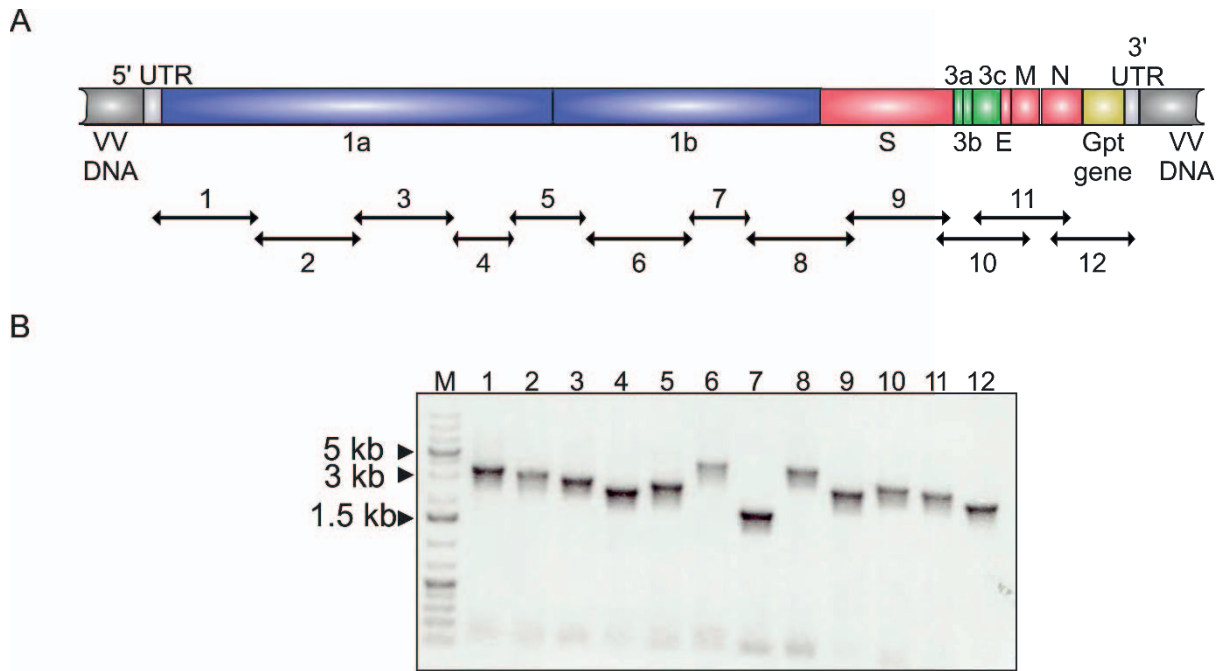


**Figure 10. Amplification of the FIPV genome in recombinant vaccinia virus vrFIPV-GPT- $\Delta$ 7ab.** (A) Schematic representation of the FIPV cDNA inserted into vrFIPV-GPT- $\Delta$ 7ab genome. Positions of 12 PCR fragments (1-12) are shown. Primer pairs used for the PCR products are listed in Table 2 (2.1.12.1). (B) PCR products were resolved in ethidium bromide-stained 1% agarose gel. The size of selected marker bands is shown on the left. M, DNA marker.

### 3.1.3 Generation of vrFIPV-7b(1-206/N68S)

In order to introduce serine instead of asparagine at amino acid position 68 in 7b protein, CV-1 cells were infected with vrFIPV-GPT- $\Delta$ 7ab and transfected with pDF1 plasmid (2.2.3.5 and 2.2.1.6.1). During incubation, vaccinia virus-mediated homologous recombination takes place between the vaccinia virus- and the plasmid-DNA that leads to the replacement of *gpt* gene by the desired FIPV sequence. After selection of *gpt*-negative recombinant vaccinia virus (2.2.6.1.3), viral DNA was isolated and analyzed with PCR (Fig. 11) (2.2.7.1). The integration of the altered FIPV sequence was confirmed by amplification and sequencing of the recombination sites (Fig. 11B and C). PCR fragment G was used as a control to show that the obtained recombinant vaccinia virus was not contaminated with the parental vrFIPV-GPT- $\Delta$ 7ab.

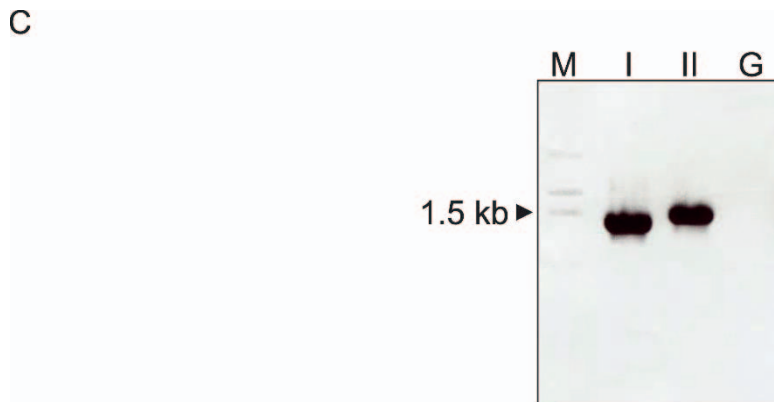
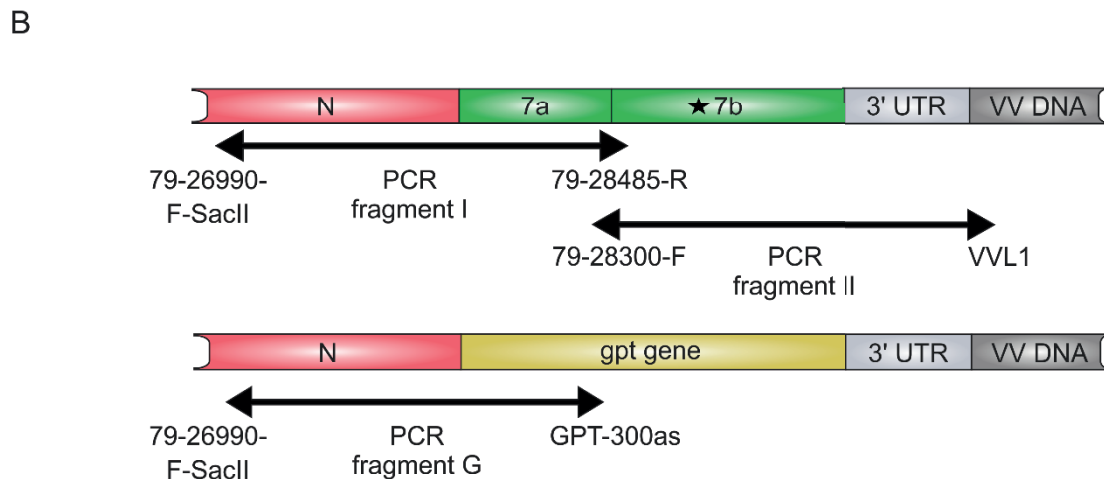
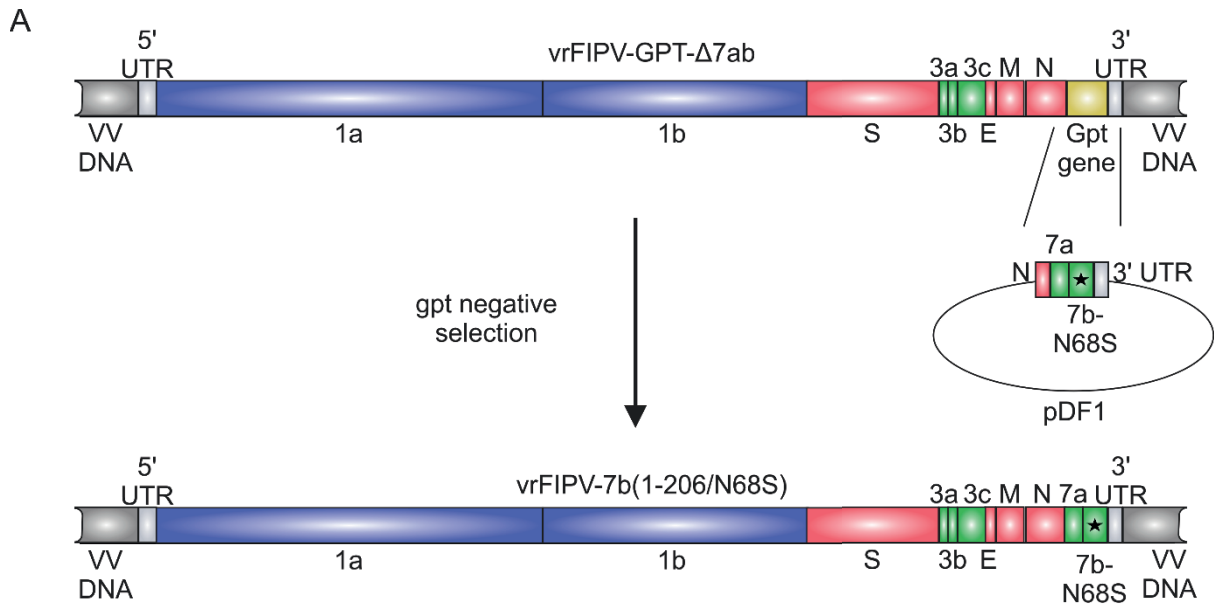


**Figure 11. Generation and analysis of recombinant vaccinia virus vrFIPV-7b(1-206/N68S).** (A) Schematic representation of the negative selection of vrFIPV-7b(1-206/N68S). (B) Positions of the PCR fragments, as well as applied primers are presented. (C) PCR analysis of vrFIPV-7b(1-206/N68S) recombinant vaccinia virus DNA. PCR products were resolved in ethidium bromide-stained 1% agarose gel. The size of selected marker band is shown on the left. I, PCR fragment I; II, PCR

fragment II; G, PCR fragment G; M, DNA marker. Asterisk indicates the substitution of asparagine with serine at amino acid position 68 (N68S) of 7b protein.

Following sequence analysis of the recombination sites, vrFIPV-7b(1-206/N68S) was plaque purified and the integrity of FIPV cDNA was analyzed with PCR (Fig.12), as described previously in Figure 10.

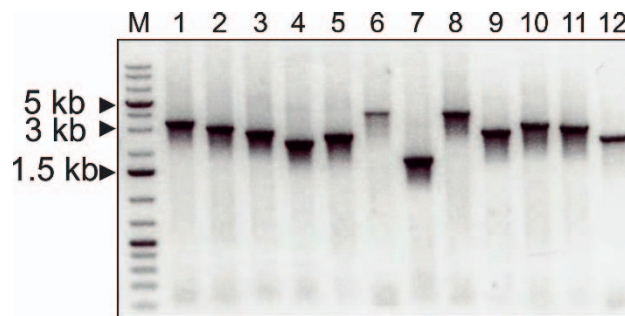


**Figure 12. Amplification of the FIPV genome in recombinant vaccinia virus vrFIPV-7b(1-206/N68S) DNA.** 12 PCR products (1-12) containing the full-length FIPV cDNA were resolved in ethidium bromide-stained 1% agarose gel. The size of selected marker bands is shown on the left. M, DNA marker.

### 3.1.4 Recovery of rFIPV-7b(1-206/N68S)

For the recovery of rFIPV-7b(1-206/N68S), the DNA of the recombinant vaccinia virus vrFIPV-7b(1-206/N68S) was isolated in preparative scale (2.2.3.3.2.2) and analyzed with agarose gel electrophoresis (Fig. 13A).

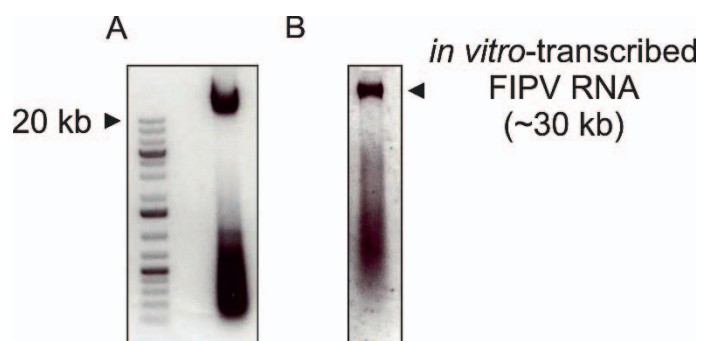
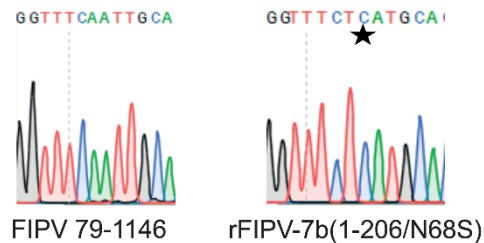


**Figure 13. Analysis of the vrFIPV-7b(1-206/N68S) DNA and the transcribed RNA. (A)** 2 µl of vrFIPV-7b(1-206/N68S) DNA was loaded on 1% agarose gel to control its quality. The size of selected marker band is shown on the left. **(B)** 2 µl of the *in vitro*-transcribed RNA (rFIPV-7b(1-206/N68S)) was resolved on 1.3% agarose gel to control its quality.

The DNA was then used as a template for *in vitro* transcription (2.2.4.3). The quality of the obtained RNA was also assessed using gel electrophoresis (Fig. 13B). Next, rFIPV-7b(1-206/N68S) RNA was electroporated (EP) (2.2.1.6.2) into BHK-FIPV-N cells. In these cells, the electroporated RNA initiates the viral replication cycle that leads to the release of infectious virions. Expression of FIPV nucleocapsid protein in BHK-FIPV-N cells facilitates the replication of the recombinant FIPVs. Since BHK-FIPV-N cells do not express receptors for FIPV, these cells cannot be infected with newly released virions. Therefore, the BHK-FIPV-N cells were co-cultured with susceptible feline cells (FCWF-4) (2.2.7.2.1). 48 hours post EP, the cell culture supernatant was harvested and centrifuged to remove cell debris. Subsequently, the supernatant was used to infect fresh FCWF-4 cells. After 24-48 h incubation, the supernatant containing rFIPV-7b(1-206/N68S) was harvested, stored at -80 °C and used for further experiments. The infected cells were used for PCR analyses. After sequencing of the PCR-products, asparagine to serine exchange at aa position 68 in 7b could be verified (Fig. 14A). The supernatant was used to determine the growth kinetics of rFIPV-7b(1-206/N68S). The analysis revealed that the growth kinetics of rFIPV-7b(1-206/N68S) were identical to those of the type II FIPV strain 79-1146 (Fig. 14B).

A



B

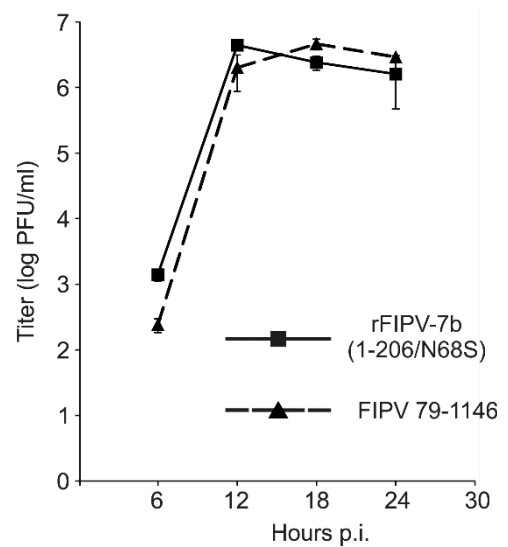


**Figure 14. Characterization of rFIPV-7b(1-206/N68S).** (A) Sequence analyses of type II FIPV strain 79-1146 and rFIPV-7b(1-206/N68S). Asterisk indicates the exchange of AAT (asparagine) to TCA (serine) at position corresponding to amino acid 68 in 7b protein. (B) Growth kinetics of rFIPV-7b(1-206/N68S) compared to type II FIPV strain 79-1146; p.i., post infection.

### 3.1.5 Characterization of the Non-glycosylated Form of 7b Protein Using rFIPV-7b(1-206/N68S)

rFIPV-7b(1-206/N68S) was used to determine the subcellular localization of the non-glycosylated form of 7b protein (Fig. 15A) in infected CRFK cells. Following infection, cells and cell culture supernatant were harvested 16 hours post infection, before cytopathic effect (CPE) developed. This time point was chosen to avoid detection of 7b protein in the supernatant caused by the lysis of infected cells. The samples were analyzed with Western Blot using anti-7b mAb 14D8 (2.2.5.3.3) (Fig. 15B). The experiment showed that 7b protein was present only in the cell lysate but not in the cell culture supernatant. Accordingly, the non-glycosylated 7b protein was probably not secreted. To determine the subcellular localization of the non-glycosylated 7b protein, rFIPV-7b(1-206/N68S)-infected CRFK cells were analyzed with indirect immunofluorescence assay using confocal microscopy with anti-7b mAb (2.2.1.5). The experiment demonstrated that 7b protein co-localized exclusively with the Golgi

apparatus (Fig.15C). These results contradict observations by Vennema et al. (1992); they described 7b protein as an endoplasmic reticulum (ER)-resident protein that is secreted from the cell.

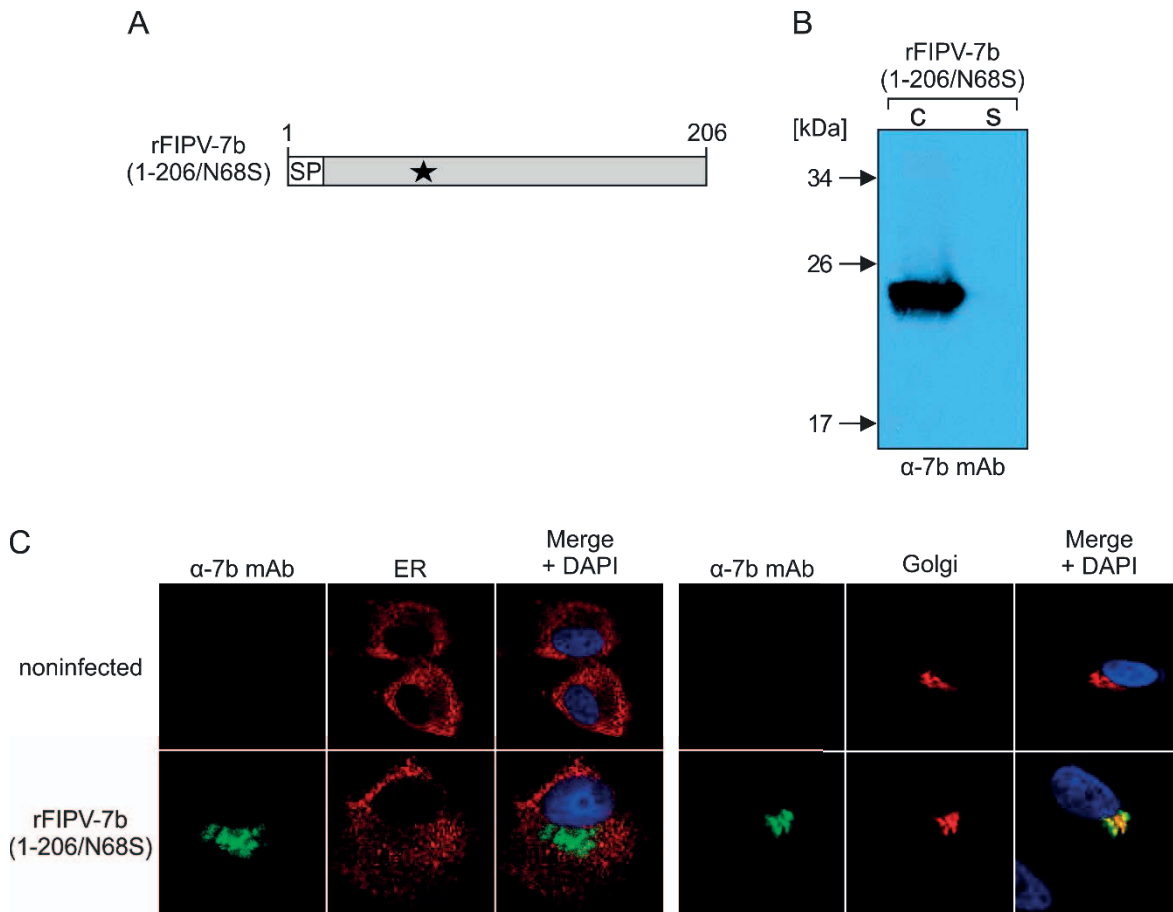


**Figure 15. 7b protein detection in FIPV-infected cells using anti-7b monoclonal antibody 14D8 (α-7b mAb).** (A) Schematic representation of 7b protein encoded by rFIPV-7b(1-206/N68S). Asterisk indicates the substitution of asparagine with serine at amino acid position 68 (N68S). SP, signal peptide; numbers indicate the amino acid positions of 7b protein. (B) rFIPV-7b(1-206/N68S) infected CRFK cells (MOI = 0.1) were harvested 16 h post infection. Cell lysate (c) and cell culture supernatant (s) were resolved in a 10% polyacrylamide gel under reducing conditions and analyzed by Western Blot with anti-7b mAb 14D8. (C) rFIPV-7b(1-206/N68S)-infected (MOI = 1) and non-infected CRFK cells were fixed 16 h p.i. and stained for immunofluorescence analysis. 7b protein was visualized using anti-7b mAb 14D8. Immunofluorescence staining of cell structures: endoplasmic reticulum (ER) (left panel) and Golgi apparatus (right panel) is demonstrated. Cell nuclei were stained blue using DAPI. Immunofluorescence staining was visualized with confocal laser scanning microscope (adapted from Florek et al., 2017).

## **3.2 FIPVs with Flag-tagged Forms of 7b Protein**

To investigate whether the observed differences with the results of Vennema and colleagues (1992) are related to the absence of glycosylation in 7b protein, a different approach was taken to study the mature, glycosylated form of 7b protein. For this, a set of recombinant FIPVs expressing flag-tagged forms of 7b protein was constructed using the above described vaccinia virus-based reverse genetic system.

### **3.2.2 Generation of rFIPV-flag-7b(1-206)**

In order to obtain recombinant vaccinia virus vrFIPV-flag-7b(1-206) where flag tag is fused to the N-terminus of 7b, CV-1 cells were infected with vrFIPV-GPT- $\Delta$ 7ab and transfected with pDF2 plasmid (2.2.7.1) as shown in Figure 11. After selection of gpt-negative recombinant vaccinia viruses, viral DNA was isolated and analyzed with PCR (Fig. 16).

After sequence analysis of the recombination sites, vrFIPV-flag-7b(1-206) was plaque purified and the integrity of the viral genome was assessed with PCR as described in Figure 10.

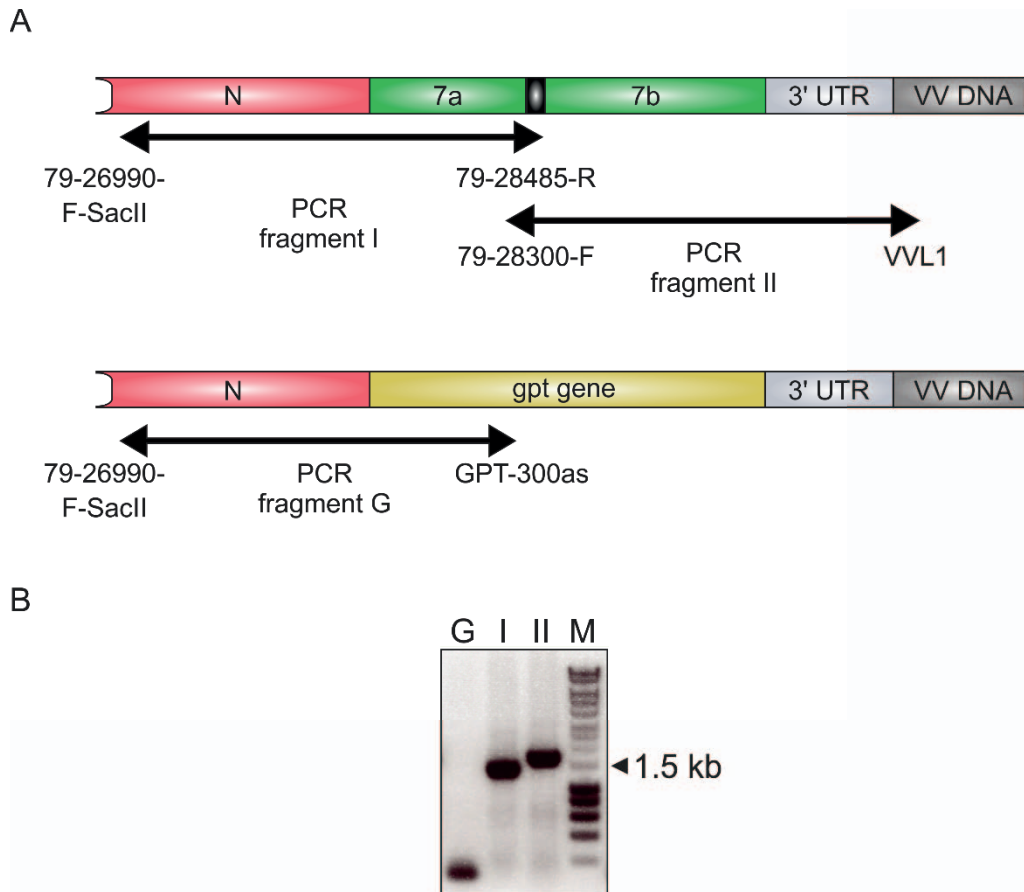


**Figure 16. Analysis of recombinant vaccinia virus vrFIPV-flag-7b(1-206).** (A) Positions of the PCR fragments, as well as applied primers are presented. Black box represents the flag tag in 7b gene. (B) PCR analysis of vrFIPV-flag-7b(1-206) recombinant vaccinia virus DNA. PCR products were resolved in ethidium bromide-stained 1% agarose gel. The size of selected marker band is shown on the right. I, PCR fragment I; II, PCR fragment II; G, PCR fragment G; M, DNA marker.

For the recovery of rFIPV-flag-7b(1-206), the DNA of the recombinant vaccinia virus vrFIPV-flag-7b(1-206) was isolated in preparative scale (2.2.3.3.2.2) and analyzed with agarose gel electrophoresis as shown in Figure 13. The DNA was then used as a template for *in vitro* transcription (2.2.4.3). In the next step, rFIPV-flag-7b(1-206) RNA was electroporated (EP) (2.2.1.6.2) into BHK-FIPV-N cells and co-cultured with FCWF-4 cells (2.2.7.2.1). 48 hours post EP, the cell culture supernatant was harvested and centrifuged to remove cell debris. Subsequently, the supernatant was used to infect fresh FCWF-4 cells. After 24-48 h incubation, the supernatant containing rFIPV-flag-7b(1-206) was harvested, stored at -80 °C and used for further experiments. The infected cells were used for PCR analyses. After sequencing of the PCR-products, insertion of the flag tag at the N-terminus of 7b was verified

(Fig.17A). Growth kinetics of rFIPV-flag-7b(1-206) were identical to those of the type II FIPV strain 79-1146 (Fig. 17B).

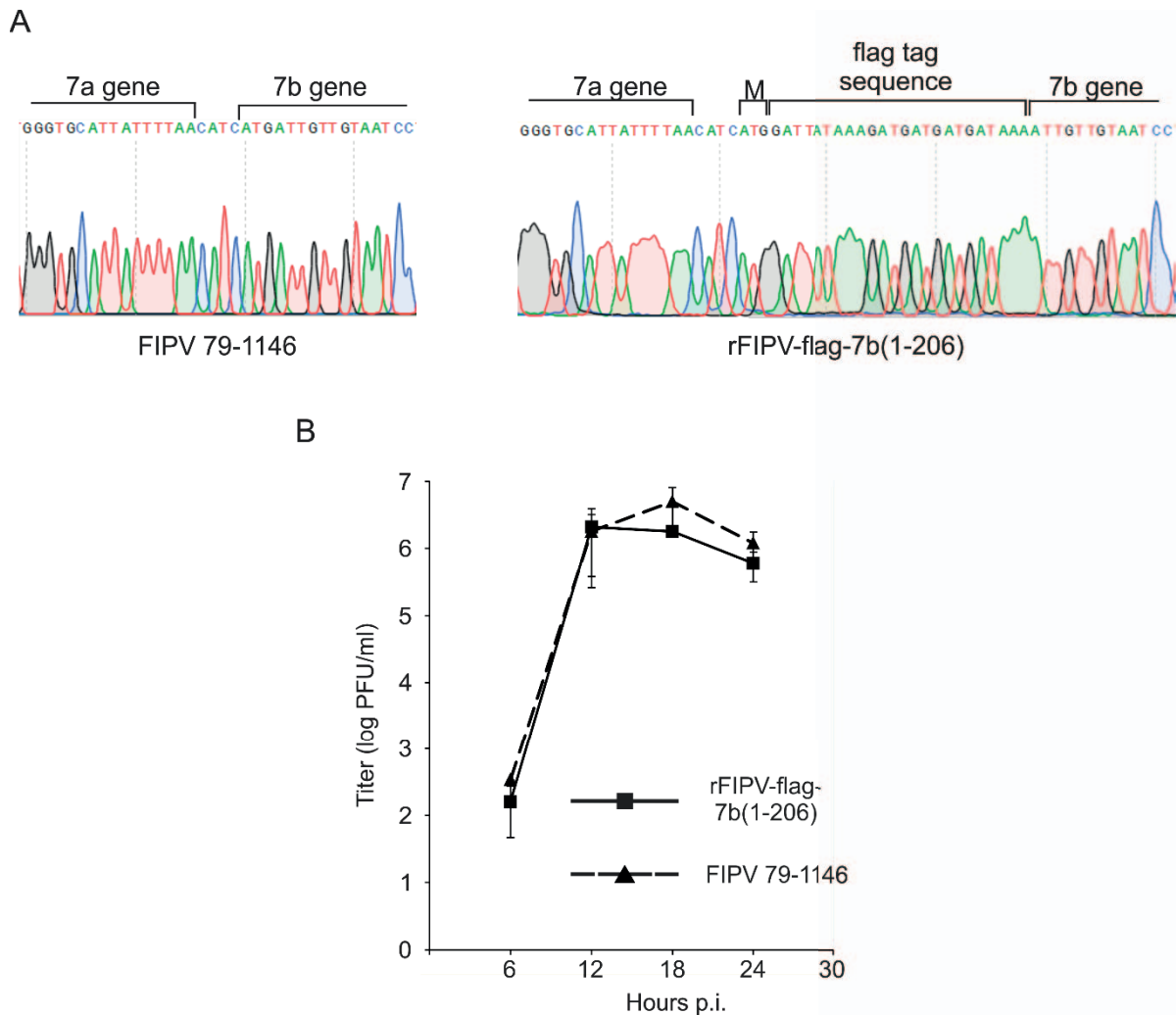


**Figure 17. Characterization of rFIPV-flag-7b(1-206).** (A) Sequence analyses of type II FIPV strain 79-1146 and rFIPV-flag-7b(1-206). Flag tag sequence preceding 7b gene is shown. M, methionine. (B) Growth kinetics of rFIPV-flag-7b(1-206) compared to type II FIPV strain 79-1146;p.i., post infection.

### 3.2.3 Detection of 7b Protein after Infection with rFIPV-flag-7b(1-206).

To investigate the expression and localization of the mature, glycosylated form of 7b protein in FIPV-infected cells, rFIPV-flag-7b(1-206) was used (Fig. 18A). CRFK cells

were infected with this virus and before CPE developed, cells and cell culture supernatant were harvested and analyzed with Western Blot (Fig. 18B).

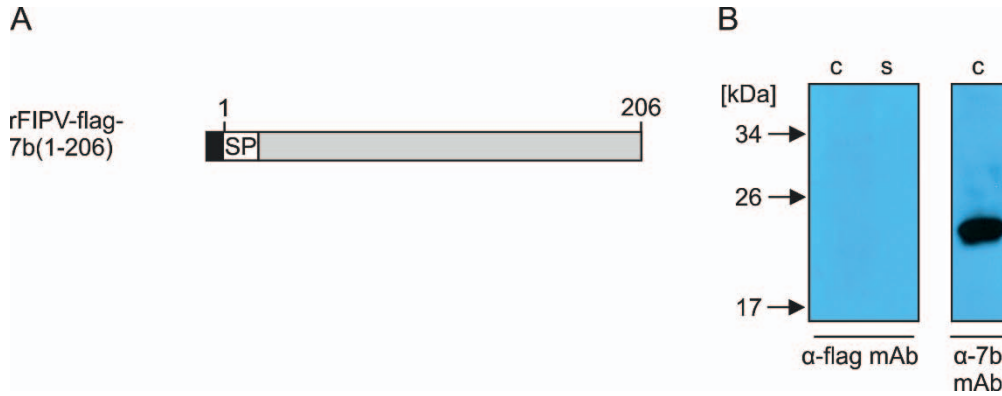


**Figure 18. Western blot analysis of N-terminal flag-tagged 7b protein in rFIPV-flag-7b(1-206)-infected CRFK cells. (A)** Schematic representation of 7b protein encoded by rFIPV-flag-7b(1-206). Black box represents the flag tag at the N-terminus of 7b protein. SP, predicted signal peptide; numbers indicate the amino acid positions in 7b protein. **(B)** CRFK cells infected with rFIPV-flag-7b(1-206) were harvested 16 h post infection. Cell lysate (c) and cell culture supernatant (s) were analyzed by Western Blot with anti-Flag<sup>®</sup> M2 ( $\alpha$ -flag mAb) or anti-7b mAb 14D8 ( $\alpha$ -7b mAb).

Using anti-flag mAb, 7b could not be detected in the cell lysate as well as in the cell culture supernatant. Only the non-glycosylated form of 7b protein (ca. 24 kDa) was detected in the cell lysate with anti-7b mAb 14D8. This result suggests that the flag tag together with the predicted N-terminal signal peptide were cleaved off by the signalase.

### 3.2.4 Signalase Cleavage Site in 7b Protein

Since the predicted signal peptide of 7b protein is obviously removed during synthesis into the ER, the flag tag had to be introduced at a different position. To enable the introduction of the flag tag downstream of the signal peptide, the exact cleavage site of the signalase was determined. 7b protein sequence was subjected to SignalP 4.1 online analyzer (Petersen et al. 2011) that predicted two potential signalase cleavage site between amino acids 17-18 and 19-20 (13-GIKA<sup>↓</sup>TA<sup>↓</sup>VQND-24) (Fig. 19).

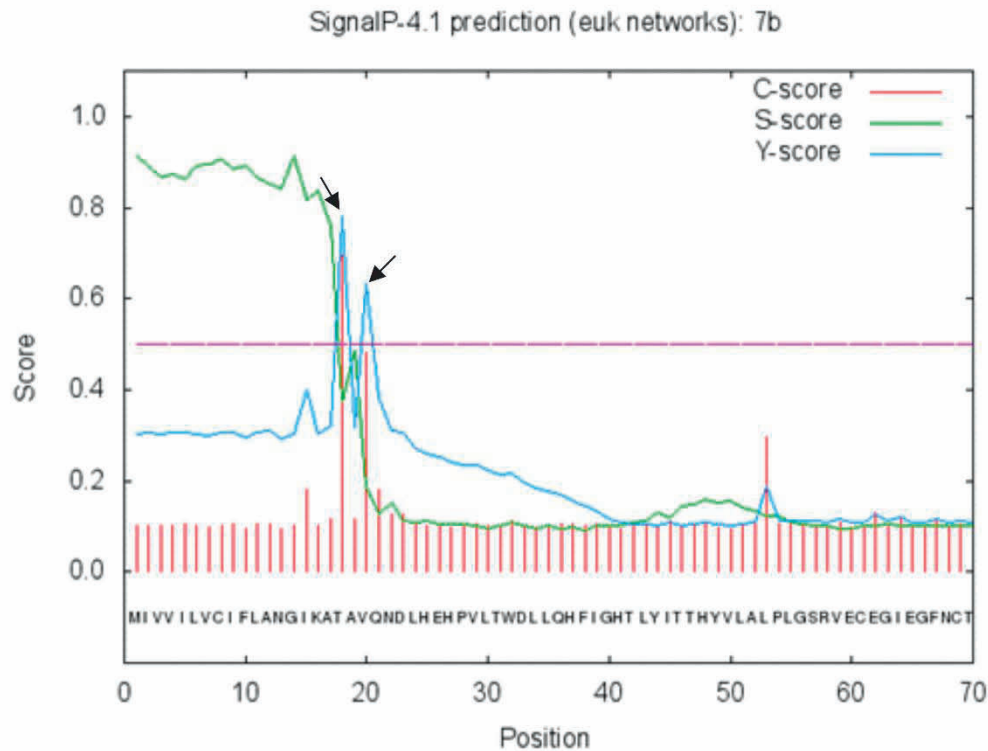


**Figure 19. Signal peptide prediction for FCoV 7b protein.** Two possible signalase cleavage sites in 7b protein are indicated by arrows. C-score demonstrates the score for signal peptide cleavage sites; S-score distinguishes amino acid positions within signal peptides from positions in the mature protein; Y-score is a combination of the C-score and the slope of the S-score and serves for better cleavage site prediction.

To experimentally determine which of the two predicted cleavage sites is used by the signalase, CRFK cells were infected with rFIPV-7b(1-206/N68S). Cells were harvested 24 hours post infection, lysed and 7b protein was immunoprecipitated with anti-7b mAb 14D8. The sample was resolved with SDS-PAGE and transferred to a PVDF membrane. Proteins on the membrane were visualized with Ponceau staining (2.2.5.3.2). The band corresponding to the non-glycosylated form of 7b protein was excised from the membrane and subjected to N-terminal Edman sequencing. It could be shown that the signalase cleavage occurred between amino acids 17 and 18. The result of the N-terminal protein sequencing is demonstrated in Table 10.

N-terminal sequence determined by Edman sequencing		Corresponding 7b protein sequence	
1	T	18	T
2	A	19	A
3	V	20	V
4	Q	21	Q
5	N	22	N
6	D	23	D
7	L	24	L
		25	H
		26	E
		27	H

**Table 10. N-terminal Edman sequencing of 7b protein.** Numbers indicate the amino acid positions in 7b protein.

### **3.2.5 Generation of rFIPV-7b(1-17/flag/18-206) and rFIPV-7b(1-17/flag/18-206/N68S).**

To detect 7b protein in infected cells with anti-flag mAb, a flag tag was introduced downstream of the determined signalase cleavage site (amino acid 17) in 7b using vaccinia virus-based reverse genetic system (rFIPV-7b(1-17/flag/18-206)). Moreover, a recombinant virus identical to rFIPV-7b(1-17/flag/18-206), but in addition with a mutation leading to substitution of asparagine with serine at amino acid position 68 (N68S) of 7b was generated (rFIPV-7b(1-17/flag/18-206/N68S)). This mutation was included to abolish N-linked glycosylation in flag-tagged 7b protein enabling the direct comparison of expression and localization of the glycosylated versus non-glycosylated forms of 7b protein in FIPV-infected cells.

For this purpose, recombinant vaccinia viruses vrFIPV-7b(1-17/flag/18-206) and vrFIPV-7b(1-17/flag/18-206/N68S) were generated. CV-1 cells were infected with vrFIPV-GPT- $\Delta$ 7ab and transfected with pDF3 and pDF5 plasmids, respectively similar as shown in Figure 11. After selection of gpt-negative recombinant vaccinia viruses, viral DNA was isolated and analyzed with PCR (Fig. 20). After sequence analysis of the recombination sites, vrFIPV-7b(1-17/flag/18-206) and vrFIPV-7b(1-17/flag/18-206/N68S) were plaque purified and the integrity of the viral genome was assessed with PCR as described in Figure 10.

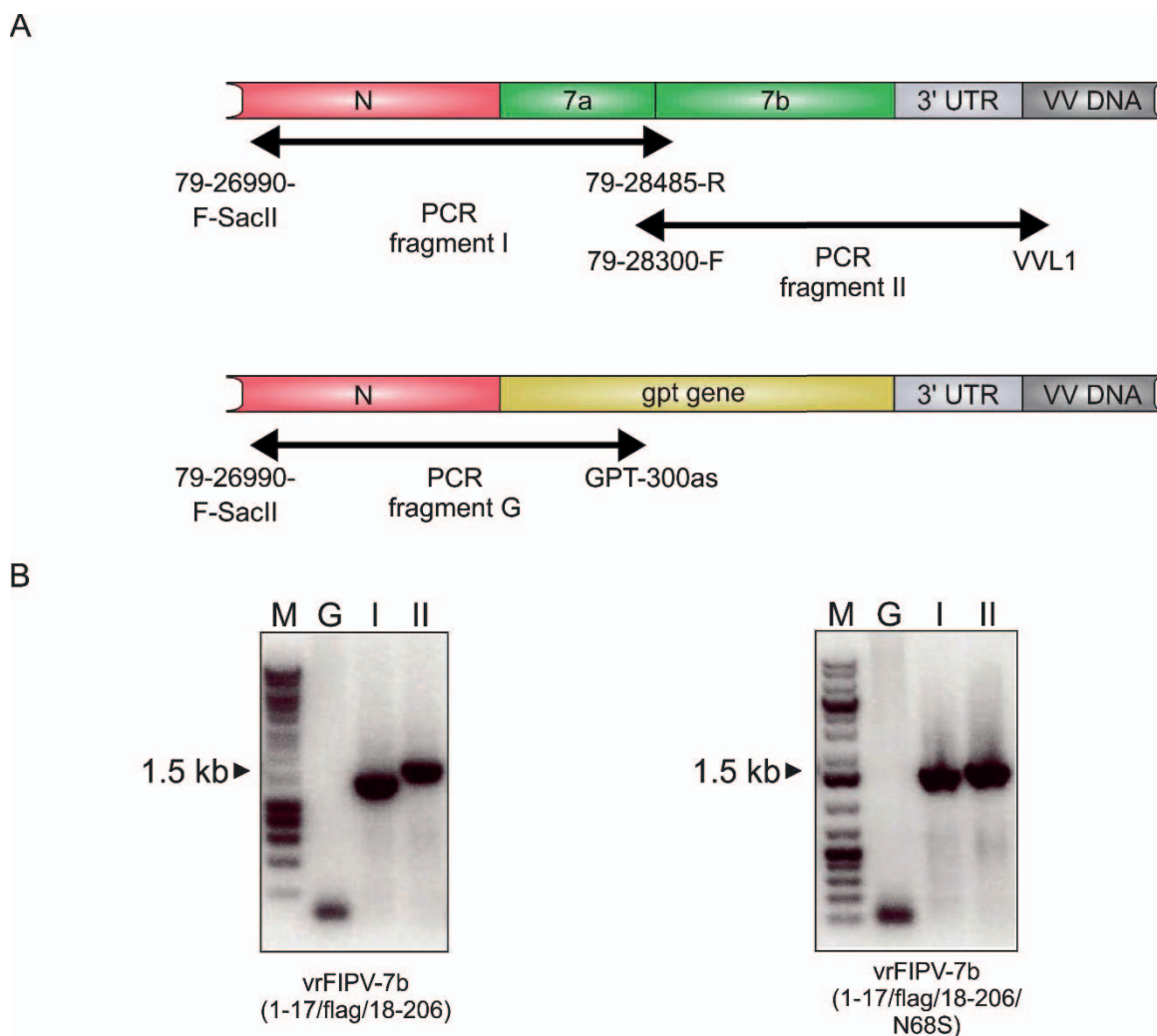


**Figure 20. Analysis of recombinant vaccinia viruses vrFIPV-7b(1-17/flag/18-206) and vrFIPV-7b(1-17/flag/18-206/N68S).** (A) Positions of the PCR fragments, as well as applied primers are presented. (B) PCR analysis of vrFIPV-7b(1-17/flag/18-206) and vrFIPV-7b(1-17/flag/18-206/N68S) recombinant vaccinia virus DNA. PCR products were resolved in ethidium bromide-stained 1%

agarose gel. The size of selected marker bands is shown on the left. I, PCR fragment I; II, PCR fragment II; G, PCR fragment G; M, DNA marker.

For the recovery of vrFIPV-7b(1-17/flag/18-206) and vrFIPV-7b(1-17/flag/18-206/N68S), the DNA of the recombinant vaccinia viruses vrFIPV-7b(1-17/flag/18-206) and rFIPV-7b(1-17/flag/18-206/N68S) was isolated in preparative scale (2.2.3.3.2.2) and analyzed with agarose gel electrophoresis as shown in Figure 13, respectively. The DNA was used as a template for *in vitro* transcription (2.2.4.3). In the next step, rFIPV-7b(1-17/flag/18-206) and rFIPV-7b(1-17/flag/18-206/N68S) RNA was electroporated (EP) (2.2.1.6.2) into BHK-FIPV-N cells and co-cultured with FCWF-4 cells, respectively (2.2.7.2.1). 48 hours post EP, the cell culture supernatant was harvested and centrifuged to remove cell debris. Subsequently, the supernatant was used to infect fresh FCWF-4 cells. After 24-48 h incubation, the supernatant containing recombinant FIPVs was harvested, stored at -80 °C and used for further experiments. The infected cells were used for PCR analyses. After sequencing of the PCR-products, insertion of the flag tag downstream of the signalase cleavage site of 7b could be verified for both rFIPV-7b(1-17/flag/18-206) and rFIPV-7b(1-17/flag/18-206/N68S) (Fig. 21A). Moreover, rFIPV-7b(1-17/flag/18-206/N68S) contained an additional mutation corresponding to N68S alteration (Fig. 21B). Growth kinetics of rFIPV-7b(1-17/flag/18-206) and rFIPV-7b(1-17/flag/18-206/N68S) were identical to those of the type II FIPV strain 79-1146 (Fig. 21C).

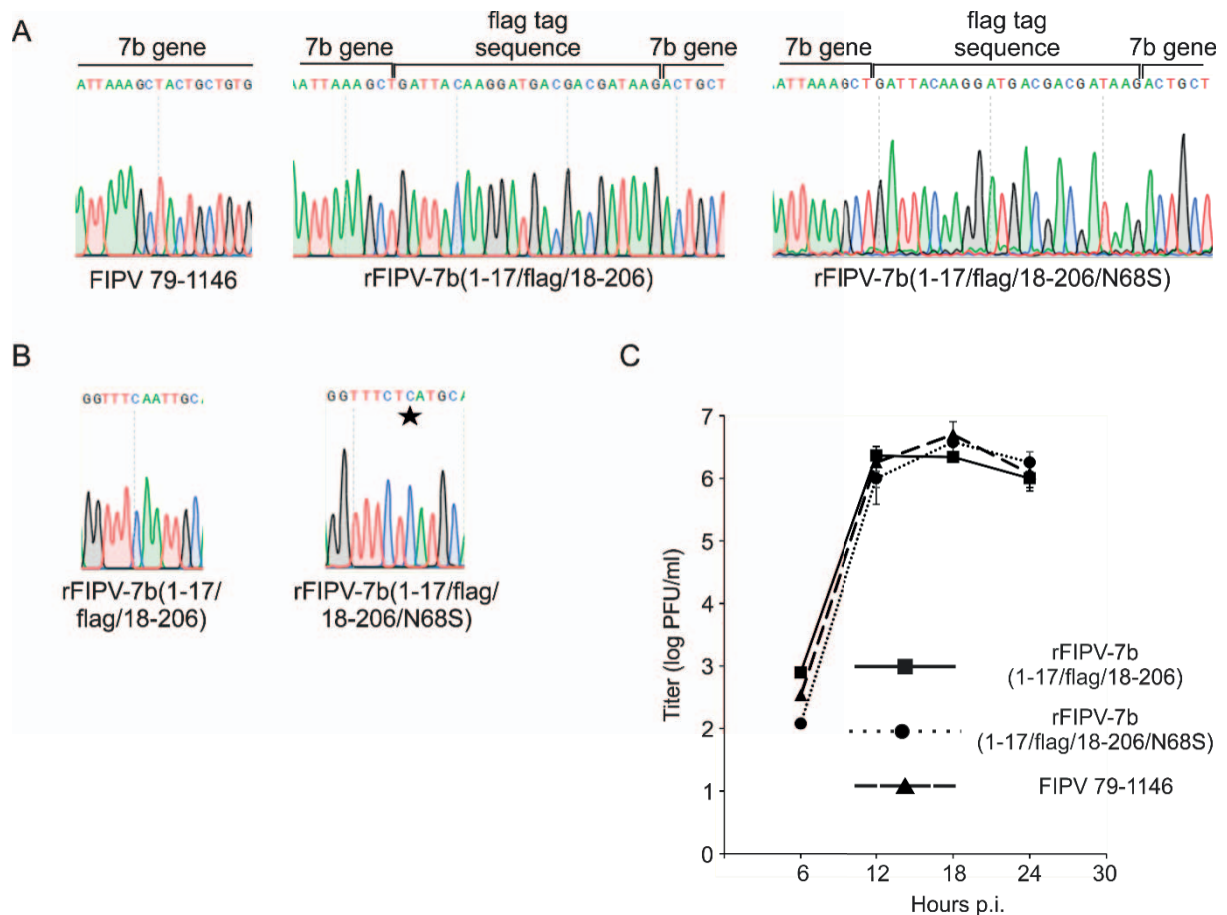


**Figure 21. Characterization of rFIPV-flag-7b(1-206) and rFIPV-flag-7b(1-206/N68S).** (A) Sequence analyses of type II FIPV strain 79-1146, rFIPV-7b(1-17/flag/18-206) and rFIPV-7b(1-17/flag/18-206/N68S). Flag tag sequence introduced downstream of the signalase cleavage site in 7b protein is demonstrated. (B) Nucleotide sequence AAT (asparagine) was substituted with TCA (serine) in rFIPV-7b(1-17/flag/18-206/N68S) (asterisk). (C) Growth kinetics of rFIPV-7b(1-17/flag/18-206) and rFIPV-7b(1-17/flag/18-206/N68S) compared to type II FIPV strain 79-1146; p.i., post infection.

### 3.2.6 Characterization of 7b Protein in rFIPV-7b(1-17/flag/18-206)- and rFIPV-7b(1-17/flag/18-206/N68S)-infected Cells.

To analyze the subcellular localization of 7b protein in infected cells, CRFK cells were infected with rFIPV-7b(1-17/flag/18-206) and rFIPV-7b(1-17/flag/18-206/N68S), respectively. 16 h post infection, before CPE developed, cells and cell culture supernatant were harvested and analyzed by Western Blot with anti-Flag® M2 (α-flag mAb) (Fig. 22B).

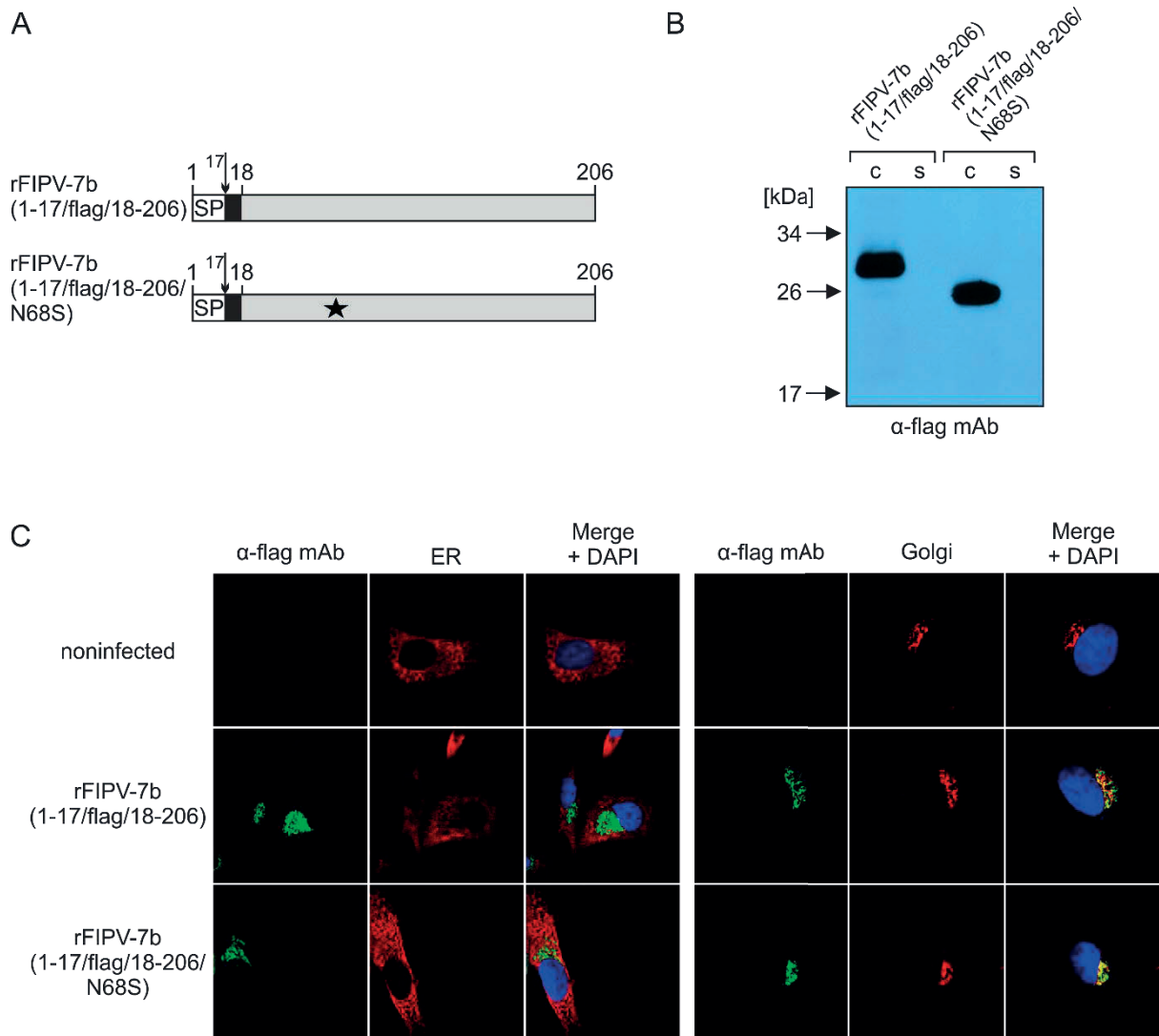


**Figure 22. Detection of 7b protein in FIPV-infected cells.** (A) Schematic representation of 7b protein encoded by rFIPV-7b(1-17/flag/18-206) and rFIPV-7b(1-17/flag/18-206/N68S). Black boxes represent the position of a flag tag in 7b protein. Asparagine to serine mutation at amino acid position 68 (N68S) is indicated by an asterisk. SP, signal peptide; numbers indicate the amino acid positions in 7b protein. Arrow: signalase cleavage site. (B) CRFK cells were infected with rFIPV-7b(1-17/flag/18-206) and rFIPV-7b(1-17/flag/18-206/N68S) at an MOI of 0.1, respectively. Cells and cell culture supernatants were harvested at 16 h p.i. Cell lysates (c) and cell culture supernatants (s) were separated by SDS-PAGE (10 %) under reducing conditions and analyzed by Western Blot using anti-flag mAb (α-flag mAb). (C) CRFK cells were infected with rFIPV-7b(1-17/flag/18-206) and rFIPV-7b(1-17/flag/18-206/N68S) at an MOI of 1 or mock infected, respectively. Cells were fixed 16 h p.i. and analyzed by confocal laser scanning microscopy. Immunofluorescence staining of 7b protein was performed with anti-flag mAb (α-flag mAb). Immunofluorescence staining of the endoplasmic reticulum (ER) (left panel) and the Golgi complex (right panel) is shown. Cell nuclei were stained blue with DAPI (adapted from Florek et al., 2017).

These experiments showed that 7b protein was detected only in both cell lysates but not in cell culture supernatants. Accordingly, independent of its glycosylation state the 7b protein is not secreted but retained in FIPV-infected cells. To determine the subcellular localization of the glycosylated versus non-glycosylated forms of 7b protein, confocal microscopy analysis was performed (Fig. 22C). CRFK cells were infected with rFIPV-7b(1-17/flag/18-206) and rFIPV-7b(1-17/flag/18-206/N68S), respectively and fixed 16 h post infection. The immunofluorescence analysis with anti-Flag<sup>®</sup> M2 ( $\alpha$ -flag mAb) revealed that both the glycosylated and the non-glycosylated forms of 7b protein co-localized exclusively with the Golgi apparatus. The results of the Western blot and confocal microscopy are identical with the outcome of the experiments performed with rFIPV-7b(1-206/N68S)-infected cells (Fig. 15) indicating that flag-tagged 7b protein at amino acid position 17 is well suited for characterization of the protein in FIPV-infected cells.

### 3.3 Subcellular Localization of 7b Protein

To determine the localization of 7b protein more precisely, cell lysates from rFIPV-7b(1-17/flag/18-206)-infected CRFK cells were subjected to either Endoglycosidase H (Endo H) or PNGase F glycosidase treatment and analyzed with Western Blot using anti-Flag<sup>®</sup> M2 antibody ( $\alpha$ -flag mAb) (Fig. 23).

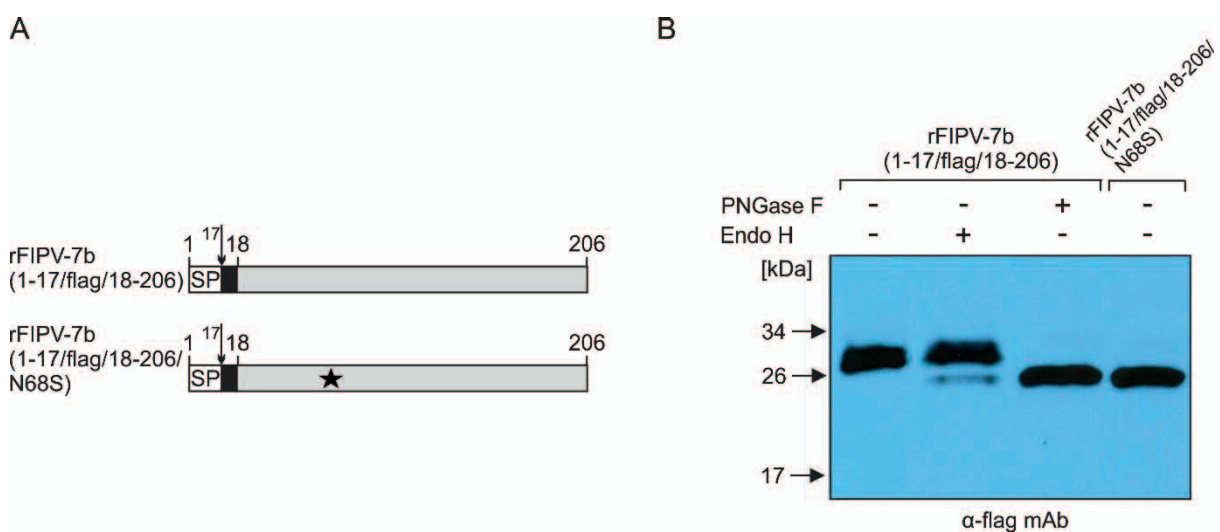


**Figure 23. Glycosidase treatment of 7b protein. (A)** Schematic representation of 7b protein encoded by rFIPV-7b(1-17/flag/18-206) and rFIPV-7b(1-17/flag/18-206/N68S). Black boxes represent

the position of a flag tag in 7b protein. Asparagine to serine mutation at amino acid position 68 (N68S) is indicated by an asterisk. SP, signal peptide; numbers indicate the amino acid positions in 7b protein. The arrow represents the signalase cleavage site. **(B)** CRFK cells were infected with rFIPV-flag-7b(18-206) at an MOI of 0.1. rFIPV-flag-7b(18-206)-N68S-infected cells were used as a control. Cells were harvested at 16 h p.i. and cell lysates subjected to glycosidase (PNGase F or Endo H) treatment (+) or left untreated (-). Subsequently, cell lysates were separated by SDS-PAGE (10%) under reducing conditions and analyzed by Western blot using anti-Flag<sup>®</sup> M2 antibody ( $\alpha$ -flag mAb) (adapted from Florek et al., 2017).

Since different steps of N-glycosylation occur in certain cellular compartments, treatment with various glycosidases allows to determine the intracellular localization of glycoproteins, like 7b in FIPV-infected cells. While PNGase F enzyme completely removes asparagine-linked sugars from glycoproteins, Endo H cleaves off high mannose oligosaccharide side chains, but not the complex glycan structures. PNGase F treatment of 7b protein originating from rFIPV-7b(1-17/flag/18-206)-infected CRFK cells led to co-migration with the non-glycosylated form of 7b protein. Endo H treatment resulted in a resistant and a sensitive form of 7b protein. The major fraction of 7b protein was Endo H-resistant suggesting that this form of 7b protein contained complex glycan structures. Since such structures are formed in *medial*- and *trans*-Golgi (Balch & Keller 1986); 7b protein is retained beyond *cis*-Golgi. The Endo H-sensitive fraction of 7b protein apparently represents the not completely glycosylated forms of 7b protein that have not yet reached the *medial*-Golgi.

## **3.4 Impact of C-terminal Sequence of 7b Protein on Subcellular Localization**

### **3.4.1 Generation of rFIPV-7b(1-206)-flag**

To elucidate whether an additional sequence at the C-terminus of 7b protein alters its intracellular localization in FIPV-infected cells, a recombinant FIPV expressing 7b protein with a flag tag at its C-terminus (rFIPV-7b(1-206)-flag) was generated using vaccinia virus-based reverse genetic system. To generate recombinant vaccinia

virus vrFIPV-7b(1-206)-flag, CV-1 cells were infected with vrFIPV-GPT- $\Delta$ 7ab and transfected with pDF4 plasmid, similar as shown in Figure 11. After selection of gpt-negative recombinant vaccinia virus, viral DNA was isolated and analyzed with PCR (Fig. 24). After sequence analysis of the recombination sites, vrFIPV-7b(1-206)-flag was plaque purified and the integrity of the viral genome was assessed with PCR as described in Figure 10.

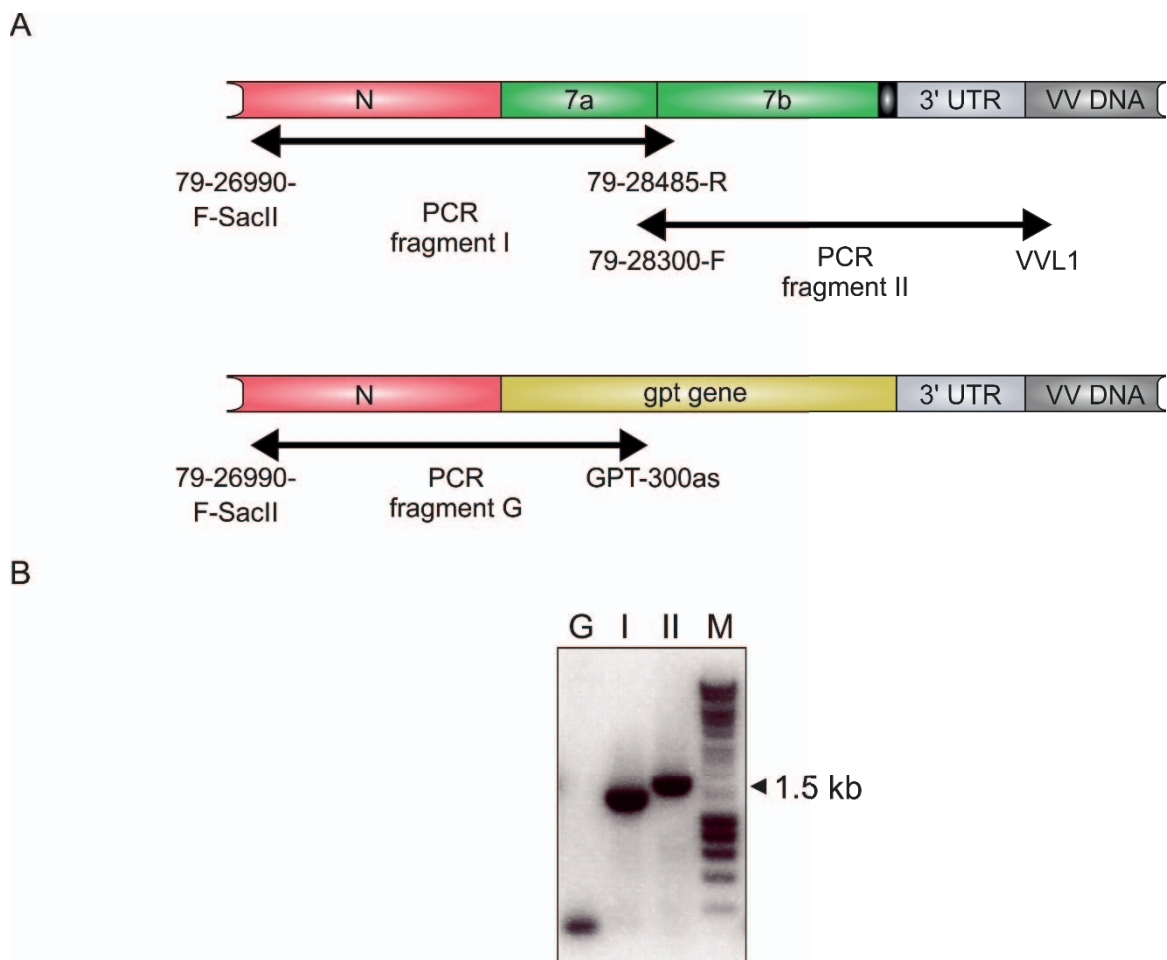


**Figure 24. Analysis of recombinant vaccinia virus vrFIPV-7b(1-206)-flag. (A)** Positions of the PCR fragments, as well as applied primers are presented. Black box represents the flag tag in 7b gene. **(B)** PCR analysis of vrFIPV-7b(1-206)-flag recombinant vaccinia virus DNA. PCR products were resolved in ethidium bromide-stained 1% agarose gel. The size of selected marker band is shown on the right. I, PCR fragment I; II, PCR fragment II; G, PCR fragment G; M, DNA marker.

For the recovery of rFIPV-7b(1-206)-flag, the DNA of the recombinant vaccinia virus vrFIPV-7b(1-206)-flag was isolated in preparative scale (2.2.3.3.2.2) and analyzed

with agarose gel electrophoresis as shown in Figure 13. The DNA was used as a template for *in vitro* transcription (2.2.4.3). In the next step, rFIPV-7b(1-206)-flag RNA was electroporated (EP) (2.2.1.6.2) into BHK-FIPV-N cells and co-cultured with FCWF-4 cells (2.2.7.2.1). 48 hours post EP, the cell culture supernatant was harvested and centrifuged to remove cell debris. Subsequently, the supernatant was used to infect fresh FCWF-4 cells. After 24-48 h incubation, the supernatant containing rFIPV-7b(1-206)-flag was harvested, stored at -80 °C and used for further experiments. The infected cells were used for PCR analyses. After sequencing of the PCR-products, insertion of the flag tag at the C-terminus of 7b could be verified (Fig. 25A). Growth kinetics of rFIPV-7b(1-206)-flag were identical to those of the type II FIPV strain 79-1146 (Fig. 25B).

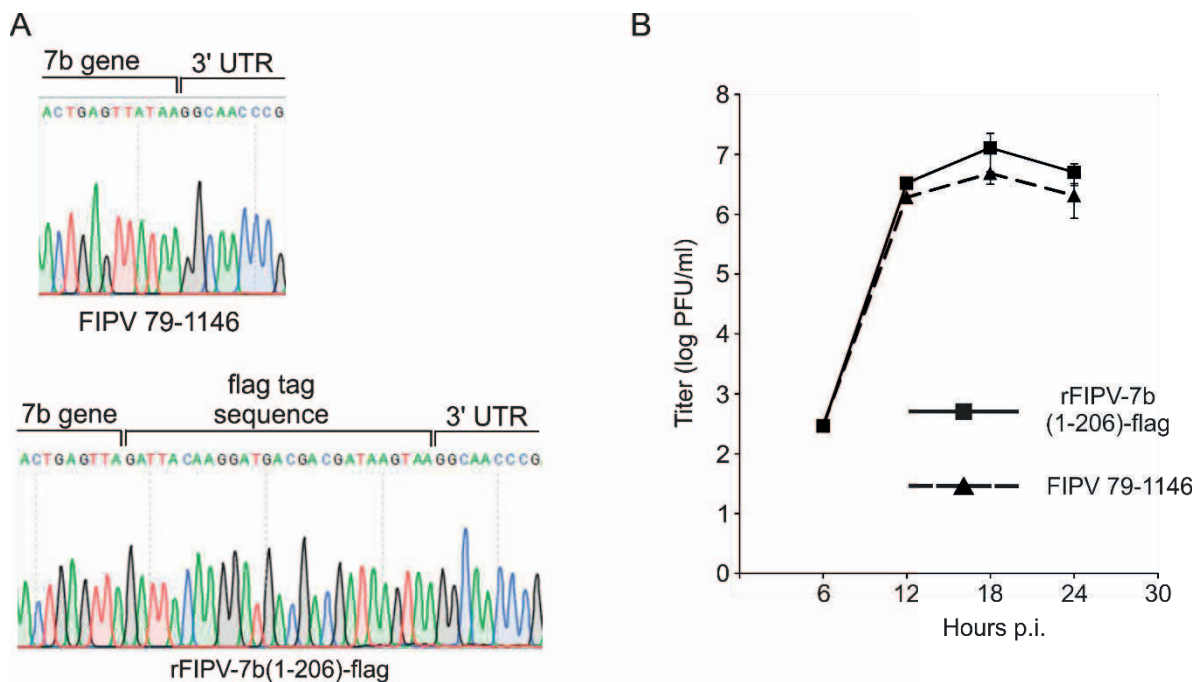


**Figure 25. Characterization of rFIPV-7b(1-206)-flag.** (A) Sequence analyses of type II FIPV strain 79-1146 and rFIPV-7b(1-206)-flag. Flag tag sequence downstream of 7b gene is demonstrated. 3' UTR, 3' untranslated region. (B) Growth kinetics of rFIPV-7b(1-206)-flag compared to type II FIPV strain 79-1146;p.i., post infection.

### 3.4.2 Characterization of 7b Protein Encoded by rFIPV-7b(1-206)-flag

CRFK cells were infected with rFIPV-7b(1-206)-flag and cells and cell culture supernatant were harvested before CPE developed. The samples were then analyzed with Western Blot using anti-Flag<sup>®</sup> M2 antibody ( $\alpha$ -flag mAb) (Fig. 26B). 7b protein was detected both in the cell lysate and the cell culture supernatant. The higher molecular weight of 7b protein in the supernatant corresponds to further glycosylation events that take place during the transport of the protein between the Golgi and the cell surface. To determine the localization of C-terminal flag-tagged 7b protein in FIPV-infected cells, confocal microscopy analysis was performed (Fig. 26C). The analysis revealed that the C-terminal flag-tagged 7b protein co-localized not only with the Golgi apparatus but it was also detected as dense spots in the cytoplasm without association of the Golgi. These data indicate that insertion of a flag tag at the C-terminus of 7b protein alters its subcellular localization and leads to secretion of 7b protein. Similar observation was made by Dedeurwaerder et. al (2014). In this recent study, 7b-GFP fusion protein expressed from a plasmid was found to localize with Golgi apparatus and as dense spots in the entire cytoplasm outside this compartment.

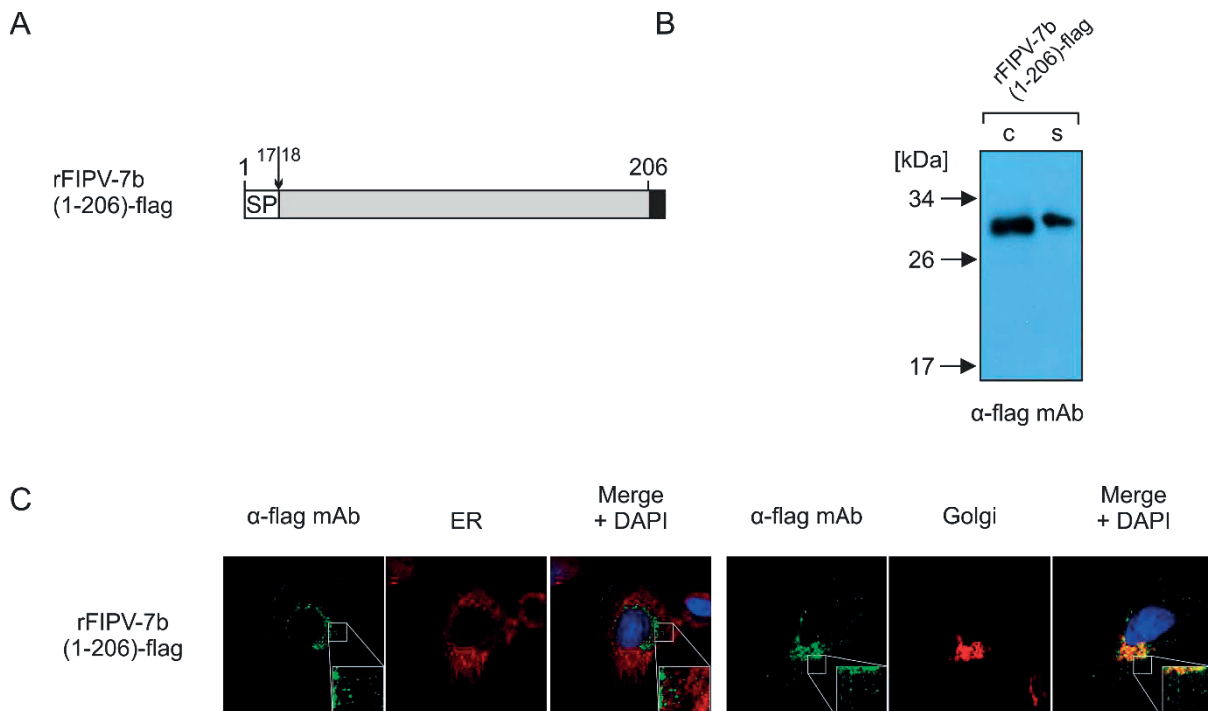
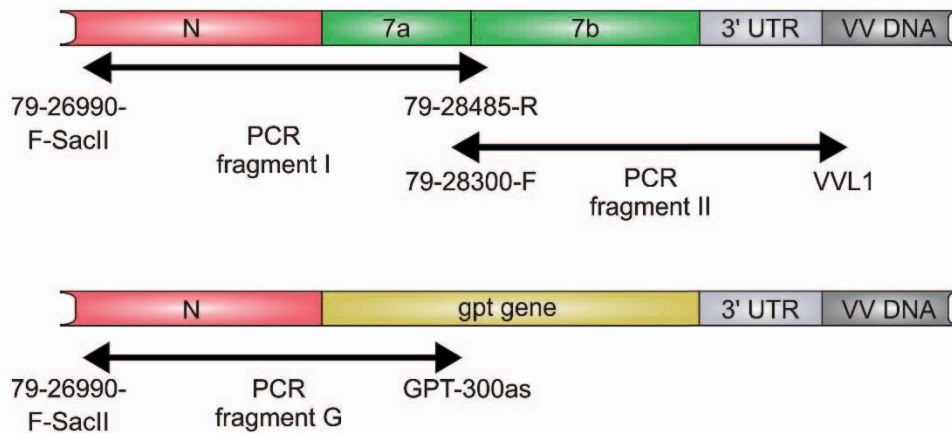


**Figure 26. Effect of the C-terminal flag tag on subcellular localization of 7b protein. (A)** Schematic representation of 7b protein encoded by rFIPV-7b(18-206)-flag. Black box represents the position of the flag tag in 7b protein. SP, signal peptide; numbers indicate the amino acid positions in 7b protein. The arrow represents the signalase cleavage site. **(B)** CRFK cells were infected with rFIPV-7b(1-206)-flag at an MOI of 0.1. Cells and cell culture supernatants were harvested at 16 h p.i.. Cell lysate (c) and cell culture supernatant (s) were separated by SDS-PAGE (10 %) under reducing conditions and analyzed by Western Blot using anti-flag mAb. **(C)** CRFK cells were infected with rFIPV-7b(1-206)-flag at an MOI of 1. Cells were fixed 16 h p.i. and analyzed by confocal laser scanning microscopy. Immunofluorescence staining of 7b protein was performed with anti-flag mAb ( $\alpha$ -flag mAb). Immunofluorescence staining of the endoplasmic reticulum (ER) (left panel) and the Golgi complex (right panel) is shown. Cell nuclei were stained blue with DAPI. The inserts in the lower right corner represent an 8x magnification of the selected area (adapted from Florek et al., 2017).

### **3.4.3 Generation of Recombinant FIPVs with Altered KTEL Motif**

To study the influence of the KTEL motif on 7b protein subcellular localization in FIPV-infected cells, we generated a set of recombinant FIPVs expressing 7b protein with altered KTEL motif. To achieve this, recombinant vaccinia viruses vrFIPV-7b(1-17/flag/18-202/KTEV), vrFIPV-7b(1-17/flag/18-202/KTE), vrFIPV-7b(1-17/flag/18-202/AAAA) and vrFIPV-7b(1-17/flag/18-202/KDEL) were generated using vaccinia virus-based reverse genetic system. CV-1 cells were infected with vrFIPV-GPT- $\Delta$ 7ab and transfected with plasmids pDF6, pDF7, pDF9 and pDF8, respectively similar as shown in Figure 11. After selection of gpt-negative recombinant vaccinia viruses, viral DNA was isolated and analyzed with PCR (Fig. 27). After sequence analysis of the recombination sites, vrFIPV-7b(1-17/flag/18-202/KTEV), vrFIPV-7b(1-17/flag/18-202/KTE), vrFIPV-7b(1-17/flag/18-202/AAAA) and vrFIPV-7b(1-17/flag/18-202/KDEL) were plaque purified and the integrity of the viral genome was assessed with PCR as described in Figure 10.

A



B

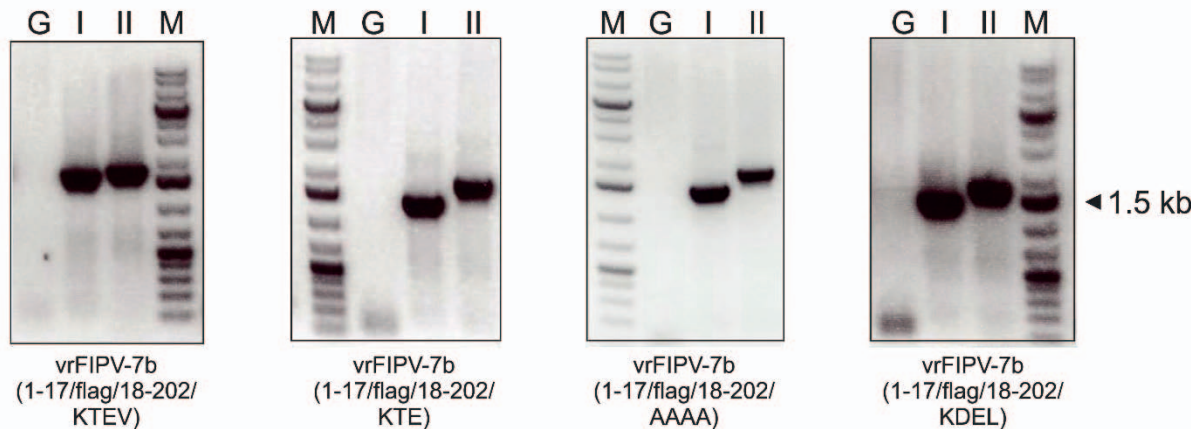


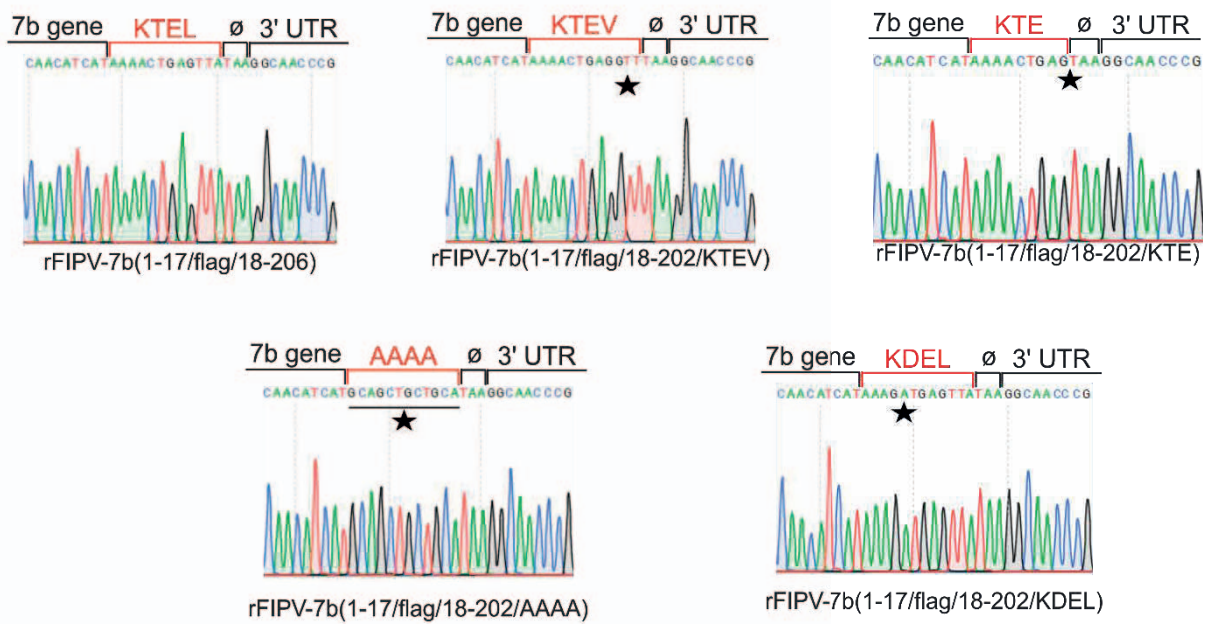
**Figure 27. Analysis of recombinant vaccinia viruses vrFIPV-7b(1-17/flag/18-202/KTEV), vrFIPV-7b(1-17/flag/18-202/KTE), vrFIPV-7b(1-17/flag/18-202/AAAA) and vrFIPV-7b(1-17/flag/18-202/KDEL).** (A) Positions of the PCR fragments as well as applied primers are presented. (B) PCR analysis of vrFIPV-7b(1-17/flag/18-202/KTEV), vrFIPV-7b(1-17/flag/18-202/KTE), vrFIPV-7b(1-17/flag/18-202/AAAA) and vrFIPV-7b(1-17/flag/18-202/KDEL) recombinant vaccinia virus DNA. PCR products were resolved in ethidium bromide-stained 1% agarose gel. The size of selected marker band is shown on the right. I, PCR fragment I; II, PCR fragment II; G, PCR fragment G; M, DNA marker.

For the recovery of recombinant FIPVs, DNA of the obtained recombinant vaccinia viruses was isolated in preparative scale (2.2.3.3.2.2) and analyzed with agarose gel electrophoresis as shown in Figure 13. The DNA was used as a template for *in vitro* transcription (2.2.4.3). In the next step, rFIPV-7b(1-17/flag/18-202/KTEV), rFIPV-7b(1-17/flag/18-202/KTE), rFIPV-7b(1-17/flag/18-202/AAAA) and rFIPV-7b(1-17/flag/18-202/KDEL) RNA was electroporated (EP) (2.2.1.6.2) into BHK-FIPV-N

cells and co-cultured with FCWF-4 cells (2.2.7.2.1). 48 hours post EP, the cell culture supernatant was harvested and centrifuged to remove cell debris. Subsequently, the supernatant was used to infect fresh FCWF-4 cells. After 24-48 h incubation, the supernatant containing rFIPVs was harvested, stored at -80 °C and used for further experiments. The infected cells were used for PCR analyses. After sequencing of the PCR-products, all respective alterations of KTEL motif could be verified (Fig. 28A). Moreover, flag tag downstream of the signalase cleavage site of 7b was successfully introduced in all rFIPVs (Fig. 28A). Growth kinetics of rFIPV-7b(1-17/flag/18-202/KTEV), rFIPV-7b(1-17/flag/18-202/KTE), rFIPV-7b(1-17/flag/18-202/AAAA) and rFIPV-7b(1-17/flag/18-202/KDEL) were identical to those of the type II FIPV strain 79-1146 (Fig. 28B).

According to Vennema and colleagues (1992), KTEL to KTEV alteration abolished ER retention and led to secretion of 7b protein. To investigate whether similar results can be observed in FIPV-infected cells rFIPV-7b(1-17/flag/18-202/KTEV) was generated. A recent study described KXD/E C-terminal motif as a Golgi retention signal for various proteins in plants (Gao et al. 2014). In order to elucidate whether KTE motif is sufficient for 7b protein retention in the Golgi, leucine at the position 206 of 7b protein was deleted (rFIPV-7b(1-17/flag/18-202/KTE)). In rFIPV-7b(1-17/flag/18-202/AAAA) the entire KTEL motif was substituted with 4 alanine residues (AAAA). In rFIPV-7b(1-17/flag/18-202/KDEL) KTEL was altered to KDEL motif, which represents a canonical ER-retention signal.

A



B

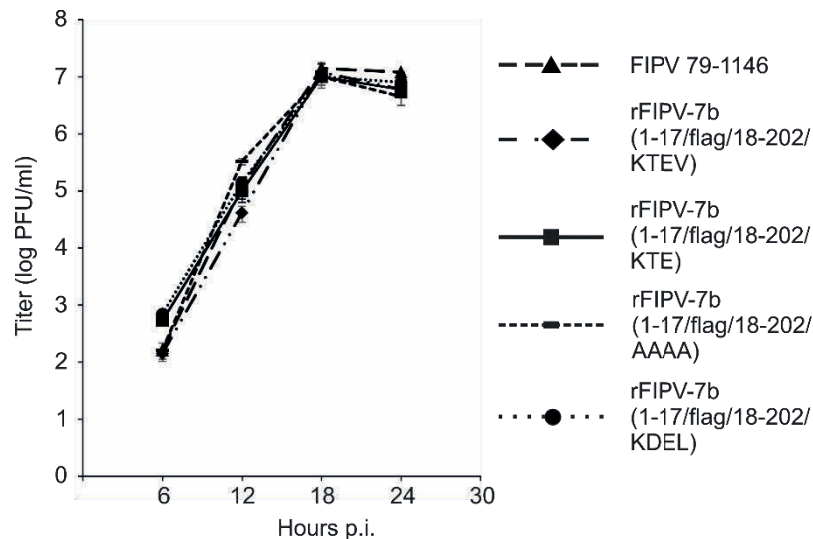


**Figure 28. Characterization of recombinant FIPVs expressing 7b protein with altered C-terminal motif. (A)** Sequence analyses of rFIPV-7b(1-17/flag/18-206), rFIPV-7b(1-17/flag/18-202/KTEV), rFIPV-7b(1-17/flag/18-202/KTE), rFIPV-7b(1-17/flag/18-202/AAAA) and rFIPV-7b(1-17/flag/18-202/KDEL). Alterations to the C-terminal KTEL motif of 7b protein are shown. In rFIPV-7b(1-17/flag/18-202/KTEV), the last 3 nucleotides (TTA, leucine) were mutated into GTT (valine). In rFIPV-7b(1-17/flag/18-202/KTE), the last 3 nucleotides (TTA, leucine) were deleted. In rFIPV-7b(1-17/flag/18-202/AAAA), the last 12 nucleotides were substituted with GCAGCTGCTGCA (AAAA). In rFIPV-7b(1-17/flag/18-202/KDEL), the nucleotides ACT (threonine) were mutated into GAT (aspartic acid). Asterisks show positions of respective alterations. 3' UTR, 3' untranslated region; ø, translational stop codon. **(B)** Growth kinetics of rFIPV-7b(1-17/flag/18-202/KTEV), rFIPV-7b(1-

17/flag/18-202/KTE), rFIPV-7b(1-17/flag/18-202/AAAA) and rFIPV-7b(1-17/flag/18-202/KDEL) compared to type II FIPV strain 79-1146; p.i., post infection.

### **3.4.4 Role of the C-terminal KTEL Motif in Subcellular Localization of 7b Protein**

CRFK cells were infected with rFIPV-7b(1-17/flag/18-206) and with viruses in which the C-terminal KTEL motif in 7b protein was altered (rFIPV-7b(1-17/flag/18-202/KTEV), rFIPV-7b(1-17/flag/18-202/KTE), rFIPV-7b(1-17/flag/18-202/AAAA) and rFIPV-7b(1-17/flag/18-202/KDEL)) (Fig. 29A). Cells and cell culture supernatants were harvested before CPE developed. The samples were subjected to SDS-PAGE and analyzed with Western Blot using anti-Flag<sup>®</sup> M2 antibody ( $\alpha$ -flag mAb) (Fig. 29B). 7b protein was detected in all cell lysates. Additionally, 7b protein was observed in the cell culture supernatants originating from cells infected with rFIPV-7b(1-17/flag/18-202/KTEV), rFIPV-7b(1-17/flag/18-202/KTE) and rFIPV-7b(1-17/flag/18-202/AAAA) suggesting that the C-terminal motifs KTEV, KTE and AAAA in 7b protein led to secretion of the protein. The higher molecular weight of 7b protein in the cell culture supernatant corresponds to further glycosylation events that take place after the protein leaves the Golgi and is transported to the cell surface. The weak signals in rFIPV-7b(1-17/flag/18-202/AAAA)-infected cells and cell culture supernatant may be due to accelerated intracellular degradation of 7b protein. The Western blot analyses further revealed that 7b with the KDEL motif was only detectable in the cell lysate.

Immunofluorescence analysis was applied to study the localization of 7b protein in cells infected with the different recombinant FIPVs listed above. Cells were fixed and 7b protein was visualized using anti-Flag<sup>®</sup> M2 antibody ( $\alpha$ -flag mAb) (Fig. 29C). The experiments revealed that 7b protein with KTEV, KTE and AAAA motifs co-localized with the Golgi apparatus and was also detected as dense spots in the entire cytoplasm outside this compartment. 7b protein with C-terminal KDEL motif co-localized exclusively with the endoplasmic reticulum.

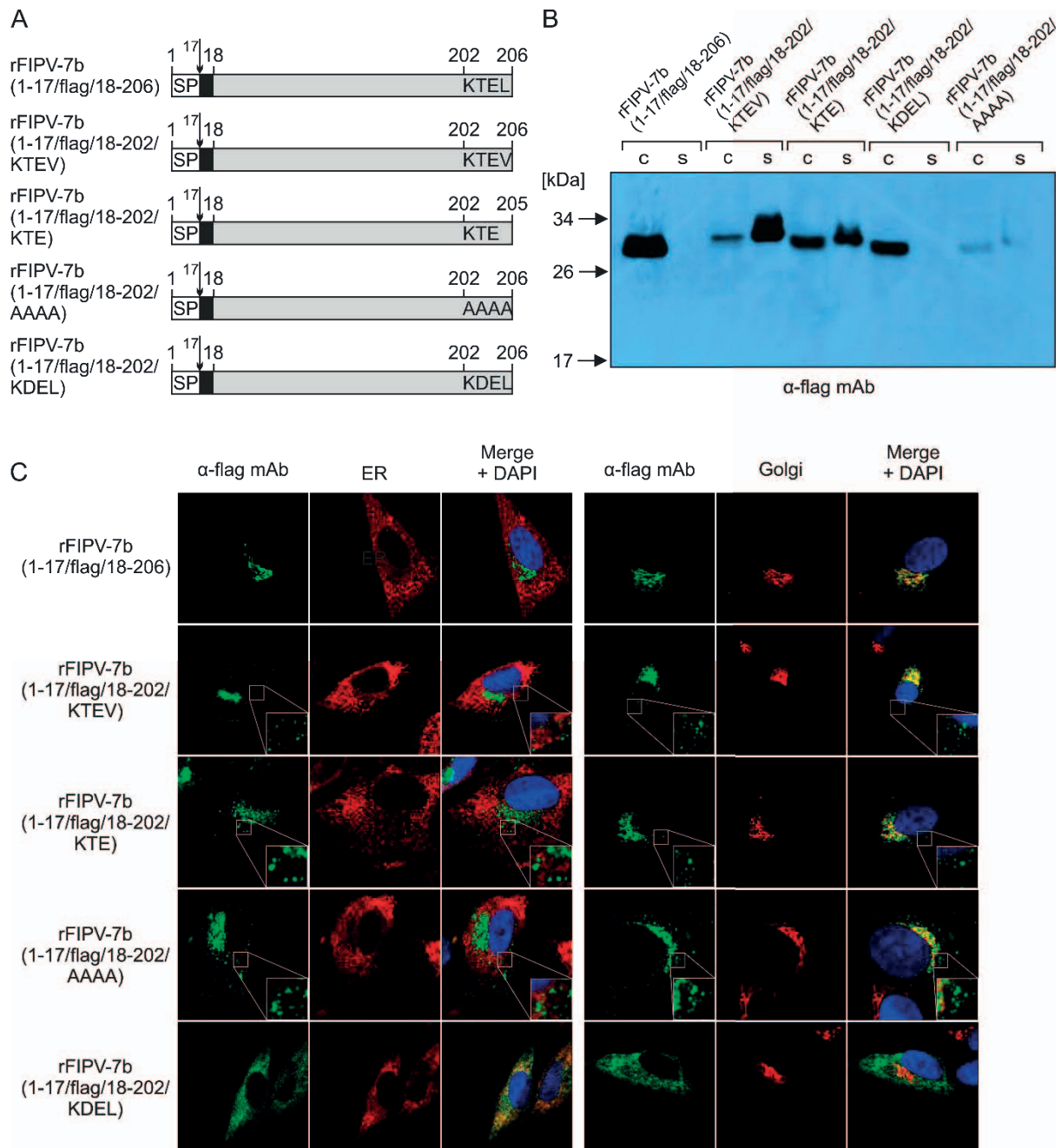


**Figure 29. Influence of altered C-terminal motifs in 7b protein on subcellular localization and secretion. (A)** Schematic representation of 7b protein encoded by rFIPV-7b(1-17/flag/18-206), rFIPV-7b(1-17/flag/18-202/KTEV), rFIPV-7b(1-17/flag/18-202/KTE), rFIPV-7b(1-17/flag/18-202/AAAA) and rFIPV-7b(1-17/flag/18-202/KDEL). Black boxes represent the position of a flag tag in 7b. The C-terminal amino acids of 7b protein are shown; SP, signal peptide; numbers indicate the amino acid positions in 7b protein. The arrows represent the signalase cleavage site **(B)** CRFK cells were infected with rFIPV-7b(1-17/flag/18-206), rFIPV-7b(1-17/flag/18-202/KTEV), rFIPV-7b(1-17/flag/18-202/KTE), rFIPV-7b(1-17/flag/18-202/AAAA) and rFIPV-7b(1-17/flag/18-202/KDEL) at an MOI of 0.1, respectively. Cells and cell culture supernatants were harvested at 16 h p.i. Cell lysates (c) and cell culture supernatants (s) were separated by SDS-PAGE (10 %) under reducing conditions and analyzed by Western Blot using anti-flag mAb (α-flag mAb). **(C)** CRFK cells were infected with rFIPV-

7b(1-17/flag/18-206), rFIPV-7b(1-17/flag/18-202/KTEV), rFIPV-7b(1-17/flag/18-202/KTE), rFIPV-7b(1-17/flag/18-202/AAAA) and rFIPV-7b(1-17/flag/18-202/KDEL) at an MOI of 1. Cells were fixed 16 h p.i. and analyzed by confocal laser scanning microscopy. Immunofluorescence staining of 7b protein was performed with anti-flag mAb ( $\alpha$ -flag mAb). Immunofluorescence staining of the endoplasmic reticulum (ER) (left panel) and the Golgi complex (right panel) is shown. Cell nuclei were stained blue with DAPI. The inserts in the lower right corner represent an 8x magnification of the selected area (adapted from Florek et al., 2017).

The results can be summarized as follows: substitution of the KTEL motif with KTEV, KTE or AAAA altered the subcellular localization of 7b protein and led to secretion of it. Replacement of the C-terminal KTEL motif by KDEL resulted in ER-, instead of Golgi-retention. Taken together, the performed experiments show that the C-terminal KTEL motif of 7b protein is responsible for its localization in the Golgi apparatus in FIPV-infected cells.

### **3.5 Subcellular Localization of 7b Protein after Inhibition of Ongoing Protein Synthesis**

Since the so far applied experimental setup cannot differentiate between ongoing protein synthesis and 7b synthesized at an earlier time point p.i. in FIPV-infected cells, translation was blocked with cycloheximide (CHX) for 2 hours prior fixation. After CHX treatment, subcellular localization of 7b protein produced before addition of cycloheximide was investigated. For this purpose, CRFK cells were infected with rFIPV-7b(1-17/flag/18-202/KTEV), rFIPV-7b(1-17/flag/18-202/KTE), rFIPV-7b(1-17/flag/18-202/AAAA), rFIPV-7b(1-17/flag/18-206) and rFIPV-7b(1-17/flag/18-202/KDEL), respectively. 15 h post infection cells were either treated with CHX or left untreated. After 2 hour of incubation (17 h post infection), both cycloheximide-treated and untreated cells were fixed and analyzed by immunofluorescence (Fig. 30). Anti-Flag<sup>®</sup> M2 antibody ( $\alpha$ -flag mAb) was used to visualize 7b protein. The subcellular localization of 7b protein with altered C-terminal motifs (KTEV, KTE or AAAA) differed between cycloheximide-treated and untreated cells. In cells treated with cycloheximide, 7b protein did not localize with the Golgi apparatus and only weak signals of 7b protein could be detected outside this compartment. In contrast, no

change in subcellular localization of 7b protein with KTEL or KDEL motifs was observed in cycloheximide-treated versus untreated cells.

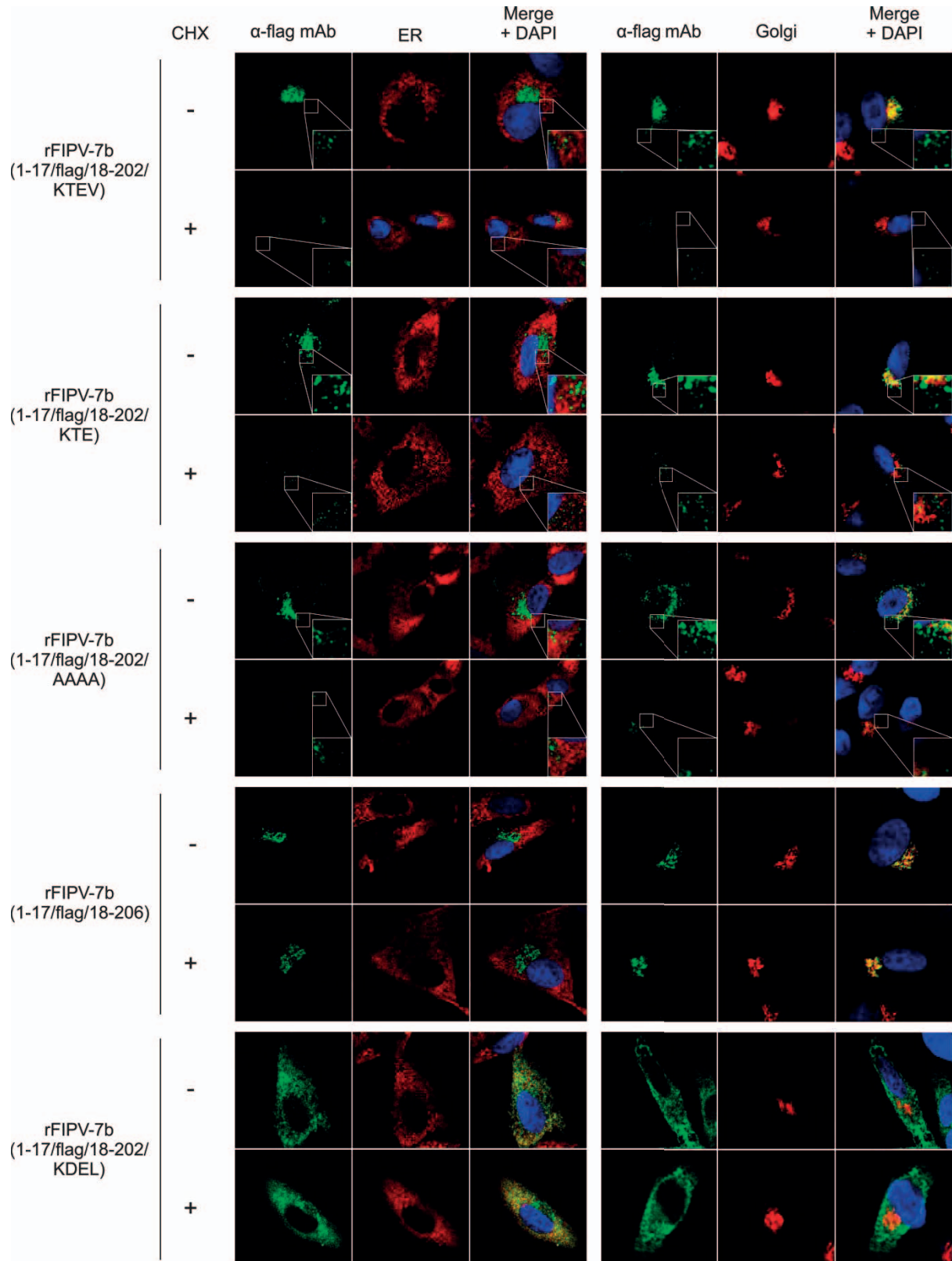


**Figure 30. Effect of cycloheximide treatment on localization of 7b protein with different C-terminal motifs.** CRFK cells were infected with rFIPV-7b(1-17/flag/18-202/KTEV), rFIPV-7b(1-17/flag/18-202/KTE), rFIPV-7b(1-17/flag/18-202/AAAA), rFIPV-7b(1-17/flag/18-206) and rFIPV-7b(1-17/flag/18-202/KDEL) at an MOI of 1, respectively. At 15 h p.i., the cells were either treated with cycloheximide (+) or left untreated (-). 17 h p.i. cells were fixed and analyzed by confocal laser scanning microscopy. Immunofluorescence staining of 7b was performed with anti-flag mAb ( $\alpha$ -flag mAb). Immunofluorescence staining of the endoplasmic reticulum (ER) (left panel) and the Golgi complex (right panel) is shown. Cell nuclei were stained blue with DAPI. CHX, cycloheximide. The inserts in the lower right corner represent an 8x magnification of the selected area (adapted from Florek et al., 2017).

The localization of 7b protein in FIPV-infected cells after inhibition of the ongoing protein synthesis was further analyzed with Endo H treatment followed by Western blot analysis (Fig. 31). CRFK cells were infected with rFIPV-7b(1-17/flag/18-206) or rFIPV-7b(1-17/flag/18-202/KDEL). 15 hours p.i. the cells were either treated with cycloheximide or left untreated. 17 h post infection the cells were harvested and the cell lysates were subjected to Endo H treatment or left untreated. The samples were then resolved on SDS-PAGE and analyzed with Western Blot using anti-Flag<sup>®</sup> M2 antibody ( $\alpha$ -flag mAb). These experiments revealed that after cycloheximide treatment, 7b protein originating from cells infected with rFIPV-7b(1-17/flag/18-206) was completely Endo H-resistant indicating that 7b protein was retained beyond *cis*-Golgi compartment. In contrast, 7b protein originating from rFIPV-7b(1-17/flag/18-202/KDEL)-infected cells was fully sensitive to Endo H digestion regardless of cycloheximide treatment suggesting that 7b protein with the C-terminal KDEL motif was exclusively retained in the endoplasmic reticulum.

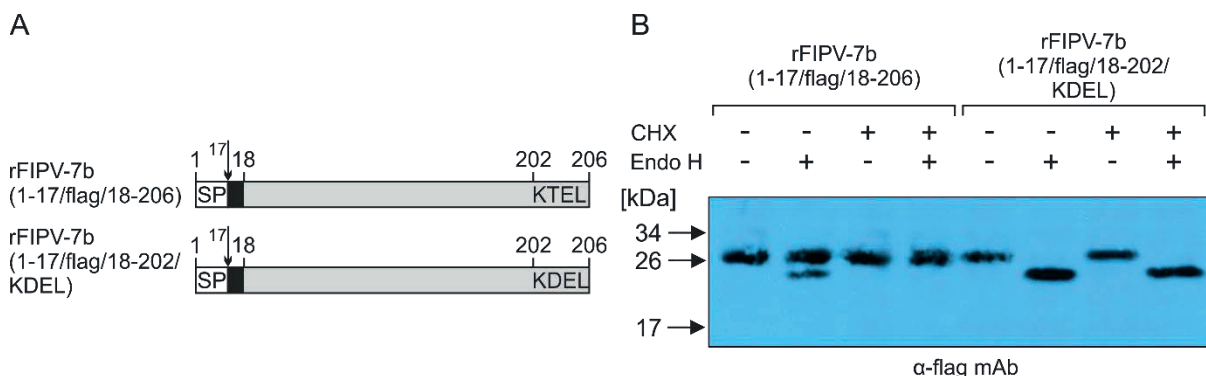


**Figure 31. Western blot analysis of CHX-treated versus non-treated FIPV-infected cells. (A)** Schematic representation of 7b protein encoded by rFIPV-7b(1-17/flag/18-206), and rFIPV-7b(1-17/flag/18-202/KDEL). Black boxes represent the flag tag in 7b protein. The C-terminal four amino acids in 7b protein are shown. SP, signal peptide; numbers indicate the amino acid positions in 7b protein. The arrows between amino acids 17 and 18 represent the signalase cleavage site. **(B)** CRFK cells infected with rFIPV-7b(1-17/flag/18-206) and rFIPV-7b(1-17/flag/18-202/KDEL) at an MOI of 0.1 were either treated with cycloheximide (+) or left untreated (-). After 2 h of incubation (17 h p.i.), the cells were harvested, lysed and subjected to treatment with Endo H glycosidase (+) or left untreated (-). The samples were then resolved in a 10% polyacrylamide gel and analyzed with Western Blot using anti-Flag<sup>®</sup> M2 antibody ( $\alpha$ -flag mAb). CHX, cycloheximide.

To verify that the observed results were not specific only to one cell line (CRFK), 7b protein localization was studied in other feline cell lines as well. For this purpose, FCWF-4 and Fc3Tg cells were infected with rFIPV-7b(1-17/flag/18-206) or rFIPV-7b(1-17/flag/18-202/KTEV). rFIPV-7b(1-17/flag/18-202/KTEV) was chosen as a representative virus, in which alteration of the 7b C-terminal KTEL motif led to secretion of the protein. Since in these cell lines cytopathic effect with recombinant FIPVs develops faster, cycloheximide treatment was performed 8 h post infection. After 2 h of incubation (10 h post infection), both cycloheximide-treated and untreated cells were fixed and analyzed with confocal microscopy using anti-Flag<sup>®</sup> M2 antibody ( $\alpha$ -flag mAb) (Fig. 32). These experiments showed no differences in 7b protein localization in FIPV-infected FCWF-4 or Fc3Tg cells in comparison with CRFK cells. Accordingly, in FCWF-4 or Fc3Tg cells 7b protein with an intact C-terminal KTEL motif was retained in the Golgi. Alteration of the KTEL motif to KTEV led to abolishment of Golgi retention and secretion of 7b protein.

Altogether, the performed experiments revealed that mutation of the C-terminal KTEL motif to KTEV, KTE or AAAA abolished Golgi retention and led to secretion of 7b protein. The results further suggest that independent of ongoing protein synthesis, the C-terminal KTEL motif in 7b protein functions as a Golgi retention signal. Exchange of only one amino acid (threonine to aspartic acid) resulting in KDEL motif turned the Golgi into an ER retention signal.

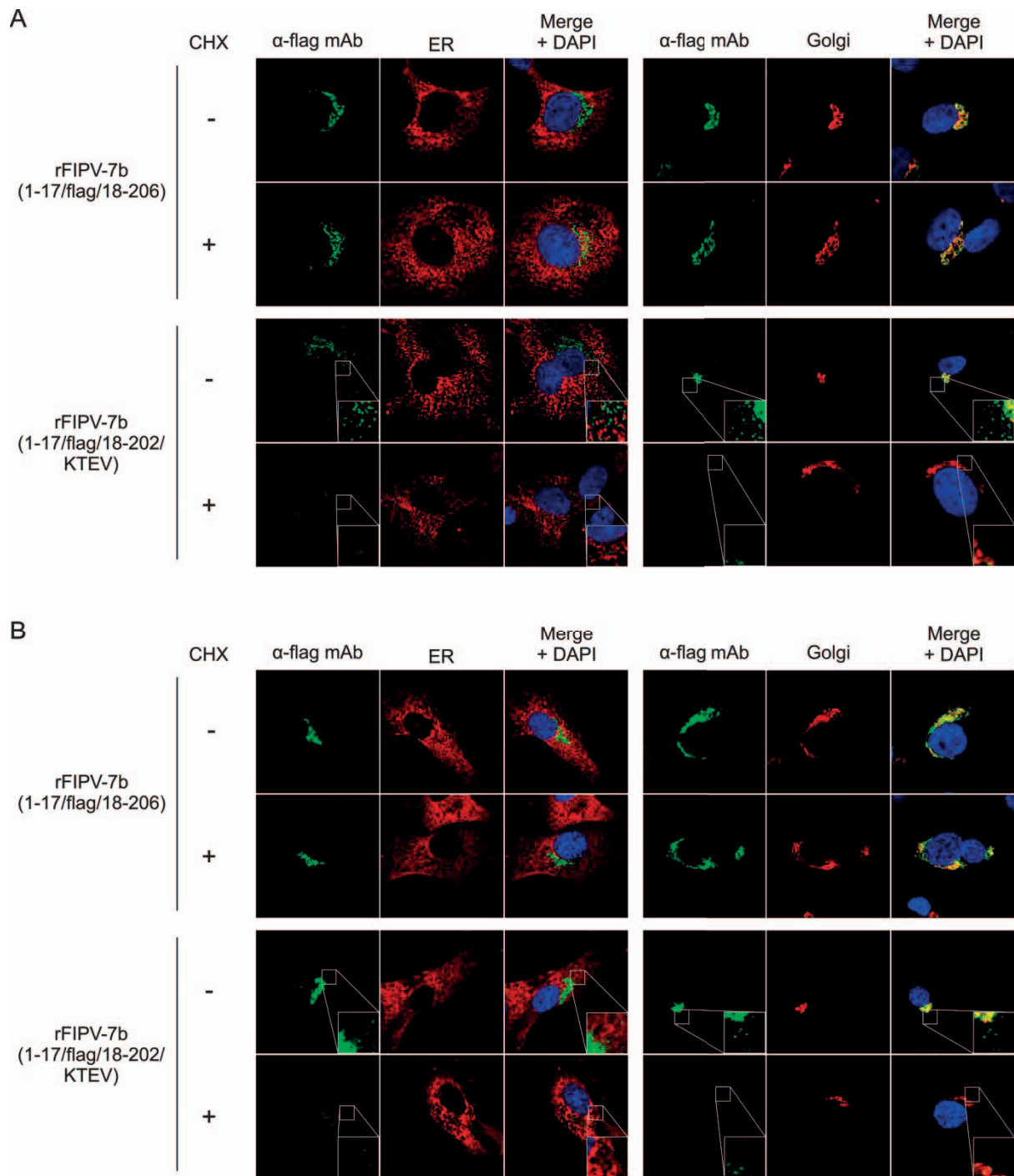


**Figure 32. Effect of cycloheximide treatment on localization of 7b protein with different C-terminal motifs in infected FCWF-4 and Fc3Tg cell lines.** FCWF-4 (A) or Fc3Tg (B) cells were infected with either rFIPV-7b(1-17/flag/18-206) or rFIPV-7b(1-17/flag/18-202/KTEV) at an MOI of 1, respectively. At 8 h post infection the cells were either treated (+) with cycloheximide or left untreated (-). 10 h post infection cells were fixed and analyzed by indirect immunofluorescence assay. 7b protein was visualized using anti-Flag® M2 ( $\alpha$ -flag mAb). Immunofluorescence staining of cell structures: endoplasmic reticulum (ER) (left panel) and Golgi apparatus (right panel) is demonstrated. Cell nuclei were stained blue using DAPI. Immunofluorescence staining was visualized with confocal

laser scanning microscope. CHX, cycloheximide. The inserts in the lower right corner represent an 8x magnification of the selected area.

## 4 Discussion

Feline coronaviruses (FCoVs) infect wild and domestic cats worldwide. In most of the cases, the infection is asymptomatic with occasional onset of mild enteritis. However, in approximately 5% of these cats a lethal disease called feline infectious peritonitis (FIP) develops (Chang et al. 2011; Haijema et al. 2007; Heeney et al. 1990; Hofmann-Lehmann et al. 1996; Munson et al. 2004; O'Brien et al. 1985; Paul-Murphy et al. 1994; Pedersen 2009). Based on antigenic differences, FCoV are divided into two serotypes (I and II) (Heeney et al. 1990; Hohdatsu et al. 1991a; Hohdatsu et al. 1991b; Kennedy et al. 2003). While serotype I FCoVs are responsible for up to 95% of the natural infections, type II FCoVs are less common (Addie et al. 2003; Hohdatsu et al. 1992; Kennedy et al. 2002; Kummrow et al. 2005). Serotype II FCoVs originate from a double homologous recombination between type I FCoVs and type II canine coronaviruses (CCoV) (Decaro & Buonavoglia 2008; Haijema et al. 2007; Herrewegh et al. 1998; Lin et al. 2013; Lorusso et al. 2008; Motokawa et al. 1996; Terada et al. 2014; Vennema 1999). Both serotypes exist in two biotypes. FECVs are responsible for asymptomatic persistent infection, while FIPV infection leads to FIP. It is widely accepted that FIPVs evolve from FECVs by acquiring mutations in persistently infected cats (Chang et al. 2011; Haijema et al. 2007; Pedersen 2009; Poland et al. 1996; Vennema et al. 1998). Mutations responsible for the biotype switch have not been identified yet, but sequence comparisons between FECVs and FIPVs suggested that alterations in the S gene, M gene and accessory genes 3c, 7a and 7b may be involved in FIPV development (Bank-Wolf et al. 2014; Brown et al. 2009; Chang et al. 2010; Chang et al. 2012; Dedeurwaerder et al. 2013; Herrewegh et al. 1995; Kennedy et al. 2001; Licitra et al. 2013; Pedersen et al. 2012; Rottier et al. 2005; Takano et al. 2011; Vennema et al. 1998).

Little is known about the FCoV accessory genes and their products. Using reverse genetics, it was shown that these genes are dispensable for virus growth *in vitro* but are important for the virulence *in vivo* (Haijema et al. 2004). Previous studies suggested that ORF 7 is necessary for FIPV replication in monocytes (Dedeurwaerder et al. 2013), while an intact ORF 3c is needed for replication in the intestine (Balint et al. 2014a; Balint et al. 2014b). Another study suggested that 7a

functions as a counteragent of IFN- $\alpha$  induced antiviral responses (Dedeurwaerder et al. 2014).

In contrast to other FCoV-encoded accessory proteins, only the expression of 7b protein was experimentally demonstrated *in vitro* (Lemmermeyer et al. 2016; Vennema et al. 1992). Additionally, FCoV 7b antibodies have been detected in sera from infected cats indicating the production of 7b protein also *in vivo* (Herrewegh et al. 1995; Kennedy et al. 2008; Vennema et al. 1992). 7b protein has been characterized in a heterologous system using recombinant vaccinia virus-infected and 7b expression plasmid-transfected HeLa cells (Vennema et al. 1992). The authors identified 7b protein as a glycoprotein (26 kDa) with one putative N-glycosylation site. The N-terminal hydrophobic sequence was suggested to represent a signal peptide. 7b protein was proposed to be an ER-resident protein containing a KDEL-like ER retention signal (KTEL) at the C-terminus. It is important to note, that the subcellular localization of 7b protein was exclusively determined by Endoglycosidase H (Endo H) digestion of cell lysates. Additionally, the authors showed that 7b protein was secreted and the C-terminal KTEL motif was responsible for its slow secretion. The KTEL motif was then characterized and mutated to either KTEV or KDEL. The former mutation led to efficient secretion of 7b protein into the cell culture supernatant, while the latter resulted in complete retention of 7b protein in the ER (Vennema et al. 1992).

Due to the lack of proper tools, so far, the characterization of FCoV accessory proteins in FIPV-infected cells was limited. To overcome this limitation, this study focused on the generation of recombinant FCOVs using reverse genetics. The recently established vaccinia virus-based reverse genetic system for type II FIPV strain 79-1146 (Tekes et al. 2012) was used for this purpose. The generated recombinant FIPVs allowed the detailed characterization of 7b protein for the first time in FCoV-infected feline cells.

#### **4.1 Localization of 7b Protein in FIPV-infected Cells**

A monoclonal antibody (mAb) against 7b protein has recently been generated to study this protein in FCoV-infected cat cells (Lemmermeyer et al. 2016). However,

results of the experiments revealed that this mAb did not recognize the mature form of 7b protein but only its non-glycosylated precursor. In order to study the localization of 7b protein in FIPV-infected cells using this antibody (anti-7b 14D8), a recombinant FIPV expressing the non-glycosylated form of 7b protein was generated using vaccinia virus-based reverse genetic system. *In silico* prediction revealed that 7b protein possesses only one N-linked glycosylation site at amino acid position 68. Since some field viruses contain at this position a serine, in rFIPV-7b(1-206/N68S) asparagine was changed to serine (N68S) to remove the glycosylation site in 7b protein. rFIPV-7b(1-206/N68S)-infected CRFK cells were then analyzed with Western blot and confocal microscopy. Cells were harvested before cytopathic effect (CPE) developed to avoid detection of 7b protein in the cell culture supernatant caused by cell lysis. The experiments revealed that the non-glycosylated form of 7b protein was not secreted but retained in the Golgi apparatus in FIPV-infected cells. These results were contradictory to the work of Vennema and colleagues (Vennema et al. 1992).

To clarify whether these discrepancies were related to the absence of glycosylation of 7b protein, a different approach was chosen to detect 7b protein. Using vaccinia virus-based reverse genetic system, a set of recombinant feline coronaviruses expressing flag-tagged 7b protein was generated. Since 7b protein was proposed to contain an N-terminal signal sequence, a flag tag was inserted downstream of the determined signalase cleavage site. Additionally, a virus expressing flag-tagged, non-glycosylated form of 7b protein was generated to enable the comparison of the subcellular localization between glycosylated and non-glycosylated forms of 7b protein. CRFK cells infected with these two viruses were then analyzed with Western blot and confocal microscopy using anti-flag mAb. The results led to the conclusion that irrespective of the glycosylation, 7b protein co-localized exclusively with the Golgi apparatus and was not secreted. To exclude that the obtained results were specific to CRFK cells, the same experiments were performed with other cell lines of cat origin. No difference in the subcellular localization of 7b protein could be detected in various cat cells (data not shown).

To determine the compartment of the Golgi, where 7b protein in FIPV-infected cells is retained, the cell lysate was subjected to PNGase F or Endoglycosidase H (Endo H) treatment. PNGase F treatment resulted in complete removal of the glycan

structure. Endo H digestion led to the detection of Endo H-resistant and -sensitive forms of 7b protein. However, the majority of 7b protein was Endo H-resistant. Since proteins become Endo H-resistant during the glycosylation process in the *medial*- and *trans*-Golgi (Balch & Keller 1986), the experiments showed that 7b protein was retained beyond the *cis*-Golgi. The Endo H-sensitive form represents probably the prematurely glycosylated forms of 7b protein that have not reached the *medial*-Golgi yet.

## **4.2 Role of the C-terminal Sequence in the Localization of 7b Protein**

In the next experiments, the influence of the C-terminus of 7b protein on its subcellular localization was investigated. In order to do so, a virus expressing 7b protein flag-tagged at the C-terminus was generated. The experiments showed that after infection of CRFK cells, 7b protein was detected both in the cell lysate and the cell culture supernatant with Western blot using anti-flag mAb. Confocal microscopy analyses revealed that C-terminal flag-tagged 7b protein co-localized not only with the Golgi apparatus, but was also observed as dense spots in the entire cytoplasm without association of the Golgi to eventually reach the cell surface. Similar results were obtained in cells transfected with a plasmid expressing 7b fused with green fluorescent protein (GFP) at its C-terminus (Dedeurwaerder et al. 2014). These results indicate that the C-terminal flag tag in 7b protein affected the subcellular localization and led to secretion of the protein.

Using the previously described heterologous expression system, the C-terminal KTEL motif of 7b protein was suggested to function as a KDEL-like ER retention signal (Vennema et al. 1992). However, our results indicated that the C-terminal KTEL motif acts as a Golgi, rather than an ER retention signal. To analyze the influence of this signal on 7b protein subcellular localization in FIPV-infected feline cells, a set of recombinant viruses encoding flag-tagged 7b protein with altered KTEL motif was generated using vaccinia virus-based reverse genetic system. (i) Vennema and coworkers (1992) showed that leucine to valine exchange in the KTEL motif abolished ER retention of the protein and facilitated its secretion. Thus, rFIPV-7b(1-17/flag/18-202/KTEV) was generated that expresses 7b protein with the C-terminal

KETV motif. (ii) A recent study described KXD/E C-terminal motif as a Golgi retention signal for various proteins in plants (Gao et al. 2014). In order to elucidate whether KTE motif is sufficient for 7b protein retention in the Golgi, rFIPV-7b(1-17/flag/18-202/KTE) was generated that encodes 7b protein without leucine at aa position 206. (iii) In rFIPV-7b(1-17/flag/18-202/AAAA), the entire KTEL motif was substituted with 4 alanine residues (AAAA). (iv) The C-terminal KDEL motif has been described as a canonical ER retention signal for proteins (Capitani & Sallese 2009; Munro & Pelham 1987; Raykhel et al. 2007). Since Vennema et al. (1992) showed that the exchange of the C-terminal KTEL with KDEL motif led to complete retention of 7b protein in the ER, rFIPV-7b(1-17/flag/18-202/KDEL) was generated. In this virus, the C-terminal KTEL motif in 7b protein was altered into KDEL to investigate whether this change will influence 7b protein retention in the Golgi of FIPV-infected cells. CRFK cells infected with recombinant FIPVs expressing 7b protein with KTEV, KTE or AAAA motif were analyzed with Western blot and confocal microscopy. These alterations of the C-terminus led to the detection of 7b protein as dense spots in the entire cytoplasm and to secretion. In contrast, the C-terminal KDEL motif conferred complete retention of 7b protein in the ER.

The intracellular localization and trafficking of 7b protein was additionally studied in CRFK cells that were treated with cycloheximide (CHX) to block ongoing protein synthesis. Only 7b protein with an authentic C-terminal KTEL motif was retained in the Golgi apparatus after 2 hours treatment with cycloheximide. In contrast, 7b protein with KTEV, KTE or AAAA alterations was barely detectable in infected cells and it did not co-localize with the Golgi suggesting that these mutations abolished Golgi retention. 7b protein with a KDEL motif was completely retained in the ER.

To further confirm the localization of 7b protein, infected cells were incubated for 2 h with CHX, lysed and subjected to Endo H digestion. 7b protein with an authentic C-terminal KTEL motif was entirely Endo H-resistant after CHX treatment indicating complete retention of the protein beyond the *cis*-Golgi compartment. Similar experiment with 7b protein containing a KDEL motif showed that the protein was Endo H-sensitive. This suggests that 7b protein with a KDEL motif did not reach the *medial*-Golgi and was retained in the ER. Altogether, the performed experiments indicate that the authentic C-terminal KTEL motif of FIPV 7b protein is crucial for its

localization in the Golgi apparatus. Identical results were observed with other feline cell lines as well.

### 4.3 Protein Retention in the ER

Different mechanisms for protein retention in the endoplasmic reticulum has been described. Specific signal motifs in the N-, or C-terminus or in the transmembrane domains of proteins were found to confer ER retention (Boulaflous et al. 2009; Capitani & Sallese 2009; Gao et al. 2014; Gomord et al. 1999; Nilsson & Warren 1994; Pelham 1990; Raykhel et al. 2007). Two major ER retention mechanisms that require the C-terminal motif of a protein have been described. Both of them are based on a COPI-dependent retrograde transport of proteins from the *cis*-Golgi to the ER (Gao et al. 2014). COPI is a protein complex that coats vesicles transporting proteins between the Golgi and the ER.

The first mechanism requires a C-terminal di-lysine motif, where two lysine residues are positioned at -3, -4 (KKXX) or -3, -5 (KXKXX) with respect to the C-terminus of a protein (Gao et al. 2014; Jackson et al. 1990; Nilsson & von Heijne 1990). This motif has been identified in a variety of yeast, plant and mammal proteins (Benghezal et al. 2000; Chen et al. 2012; Gaynor et al. 1994; Jackson et al. 1990; Langhans et al. 2008; Montesinos et al. 2012; Montesinos et al. 2013; Nilsson & von Heijne 1990; Townsley & Pelham 1994). The C-terminal di-lysine motif in proteins is recognized by subunits of the COPI complex in the *cis*-Golgi and the protein is transported back to the ER (Contreras et al. 2004; Cosson & Letourneur 1994; Langhans et al. 2008; Letourneur et al. 1994; Montesinos et al. 2012; Montesinos et al. 2013). However, the presence of the KKXX motif at the C-terminus of proteins does not always confer ER retention suggesting that other factors might also be important for the retention of proteins in the ER (Schroder et al. 1995).

The second mechanism requires a C-terminal motif different from KKXX. Based on current knowledge, proteins with KDEL or similar C-terminal motifs (e.g. KTEL, HDEL) are recognized by KDEL receptors located in the *cis*-Golgi compartment and retrieved to the ER by a COPI-dependent retrograde transport (Capitani & Sallese 2009; Gupta et al. 2012; Raykhel et al. 2007; Vennema et al. 1992) (Fig. 33). ER

retention of various proteins has been associated with the presence of a KDEL/KTEL motif at their C-terminus (Byun et al. 2007; Gupta et al. 2012; McCoy et al. 2012). Binding of the target protein to the KDEL receptor is pH dependent. Lower pH of the Golgi apparatus results in association, while higher pH in the lumen of the ER leads to the dissociation of the receptor-protein complex (Wilson et al. 1993).

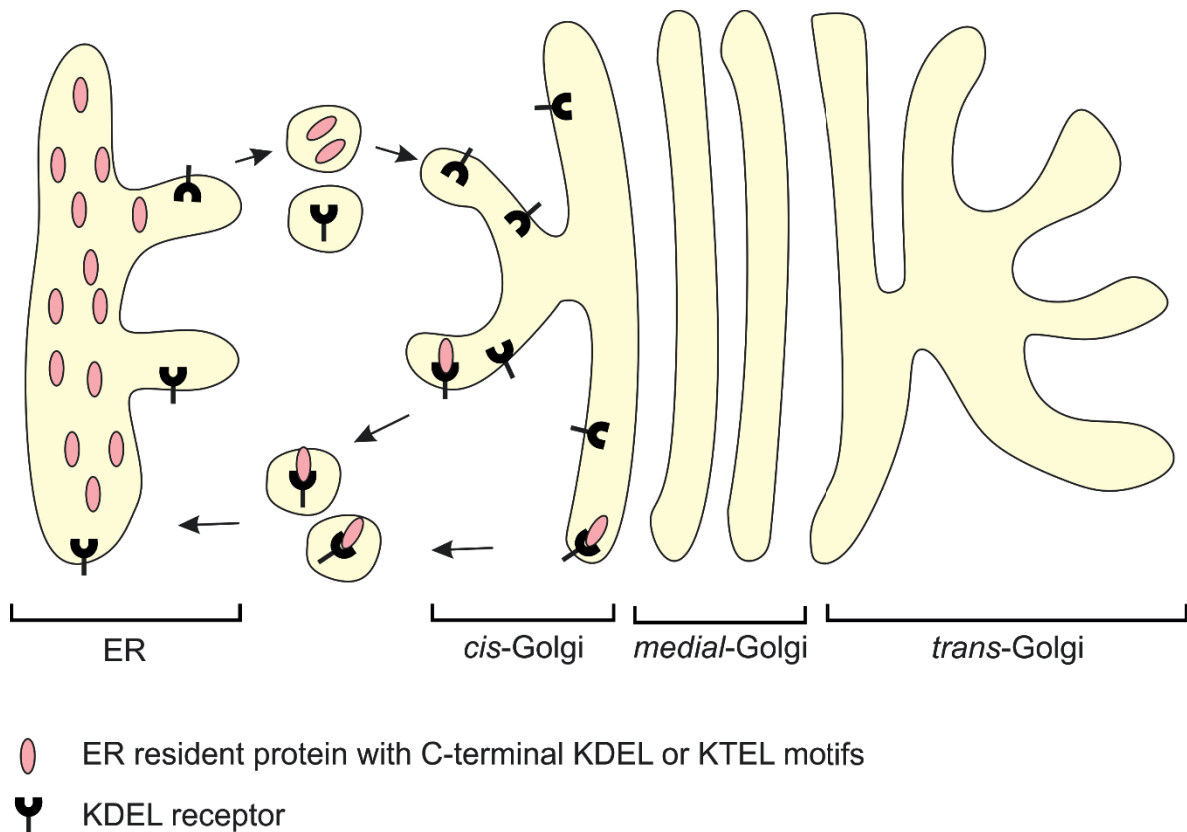


**Figure 33. Retention of proteins with C-terminal KDEL/KTEL motifs in the ER.** Following translation, a protein with C-terminal KDEL/KTEL motifs (red) is transported to the Golgi apparatus. KDEL receptors (black) recognize KDEL/KTEL motifs and induce retrograde transport of the protein to the endoplasmic reticulum (ER).

Up to date, three isoforms of KDEL receptors have been identified with a sequence identity between 80% and 90% (Capitani & Sallese 2009). These isoforms recognize and bind proteins with a variety of C-terminal motifs with variable efficiency, suggesting that certain proteins bind preferentially to one specific isoform (Capitani & Sallese 2009; Raykhel et al. 2007). The efficiency of binding of proteins containing different C-terminal motifs by KDEL receptors was compared in human (HeLa) cells

(Raykhel et al. 2007). The analyses revealed that the KTEL motif was recognized by KDEL receptors with almost the same efficiency as the KDEL motif. KDEL receptors homologs are present in other mammalian species as well. The amino acid sequence comparisons between the corresponding cat and human KDEL receptors revealed 99%, 98.6% and 95% amino acid identity, respectively. The ligand binding specificity of the cat KDEL receptors in comparison with human isoforms is not known.

We assume that, in the study of Vennema et al. (1992), 7b protein was efficiently recognized by KDEL receptors in HeLa cells and thereby retained in the ER. By contrast, the results of the experiments performed in this work suggest that KDEL receptors in cat cell lines do not recognize the KTEL motif at the C-terminus of 7b protein. Accordingly, 7b protein is transported to the Golgi. It is important to note, that the lack of 7b protein binding by the KDEL receptors does not explain its retention in the Golgi apparatus. It appears likely that FIPV 7b protein interacts with a so far unidentified viral or cellular protein that confers Golgi retention in FIPV-infected cells (Fig. 34). Similar mechanisms were described for numerous proteins, for which Golgi retention was accomplished by protein-protein interactions (Banfield 2011; Fukasawa et al. 2004; Gao et al. 2014; Kamena et al. 2008; Munro 1998; Setty et al. 2004).

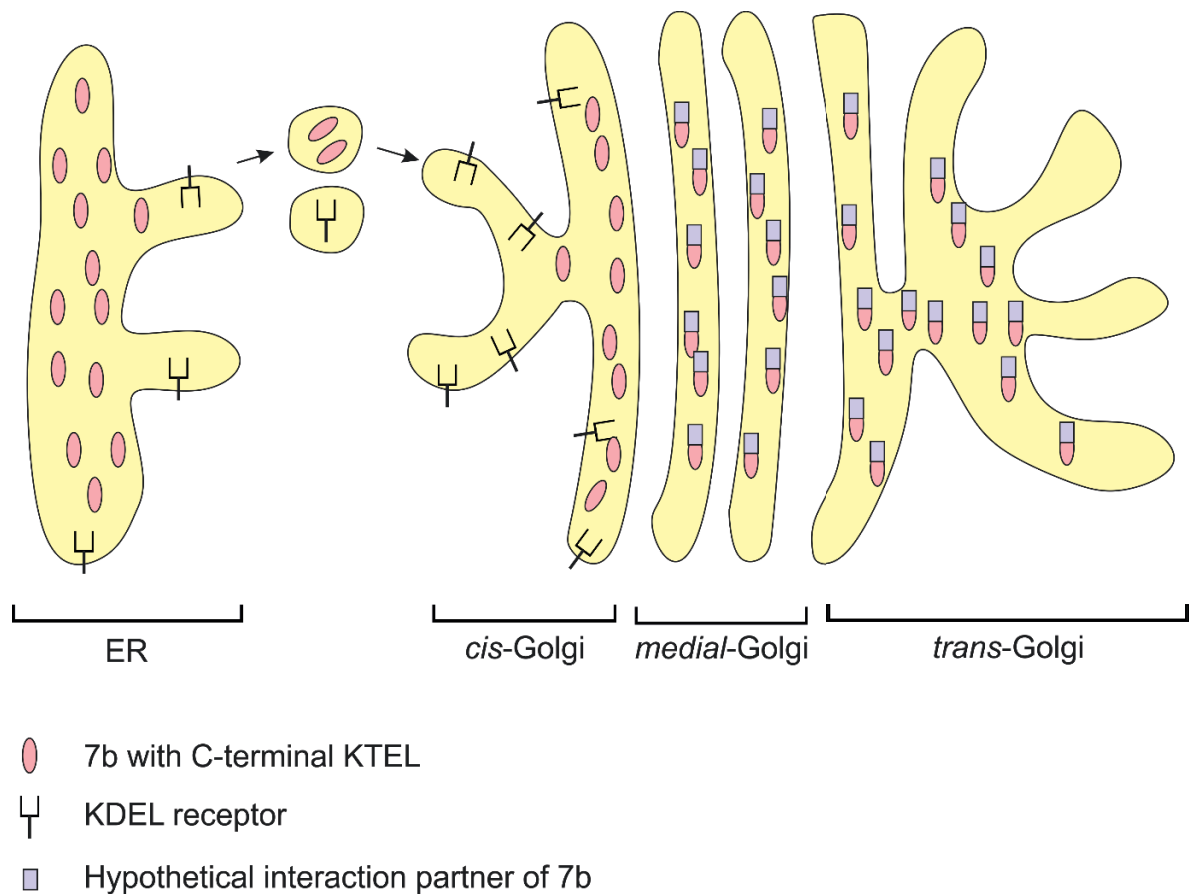


**Figure 34. Model for FCoV 7b Golgi retention in FCoV-infected feline cells.** Following translation, 7b protein with C-terminal KTEL motif (red) is transported to the Golgi apparatus. Feline KDEL receptors (black) are unable to recognize KTEL motif in 7b protein and fail to induce retrograde transport of the protein to the endoplasmic reticulum (ER). Accordingly, 7b protein is transported to the *medial/trans*-Golgi where it interacts with a so far unidentified protein (blue) that confers Golgi retention.

The experiments performed in this work further suggest that alterations of the C-terminal KTEL motif of 7b protein either by mutation (KTEV, KTE and AAAA motifs) or by insertion of a flag tag abolish this interaction that consequently leads to secretion of 7b protein (Fig. 35).

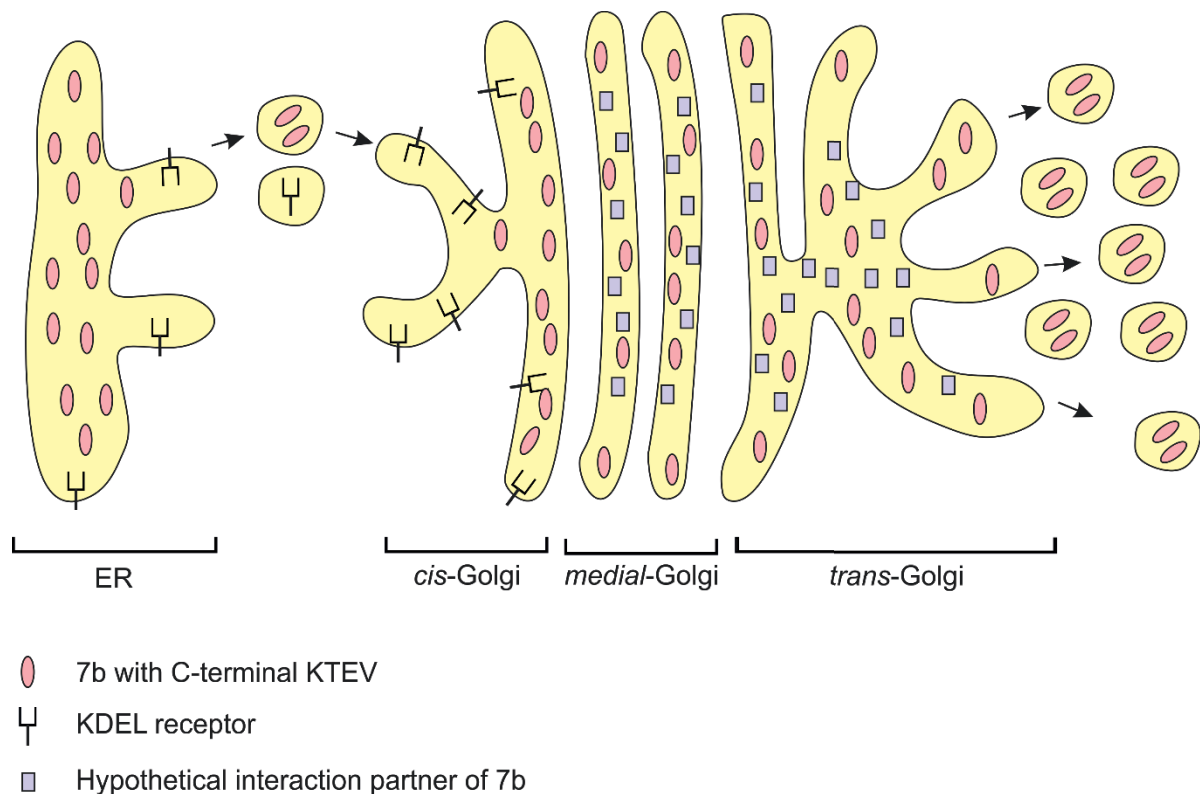


**Figure 35. Model for FCoV 7b trafficking with C-terminal KTEV motif in FCoV-infected feline cells.** Following translation, 7b protein with C-terminal KTEV motif (red) is transported to the Golgi apparatus. Feline KDEL receptors (black) are unable to recognize KTEV motif in 7b protein and fail to induce retrograde transport of the protein to the endoplasmic reticulum (ER). 7b protein with the altered C-terminal motif cannot bind to its hypothetical interaction partner (blue) and Golgi retention is abolished. Accordingly, 7b protein follows the secretory pathway through the *medial/trans*-Golgi to the cell membrane, where it is released.

KDEL receptor-mediated retrograde protein transport may also provide a reasonable explanation for the different observations in 7b protein secretion in the present work and a previous study (Vennema et al. 1992). It has been reported that overproduction of an ER resident protein can lead to secretion by saturation of the KDEL receptor-triggered retention system (Gupta et al. 2012; Munro & Pelham 1987; Semenza et al. 1990). Such a mechanism could serve as an explanation why in HeLa cells the vaccinia virus-based robust expression system used by Vennema and colleagues (1992) led to secretion of 7b protein despite efficient ER retention. Vennema and coworkers (1992) also reported 7b protein secretion in infected cat cells. However, they did not provide any data at which time p.i. 7b protein was detected in the cell culture supernatant. It is likely, that 7b protein was released into

the supernatant due to cell damage caused by FCoV infection at late time points p.i.. This is consistent with our own data, since 7b protein was also found in the supernatant of FCoV-infected cat cells after development of CPE (data not shown).

What is the function of 7b protein and why intercellular retention of this protein is beneficial for the virus remain to be elucidated. We speculate that retention of 7b protein in the Golgi apparatus may contribute to avoid immune recognition and consequently be important for establishment of persistent infection. Further studies are required to test this hypothesis.

Taken together, the data of the current study provides important information on 7b protein and new insight into a Golgi retention signal that controls the trafficking of this protein in FIPV-infected cells.

## 5 Summary

Feline infectious peritonitis (FIP) is one of the most important lethal infectious diseases of cats. The genome of Feline infectious peritonitis virus (FIPV) contains five accessory genes: 3a, 3b, 3c, 7a and 7b. Due to the lack of proper immunological tools, so far, the characterization of putative FIPV accessory proteins was limited. In this study, expression, processing, glycosylation, subcellular localization and trafficking of the accessory protein 7b was studied for the first time in FIPV-infected cells. The following results were obtained:

1. Recombinant FIPV (rFIPV) expressing non-glycosylated form of 7b protein was generated using vaccinia virus-based reverse genetic system. Expression and subcellular localization of this protein in FIPV-infected cells was analyzed with Western blot and confocal microscopy using anti-7b monoclonal antibody (mAb). The data showed that the non-glycosylated form of 7b protein is not secreted but co-localizes with the Golgi apparatus.
2. To characterize the mature, glycosylated form of 7b protein, rFIPVs expressing flag-tagged 7b proteins were generated by reverse genetics. The flag tag was positioned downstream of the signalase cleavage site that was determined with N-terminal Edman sequencing. Expression and subcellular localization of the flag-tagged, mature form of 7b protein in FIPV-infected cells was investigated using Western blot and confocal microscopy with anti-flag mAb. Furthermore, the state of glycosylation of 7b protein was determined with Western blot after treatment with glycosidases. The obtained results indicated that the mature form of 7b protein is not secreted but retained in the medial/trans Golgi.
3. The C-terminal KTEL motif in 7b protein was altered to investigate its influence on the protein subcellular localization in FIPV-infected cells.

Recombinant FIPVs expressing flag-tagged 7b protein with modifications in the C-terminal KTEL motif were generated using reverse genetics. Expression and subcellular localization of the 7b protein with altered C-terminal KTEL motifs in FIPV-infected cells was investigated with Western blot and confocal microscopy using anti-flag mAb. Additionally, the subcellular localization and trafficking of the 7b protein with altered C-terminal motifs was analyzed after inhibition of ongoing protein synthesis. It was shown that 7b protein only with an intact C-terminal KTEL motif was retained in the Golgi apparatus. KTEL to KDEL exchange led to ER retention of the protein, while KTEV, KTE and AAAA alterations abolished Golgi retention and led to efficient secretion of 7b protein.

The results of the current work provide important information on 7b protein and new insight into a Golgi retention signal that controls the trafficking of this protein in FIPV-infected cells. Further studies are required to elucidate the exact role of 7b in the coronaviral life cycle.

## 6 Zusammenfassung

Feline infektiöse Peritonitis (FIP) gehört zu den wichtigsten meist tödlich verlaufenden infektiösen Erkrankungen der Katze. Das FIPV Genom enthält fünf akzessorische Gene: 3a, 3b, 3c, 7a und 7b. Da keine geeigneten immunologischen Reagenzien gegen die akzessorischen Proteine zur Verfügung stehen, war die bisherige Charakterisierung dieser Proteine limitiert. In Rahmen dieser Arbeit wurden die Expression, Prozessierung, Glycosylierung, subzelluläre Lokalisierung und Transport des akzessorischen Proteins 7b zum ersten Mal in FIPV-infizierten Zellen untersucht. Folgende Ergebnisse wurden erhalten:

1. Rekombinantes FIPV (rFIPV), welches eine nicht-glykosylierte Form des 7b Proteins exprimiert, wurde unter Nutzung eines Vaccinia Virus-basierten revers-genetischen Systems erzeugt. Die Expression und die subzelluläre Lokalisierung dieses Proteins wurden sowohl mit Western Blot als auch mit konfokaler Mikroskopie unter Verwendung von anti-7b monoklonalem Antikörper (mAk) in FIPV-infizierten Zellen analysiert. Die erhaltenen Daten zeigten, dass die nicht-glykosylierte Form von 7b Protein nicht sezerniert wird und mit dem Golgi-Apparat kolokalisiert.
2. Zur Charakterisierung der glykosylierten Form des 7b Proteins wurden rFIPVs, die das 7b Protein mit Flag-Tag exprimieren, mit Hilfe eines revers-genetischen Systems erzeugt. Der Flag-Tag wurde stromabwärts der Signalase-Spaltstelle positioniert, welche mittels N-terminaler Edman-Sequenzierung bestimmt wurde. Die Expression und die subzelluläre Lokalisierung der Flag-Tag-markierten, glykosylierten Form des 7b Proteins wurden unter Verwendung von Western Blot und konfokaler Mikroskopie mit anti-Flag mAk in FIPV-infizierten Zellen untersucht. Weiterhin wurde der Glycosylierungszustand des 7b Proteins nach Behandlung mit Glycosidasen mittels Western Blot ermittelt. Die erhaltenen Ergebnisse zeigten, dass die

glykosylierte Form von 7b nicht sezerniert, sondern in dem medial/trans Golgi-Apparat zurückgehalten wird.

3. Um den Einfluss des C-terminalen KTEL-Motivs auf die subzelluläre Lokalisation von 7b in FIPV-infizierten Zellen zu untersuchen, wurde diese Sequenz verändert. Rekombinante FIPVs, die ein Flag-Tag-markiertes 7b Protein mit Modifikationen im C-terminalen KTEL-Motiv exprimieren, wurden unter Nutzung reverser Genetik erzeugt. Die Expression und die subzelluläre Lokalisation des 7b Proteins mit veränderten C-terminalen KTEL-Motiven wurden mit Western Blot und konfokaler Mikroskopie unter Verwendung von anti-Flag mAk in FIPV-infizierten Zellen untersucht. Weiterhin wurden die subzelluläre Lokalisierung und der Transport von 7b Protein mit veränderten C-terminalen Motiven nach Inhibierung der fortlaufenden Proteinsynthese analysiert. Es konnte gezeigt werden, dass 7b Protein nur mit einem intakten C-terminalen KTEL-Motiv im Golgi-Apparat zurückgehalten wird. KTEL-zu-KDEL-Austausch führte zur ER-Retention des Proteins, während KTEV-, KTE- und AAAA-Veränderungen die Golgi-Retention aufhoben und zu einer effizienten Sekretion des 7b Proteins führten.

Die präsentierten Ergebnisse der vorliegenden Arbeit liefern wichtige Informationen über 7b und ein neues Golgi-Retentionssignal, welches den subzellulären Transport von diesem Protein in FIPV-infizierten Zellen bestimmt. Weitere Versuche sind nötig, um die genaue Funktion von 7b in dem coronaviralen Lebenszyklus zu erforschen.

## 7 References

- Adams, M. J., King, A. M. & Carstens, E. B. (2013). Ratification vote on taxonomic proposals to the International Committee on Taxonomy of Viruses (2013). *Arch Virol*, 158 (9): 2023-30.
- Addie, D., Belak, S., Boucraut-Baralon, C., Egberink, H., Frymus, T., Gruffydd-Jones, T., Hartmann, K., Hosie, M. J., Lloret, A., Lutz, H., et al. (2009). Feline infectious peritonitis. ABCD guidelines on prevention and management. *J Feline Med Surg*, 11 (7): 594-604.
- Addie, D. D. & Jarrett, O. (2001). Use of a reverse-transcriptase polymerase chain reaction for monitoring the shedding of feline coronavirus by healthy cats. *Vet Rec*, 148 (21): 649-53.
- Addie, D. D., Schaap, I. A., Nicolson, L. & Jarrett, O. (2003). Persistence and transmission of natural type I feline coronavirus infection. *J Gen Virol*, 84 (Pt 10): 2735-44.
- Almazan, F., Gonzalez, J. M., Penzes, Z., Izeta, A., Calvo, E., Plana-Duran, J. & Enjuanes, L. (2000). Engineering the largest RNA virus genome as an infectious bacterial artificial chromosome. *Proc Natl Acad Sci U S A*, 97 (10): 5516-21.
- Almazan, F., Galan, C. & Enjuanes, L. (2004). The nucleoprotein is required for efficient coronavirus genome replication. *J Virol*, 78 (22): 12683-8.
- Alvarado-Facundo, E., Vassell, R., Schmeisser, F., Weir, J. P., Weiss, C. D. & Wang, W. (2016). Glycosylation of Residue 141 of Subtype H7 Influenza A Hemagglutinin (HA) Affects HA-Pseudovirus Infectivity and Sensitivity to Site A Neutralizing Antibodies. *PLoS One*, 11 (2): e0149149.
- Amer, A., Siti Suri, A., Abdul Rahman, O., Mohd, H. B., Faruku, B., Saeed, S. & Tengku Azmi, T. I. (2012). Isolation and molecular characterization of type I and type II feline coronavirus in Malaysia. *Virology*, 9: 278.
- An, D. J., Jeoung, H. Y., Jeong, W., Park, J. Y., Lee, M. H. & Park, B. K. (2011). Prevalence of Korean cats with natural feline coronavirus infections. *Virology*, 8: 455.

- Balch, W. E. & Keller, D. S. (1986). ATP-coupled transport of vesicular stomatitis virus G protein. Functional boundaries of secretory compartments. *J Biol Chem*, 261 (31): 14690-6.
- Balint, A., Farsang, A., Zadori, Z., Hornyak, A., Dencso, L., Almazan, F., Enjuanes, L. & Belak, S. (2012). Molecular characterization of feline infectious peritonitis virus strain DF-2 and studies of the role of ORF3abc in viral cell tropism. *J Virol*, 86 (11): 6258-67.
- Balint, A., Farsang, A., Szeredi, L., Zadori, Z. & Belak, S. (2014a). Recombinant feline coronaviruses as vaccine candidates confer protection in SPF but not in conventional cats. *Vet Microbiol*, 169 (3-4): 154-62.
- Balint, A., Farsang, A., Zadori, Z. & Belak, S. (2014b). Comparative in vivo analysis of recombinant type II feline coronaviruses with truncated and completed ORF3 region. *PLoS One*, 9 (2): e88758.
- Banfield, D. K. (2011). Mechanisms of protein retention in the Golgi. *Cold Spring Harb Perspect Biol*, 3 (8): a005264.
- Bank-Wolf, B. R., Stallkamp, I., Wiese, S., Moritz, A., Tekes, G. & Thiel, H.-J. (2014). Mutations of 3c and spike protein genes correlate with the occurrence of feline infectious peritonitis. *Vet Microbiol*, 173 (3-4): 177-88.
- Baric, R. S., Nelson, G. W., Fleming, J. O., Deans, R. J., Keck, J. G., Casteel, N. & Stohlman, S. A. (1988). Interactions between coronavirus nucleocapsid protein and viral RNAs: implications for viral transcription. *J Virol*, 62 (11): 4280-7.
- Benghezal, M., Wasteneys, G. O. & Jones, D. A. (2000). The C-terminal dilysine motif confers endoplasmic reticulum localization to type I membrane proteins in plants. *Plant Cell*, 12 (7): 1179-201.
- Bentley, K., Keep, S. M., Armesto, M. & Britton, P. (2013). Identification of a Noncanonically Transcribed Subgenomic mRNA of Infectious Bronchitis Virus and Other Gammacoronaviruses. *Journal of Virology*, 87 (4): 2128-2136.
- Blau, D. M. & Holmes, K. V. (2001). Human coronavirus HCoV-229E enters susceptible cells via the endocytic pathway. *Adv Exp Med Biol*, 494: 193-8.
- Boulaflous, A., Saint-Jore-Dupas, C., Herranz-Gordo, M. C., Pagny-Salehabadi, S., Plasson, C., Garidou, F., Kiefer-Meyer, M. C., Ritzenthaler, C., Faye, L. & Gomord, V. (2009). Cytosolic N-terminal arginine-based signals together with

- a luminal signal target a type II membrane protein to the plant ER. *BMC Plant Biol*, 9: 144.
- Brierley, I., Bournnell, M. E., Binns, M. M., Bilimoria, B., Blok, V. C., Brown, T. D. & Inglis, S. C. (1987). An efficient ribosomal frame-shifting signal in the polymerase-encoding region of the coronavirus IBV. *EMBO J*, 6 (12): 3779-85.
- Brierley, I., Digard, P. & Inglis, S. C. (1989). Characterization of an efficient coronavirus ribosomal frameshifting signal: requirement for an RNA pseudoknot. *Cell*, 57 (4): 537-47.
- Brierley, I. (1995). Ribosomal frameshifting viral RNAs. *J Gen Virol*, 76 ( Pt 8): 1885-92.
- Brown, M. A., Troyer, J. L., Pecon-Slaterry, J., Roelke, M. E. & O'Brien, S. J. (2009). Genetics and pathogenesis of feline infectious peritonitis virus. *Emerg Infect Dis*, 15 (9): 1445-52.
- Brown, P. A., Touzain, F., Briand, F. X., Gouilh, A. M., Courtillon, C., Allee, C., Lemaitre, E., De Boisseson, C., Blanchard, Y. & Etteradossi, N. (2016). First complete genome sequence of European turkey coronavirus suggests complex recombination history related with US turkey and guinea fowl coronaviruses. *J Gen Virol*, 97 (1): 110-20.
- Burda, P. & Aebi, M. (1999). The dolichol pathway of N-linked glycosylation. *Biochim Biophys Acta*, 1426 (2): 239-57.
- Byun, M., Wang, X., Pak, M., Hansen, T. H. & Yokoyama, W. M. (2007). Cowpox virus exploits the endoplasmic reticulum retention pathway to inhibit MHC class I transport to the cell surface. *Cell Host Microbe*, 2 (5): 306-15.
- Capitani, M. & Sallese, M. (2009). The KDEL receptor: new functions for an old protein. *FEBS Lett*, 583 (23): 3863-71.
- Casais, R., Thiel, V., Siddell, S. G., Cavanagh, D. & Britton, P. (2001). Reverse genetics system for the avian coronavirus infectious bronchitis virus. *J Virol*, 75 (24): 12359-69.
- Casais, R., Davies, M., Cavanagh, D. & Britton, P. (2005). Gene 5 of the avian coronavirus infectious bronchitis virus is not essential for replication. *J Virol*, 79 (13): 8065-78.

- Cavanagh, D. (1983). Coronavirus IBV: structural characterization of the spike protein. *J Gen Virol*, 64 ( Pt 12): 2577-83.
- Cavanagh, D., Mawditt, K., Welchman Dde, B., Britton, P. & Gough, R. E. (2002). Coronaviruses from pheasants (*Phasianus colchicus*) are genetically closely related to coronaviruses of domestic fowl (infectious bronchitis virus) and turkeys. *Avian Pathol*, 31 (1): 81-93.
- Chang, H. W., de Groot, R. J., Egberink, H. F. & Rottier, P. J. (2010). Feline infectious peritonitis: insights into feline coronavirus pathobiogenesis and epidemiology based on genetic analysis of the viral 3c gene. *J Gen Virol*, 91 (Pt 2): 415-20.
- Chang, H. W., Egberink, H. F. & Rottier, P. J. (2011). Sequence analysis of feline coronaviruses and the circulating virulent/avirulent theory. *Emerg Infect Dis*, 17 (4): 744-6.
- Chang, H. W., Egberink, H. F., Halpin, R., Spiro, D. J. & Rottier, P. J. (2012). Spike protein fusion peptide and feline coronavirus virulence. *Emerg Infect Dis*, 18 (7): 1089-95.
- Chang, R. Y., Hofmann, M. A., Sethna, P. B. & Brian, D. A. (1994). A cis-acting function for the coronavirus leader in defective interfering RNA replication. *J Virol*, 68 (12): 8223-31.
- Chen, J., Qi, X. & Zheng, H. (2012). Subclass-specific localization and trafficking of Arabidopsis p24 proteins in the ER-Golgi interface. *Traffic*, 13 (3): 400-15.
- Christianson, K. K., Ingersoll, J. D., Landon, R. M., Pfeiffer, N. E. & Gerber, J. D. (1989). Characterization of a temperature sensitive feline infectious peritonitis coronavirus. *Arch Virol*, 109 (3-4): 185-96.
- Chu, V. C., McElroy, L. J., Chu, V., Bauman, B. E. & Whittaker, G. R. (2006). The avian coronavirus infectious bronchitis virus undergoes direct low-pH-dependent fusion activation during entry into host cells. *J Virol*, 80 (7): 3180-8.
- Compton, S. R., Barthold, S. W. & Smith, A. L. (1993). The cellular and molecular pathogenesis of coronaviruses. *Lab Anim Sci*, 43 (1): 15-28.
- Contreras, I., Ortiz-Zapater, E. & Aniento, F. (2004). Sorting signals in the cytosolic tail of membrane proteins involved in the interaction with plant ARF1 and coatomer. *Plant J*, 38 (4): 685-98.

- Corman, V. M., Kallies, R., Philipps, H., Gopner, G., Muller, M. A., Eckerle, I., Brunink, S., Drosten, C. & Drexler, J. F. (2014). Characterization of a novel betacoronavirus related to middle East respiratory syndrome coronavirus in European hedgehogs. *J Virol*, 88 (1): 717-24.
- Cosson, P. & Letourneur, F. (1994). Coatomer interaction with di-lysine endoplasmic reticulum retention motifs. *Science*, 263 (5153): 1629-31.
- Cowley, J. A., Dimmock, C. M., Spann, K. M. & Walker, P. J. (2000). Gill-associated virus of *Penaeus monodon* prawns: an invertebrate virus with ORF1a and ORF1b genes related to arteri- and coronaviruses. *J Gen Virol*, 81 (Pt 6): 1473-84.
- Davies, H. A. & Macnaughton, M. R. (1979). Comparison of the morphology of three coronaviruses. *Arch Virol*, 59 (1-2): 25-33.
- de Brogniez, A., Bouzar, A. B., Jacques, J. R., Cosse, J. P., Gillet, N., Callebaut, I., Reichert, M. & Willems, L. (2015). Mutation of a Single Envelope N-Linked Glycosylation Site Enhances the Pathogenicity of Bovine Leukemia Virus. *J Virol*, 89 (17): 8945-56.
- de Groot, R., Baker, S., Baric, R., Enjuanes, L., Gorbalenya, A., Holmes, K., Perlman, S., Poon, L., Rottier, P., Talbot, P., et al. (2012a). Family Coronaviridae. In King AMQ, A. M., Carstens EB, Lefkowitz EJ (ed.) *Virus taxonomy. Ninth Report of the International Committee on Taxonomy of Viruses.*, pp. 806-828. Amsterdam, NL: Elsevier Academic Press.
- de Groot, R., Cowley, J., Enjuanes, L., Faaberg, K., Perlman, S., Rottier, P., Snijder, E., Ziebuhr, J. & Gorbalenya, A. (2012b). Order Nidovirales. In King AMQ, A. M., Carstens EB, Lefkowitz EJ (ed.) *Virus taxonomy. Ninth Report of the International Committee on Taxonomy of Viruses.*, pp. 785-795. Amsterdam, NL: Elsevier Academic Press.
- de Haan, C. A., Volders, H., Koetzner, C. A., Masters, P. S. & Rottier, P. J. (2002). Coronaviruses maintain viability despite dramatic rearrangements of the strictly conserved genome organization. *J Virol*, 76 (24): 12491-502.
- de Haan, C. A., Haijema, B. J., Boss, D., Heuts, F. W. & Rottier, P. J. (2005). Coronaviruses as vectors: stability of foreign gene expression. *J Virol*, 79 (20): 12742-51.

- Dean, N. (1999). Asparagine-linked glycosylation in the yeast Golgi. *Biochim Biophys Acta*, 1426 (2): 309-22.
- Decaro, N. & Buonavoglia, C. (2008). An update on canine coronaviruses: viral evolution and pathobiology. *Vet Microbiol*, 132 (3-4): 221-34.
- Dedeurwaerder, A., Desmarests, L. M., Olyslaegers, D. A., Vermeulen, B. L., Dewerchin, H. L. & Nauwynck, H. J. (2013). The role of accessory proteins in the replication of feline infectious peritonitis virus in peripheral blood monocytes. *Vet Microbiol*, 162 (2-4): 447-55.
- Dedeurwaerder, A., Olyslaegers, D. A., Desmarests, L. M., Roukaerts, I. D., Theuns, S. & Nauwynck, H. J. (2014). ORF7-encoded accessory protein 7a of feline infectious peritonitis virus as a counteragent against IFN-alpha-induced antiviral response. *J Gen Virol*, 95 (Pt 2): 393-402.
- DeDiego, M. L., Nieto-Torres, J. L., Jimenez-Guardeno, J. M., Regla-Nava, J. A., Alvarez, E., Oliveros, J. C., Zhao, J., Fett, C., Perlman, S. & Enjuanes, L. (2011). Severe acute respiratory syndrome coronavirus envelope protein regulates cell stress response and apoptosis. *PLoS Pathog*, 7 (10): e1002315.
- Delmas, B. & Laude, H. (1990). Assembly of coronavirus spike protein into trimers and its role in epitope expression. *J Virol*, 64 (11): 5367-75.
- Delmas, B., Gelfi, J., L'Haridon, R., Vogel, L. K., Sjostrom, H., Noren, O. & Laude, H. (1992). Aminopeptidase N is a major receptor for the entero-pathogenic coronavirus TGEV. *Nature*, 357 (6377): 417-20.
- Dewerchin, H. L., Cornelissen, E. & Nauwynck, H. J. (2005). Replication of feline coronaviruses in peripheral blood monocytes. *Arch Virol*, 150 (12): 2483-500.
- Ding, Z., Fang, L., Jing, H., Zeng, S., Wang, D., Liu, L., Zhang, H., Luo, R., Chen, H. & Xiao, S. (2014). Porcine epidemic diarrhea virus nucleocapsid protein antagonizes beta interferon production by sequestering the interaction between IRF3 and TBK1. *J Virol*, 88 (16): 8936-45.
- Drechsler, Y., Alcaraz, A., Bossong, F. J., Collisson, E. W. & Diniz, P. P. (2011). Feline coronavirus in multicat environments. *Vet Clin North Am Small Anim Pract*, 41 (6): 1133-69.
- Dveksler, G. S., Pensiero, M. N., Cardellichio, C. B., Williams, R. K., Jiang, G. S., Holmes, K. V. & Dieffenbach, C. W. (1991). Cloning of the mouse hepatitis

- virus (MHV) receptor: expression in human and hamster cell lines confers susceptibility to MHV. *J Virol*, 65 (12): 6881-91.
- Dveksler, G. S., Dieffenbach, C. W., Cardellicchio, C. B., McCuaig, K., Pensiero, M. N., Jiang, G. S., Beauchemin, N. & Holmes, K. V. (1993). Several members of the mouse carcinoembryonic antigen-related glycoprotein family are functional receptors for the coronavirus mouse hepatitis virus-A59. *J Virol*, 67 (1): 1-8.
- Dye, C. & Siddell, S. G. (2005). Genomic RNA sequence of Feline coronavirus strain FIPV WSU-79/1146. *J Gen Virol*, 86 (Pt 8): 2249-53.
- Ellgaard, L. & Helenius, A. (2003). Quality control in the endoplasmic reticulum. *Nature Reviews Molecular Cell Biology*, 4 (3): 181-191.
- Eriksson, K. K., Makia, D. & Thiel, V. (2008). Generation of recombinant coronaviruses using vaccinia virus as the cloning vector and stable cell lines containing coronaviral replicon RNAs. *Methods Mol Biol*, 454: 237-54.
- Ermonval, M., Kitzmuller, C., Mir, A. M., Cacan, R. & Ivessa, N. E. (2001). N-glycan structure of a short-lived variant of ribophorin I expressed in the MadIA214 glycosylation-defective cell line reveals the role of a mannosidase that is not ER mannosidase I in the process of glycoprotein degradation. *Glycobiology*, 11 (7): 565-76.
- Escors, D., Ortego, J., Laude, H. & Enjuanes, L. (2001). The membrane M protein carboxy terminus binds to transmissible gastroenteritis coronavirus core and contributes to core stability. *J Virol*, 75 (3): 1312-24.
- Fang, P., Fang, L., Liu, X., Hong, Y., Wang, Y., Dong, N., Ma, P., Bi, J., Wang, D. & Xiao, S. (2016). Identification and subcellular localization of porcine deltacoronavirus accessory protein NS6. *Virology*, 499: 170-177.
- Florek, D., Ehmann, R., Kristen-Burmann, C., Lemmermeyer, T., Lochnit, G., Ziebuhr, J., Thiel, H.-J. & Tekes, G. (2017). Identification and characterization of a Golgi retention signal in feline coronavirus accessory protein 7b. *J Gen Virol*, 98 (8): 2017-29.
- Foley, J. E., Poland, A., Carlson, J. & Pedersen, N. C. (1997). Patterns of feline coronavirus infection and fecal shedding from cats in multiple-cat environments. *J Am Vet Med Assoc*, 210 (9): 1307-12.

- Frenkel, Z., Gregory, W., Kornfeld, S. & Lederkremer, G. Z. (2003). Endoplasmic reticulum-associated degradation of mammalian glycoproteins involves sugar chain trimming to Man6-5GlcNAc2. *J Biol Chem*, 278 (36): 34119-24.
- Fukasawa, M., Varlamov, O., Eng, W. S., Sollner, T. H. & Rothman, J. E. (2004). Localization and activity of the SNARE Ykt6 determined by its regulatory domain and palmitoylation. *Proc Natl Acad Sci U S A*, 101 (14): 4815-20.
- Gao, C., Cai, Y., Wang, Y., Kang, B. H., Aniento, F., Robinson, D. G. & Jiang, L. (2014). Retention mechanisms for ER and Golgi membrane proteins. *Trends Plant Sci*, 19 (8): 508-15.
- Garner, M. M., Ramsell, K., Morera, N., Juan-Salles, C., Jimenez, J., Ardiaca, M., Montesinos, A., Teifke, J. P., Lohr, C. V., Evermann, J. F., et al. (2008). Clinicopathologic features of a systemic coronavirus-associated disease resembling feline infectious peritonitis in the domestic ferret (*Mustela putorius*). *Vet Pathol*, 45 (2): 236-46.
- Gaynor, E. C., te Heesen, S., Graham, T. R., Aebi, M. & Emr, S. D. (1994). Signal-mediated retrieval of a membrane protein from the Golgi to the ER in yeast. *J Cell Biol*, 127 (3): 653-65.
- Gerber, J. D., Ingersoll, J. D., Gast, A. M., Christianson, K. K., Selzer, N. L., Landon, R. M., Pfeiffer, N. E., Sharpee, R. L. & Beckenhauer, W. H. (1990a). Protection against feline infectious peritonitis by intranasal inoculation of a temperature-sensitive FIPV vaccine. *Vaccine*, 8 (6): 536-42.
- Gerber, J. D., Pfeiffer, N. E., Ingersoll, J. D., Christianson, K. K., Landon, R. M., Selzer, N. L. & Beckenhauer, W. H. (1990b). Characterization of an attenuated temperature sensitive feline infectious peritonitis vaccine virus. *Adv Exp Med Biol*, 276: 481-9.
- Goitsuka, R., Ohashi, T., Ono, K., Yasukawa, K., Koishibara, Y., Fukui, H., Ohsugi, Y. & Hasegawa, A. (1990). IL-6 activity in feline infectious peritonitis. *J Immunol*, 144 (7): 2599-603.
- Gomord, V., Wee, E. & Faye, L. (1999). Protein retention and localization in the endoplasmic reticulum and the golgi apparatus. *Biochimie*, 81 (6): 607-18.
- Gorbalenya, A. E., Enjuanes, L., Ziebuhr, J. & Snijder, E. J. (2006). Nidovirales: evolving the largest RNA virus genome. *Virus Res*, 117 (1): 17-37.

- Gosert, R., Kanjanahaluethai, A., Egger, D., Bienz, K. & Baker, S. C. (2002). RNA replication of mouse hepatitis virus takes place at double-membrane vesicles. *J Virol*, 76 (8): 3697-708.
- Gunn-Moore, D. A., Gruffydd-Jones, T. J. & Harbour, D. A. (1998). Detection of feline coronaviruses by culture and reverse transcriptase-polymerase chain reaction of blood samples from healthy cats and cats with clinical feline infectious peritonitis. *Vet Microbiol*, 62 (3): 193-205.
- Gupta, A., Dong, A. & Lowe, A. W. (2012). AGR2 gene function requires a unique endoplasmic reticulum localization motif. *J Biol Chem*, 287 (7): 4773-82.
- Haijema, B., Rottier, P. & de Groot, R. (2007). Feline Coronaviruses: A tale of two-faced types. In Thiel V (ed.) *Coronaviruses - Molecular and Cellular Biology*., pp. 183-208. Norfolk, UK: Caister Academic Press.
- Haijema, B. J., Volders, H. & Rottier, P. J. (2003). Switching species tropism: an effective way to manipulate the feline coronavirus genome. *J Virol*, 77 (8): 4528-38.
- Haijema, B. J., Volders, H. & Rottier, P. J. (2004). Live, attenuated coronavirus vaccines through the directed deletion of group-specific genes provide protection against feline infectious peritonitis. *J Virol*, 78 (8): 3863-71.
- Hanke, D., Jenckel, M., Petrov, A., Ritzmann, M., Stadler, J., Akimkin, V., Blome, S., Pohlmann, A., Schirrmeyer, H., Beer, M., et al. (2015). Comparison of porcine epidemic diarrhea viruses from Germany and the United States, 2014. *Emerg Infect Dis*, 21 (3): 493-6.
- Hansen, G. H., Delmas, B., Besnardeau, L., Vogel, L. K., Laude, H., Sjostrom, H. & Noren, O. (1998). The coronavirus transmissible gastroenteritis virus causes infection after receptor-mediated endocytosis and acid-dependent fusion with an intracellular compartment. *J Virol*, 72 (1): 527-34.
- Harcourt, B. H., Jukneliene, D., Kanjanahaluethai, A., Bechill, J., Severson, K. M., Smith, C. M., Rota, P. A. & Baker, S. C. (2004). Identification of severe acute respiratory syndrome coronavirus replicase products and characterization of papain-like protease activity. *J Virol*, 78 (24): 13600-12.
- Hartmann, K. (2005). Feline infectious peritonitis. *Vet Clin North Am Small Anim Pract*, 35 (1): 39-79, vi.

- Heeney, J. L., Evermann, J. F., McKeirnan, A. J., Marker-Kraus, L., Roelke, M. E., Bush, M., Wildt, D. E., Meltzer, D. G., Colly, L., Lukas, J., et al. (1990). Prevalence and implications of feline coronavirus infections of captive and free-ranging cheetahs (*Acinonyx jubatus*). *J Virol*, 64 (5): 1964-72.
- Herrewegh, A. A., Vennema, H., Horzinek, M. C., Rottier, P. J. & de Groot, R. J. (1995). The molecular genetics of feline coronaviruses: comparative sequence analysis of the ORF7a/7b transcription unit of different biotypes. *Virology*, 212 (2): 622-31.
- Herrewegh, A. A., Mahler, M., Hedrich, H. J., Haagmans, B. L., Egberink, H. F., Horzinek, M. C., Rottier, P. J. & de Groot, R. J. (1997). Persistence and evolution of feline coronavirus in a closed cat-breeding colony. *Virology*, 234 (2): 349-63.
- Herrewegh, A. A., Smeenk, I., Horzinek, M. C., Rottier, P. J. & de Groot, R. J. (1998). Feline coronavirus type II strains 79-1683 and 79-1146 originate from a double recombination between feline coronavirus type I and canine coronavirus. *J Virol*, 72 (5): 4508-14.
- Hertzog, T., Scandella, E., Schelle, B., Ziebuhr, J., Siddell, S. G., Ludewig, B. & Thiel, V. (2004). Rapid identification of coronavirus replicase inhibitors using a selectable replicon RNA. *J Gen Virol*, 85 (Pt 6): 1717-25.
- Hodgson, T., Britton, P. & Cavanagh, D. (2006). Neither the RNA nor the proteins of open reading frames 3a and 3b of the coronavirus infectious bronchitis virus are essential for replication. *J Virol*, 80 (1): 296-305.
- Hofmann-Lehmann, R., Fehr, D., Grob, M., Elgizoli, M., Packer, C., Martenson, J. S., O'Brien, S. J. & Lutz, H. (1996). Prevalence of antibodies to feline parvovirus, calicivirus, herpesvirus, coronavirus, and immunodeficiency virus and of feline leukemia virus antigen and the interrelationship of these viral infections in free-ranging lions in east Africa. *Clin Diagn Lab Immunol*, 3 (5): 554-62.
- Hofmann, H., Pyrc, K., van der Hoek, L., Geier, M., Berkhout, B. & Pohlmann, S. (2005). Human coronavirus NL63 employs the severe acute respiratory syndrome coronavirus receptor for cellular entry. *Proc Natl Acad Sci U S A*, 102 (22): 7988-93.
- Hohdatsu, T., Okada, S. & Koyama, H. (1991a). Characterization of Monoclonal Antibodies against Feline Infectious Peritonitis Virus Type-I and Antigenic

- Relationship between Feline, Porcine, and Canine Coronaviruses. *Archives of Virology*, 117 (1-2): 85-95.
- Hohdatsu, T., Sasamoto, T., Okada, S. & Koyama, H. (1991b). Antigenic Analysis of Feline Coronaviruses with Monoclonal-Antibodies (Mabs) - Preparation of Mabs Which Discriminate between Fipv Strain-79-1146 and Fecv Strain-79-1683. *Veterinary Microbiology*, 28 (1): 13-24.
- Hohdatsu, T., Okada, S., Ishizuka, Y., Yamada, H. & Koyama, H. (1992). The prevalence of types I and II feline coronavirus infections in cats. *J Vet Med Sci*, 54 (3): 557-62.
- Hohdatsu, T., Izumiya, Y., Yokoyama, Y., Kida, K. & Koyama, H. (1998). Differences in virus receptor for type I and type II feline infectious peritonitis virus. *Arch Virol*, 143 (5): 839-50.
- Holzworth, J. (1963). Some important disorders of cats. *Cornell Vet*, 53: 157-60.
- Hosokawa, N., Tremblay, L. O., You, Z., Herscovics, A., Wada, I. & Nagata, K. (2003). Enhancement of endoplasmic reticulum (ER) degradation of misfolded Null Hong Kong alpha1-antitrypsin by human ER mannosidase I. *J Biol Chem*, 278 (28): 26287-94.
- Jackson, M. R., Nilsson, T. & Peterson, P. A. (1990). Identification of a consensus motif for retention of transmembrane proteins in the endoplasmic reticulum. *EMBO J*, 9 (10): 3153-62.
- Kamena, F., Diefenbacher, M., Kilchert, C., Schwarz, H. & Spang, A. (2008). Ypt1p is essential for retrograde Golgi-ER transport and for Golgi maintenance in *S. cerevisiae*. *J Cell Sci*, 121 (Pt 8): 1293-302.
- Kariwa, H., Murata, R., Totani, M., Yoshii, K. & Takashima, I. (2013). Increased pathogenicity of West Nile virus (WNV) by glycosylation of envelope protein and seroprevalence of WNV in wild birds in Far Eastern Russia. *Int J Environ Res Public Health*, 10 (12): 7144-64.
- Kennedy, M., Boedeker, N., Gibbs, P. & Kania, S. (2001). Deletions in the 7a ORF of feline coronavirus associated with an epidemic of feline infectious peritonitis. *Vet Microbiol*, 81 (3): 227-34.
- Kennedy, M., Citino, S., McNabb, A. H., Moffatt, A. S., Gertz, K. & Kania, S. (2002). Detection of feline coronavirus in captive Felidae in the USA. *J Vet Diagn Invest*, 14 (6): 520-2.

- Kennedy, M., Kania, S., Stylianides, E., Bertschinger, H., Keet, D. & van Vuuren, M. (2003). Detection of feline coronavirus infection in southern African nondomestic felids. *J Wildl Dis*, 39 (3): 529-35.
- Kennedy, M. A., Abd-Eldaim, M., Zika, S. E., Mankin, J. M. & Kania, S. A. (2008). Evaluation of antibodies against feline coronavirus 7b protein for diagnosis of feline infectious peritonitis in cats. *Am J Vet Res*, 69 (9): 1179-82.
- Kerr, S. M. & Smith, G. L. (1991). Vaccinia virus DNA ligase is nonessential for virus replication: recovery of plasmids from virus-infected cells. *Virology*, 180 (2): 625-32.
- Kim, Y., Liu, H., Galasiti Kankanamalage, A. C., Weerasekara, S., Hua, D. H., Groutas, W. C., Chang, K. O. & Pedersen, N. C. (2016). Reversal of the Progression of Fatal Coronavirus Infection in Cats by a Broad-Spectrum Coronavirus Protease Inhibitor. *PLoS Pathog*, 12 (3): e1005531.
- King, B., Potts, B. J. & Brian, D. A. (1985). Bovine coronavirus hemagglutinin protein. *Virus Res*, 2 (1): 53-9.
- Kipar, A., May, H., Menger, S., Weber, M., Leukert, W. & Reinacher, M. (2005). Morphologic features and development of granulomatous vasculitis in feline infectious peritonitis. *Vet Pathol*, 42 (3): 321-30.
- Kipar, A., Meli, M. L., Failing, K., Euler, T., Gomes-Keller, M. A., Schwartz, D., Lutz, H. & Reinacher, M. (2006). Natural feline coronavirus infection: differences in cytokine patterns in association with the outcome of infection. *Vet Immunol Immunopathol*, 112 (3-4): 141-55.
- Kipar, A., Meli, M. L., Baptiste, K. E., Bowker, L. J. & Lutz, H. (2010). Sites of feline coronavirus persistence in healthy cats. *J Gen Virol*, 91 (Pt 7): 1698-707.
- Kipar, A. & Meli, M. L. (2014). Feline infectious peritonitis: still an enigma? *Vet Pathol*, 51 (2): 505-26.
- Kiss, I., Poland, A. M. & Pedersen, N. C. (2004). Disease outcome and cytokine responses in cats immunized with an avirulent feline infectious peritonitis virus (FIPV)-UCD1 and challenge-exposed with virulent FIPV-UCD8. *J Feline Med Surg*, 6 (2): 89-97.
- Kitzmuller, C., Caprini, A., Moore, S. E., Frenoy, J. P., Schwaiger, E., Kellermann, O., Ivessa, N. E. & Ermonval, M. (2003). Processing of N-linked glycans

- during endoplasmic-reticulum-associated degradation of a short-lived variant of ribophorin I. *Biochem J*, 376 (Pt 3): 687-96.
- Klumperman, J., Locker, J. K., Meijer, A., Horzinek, M. C., Geuze, H. J. & Rottier, P. J. (1994). Coronavirus M proteins accumulate in the Golgi complex beyond the site of virion budding. *J Virol*, 68 (10): 6523-34.
- Kolb, A. F., Hegyi, A., Maile, J., Heister, A., Hagemann, M. & Siddell, S. G. (1998). Molecular analysis of the coronavirus-receptor function of aminopeptidase N. *Adv Exp Med Biol*, 440: 61-7.
- Krempl, C., Schultze, B. & Herrler, G. (1995). Analysis of cellular receptors for human coronavirus OC43. *Adv Exp Med Biol*, 380: 371-4.
- Kubo, H., Yamada, Y. K. & Taguchi, F. (1994). Localization of neutralizing epitopes and the receptor-binding site within the amino-terminal 330 amino acids of the murine coronavirus spike protein. *J Virol*, 68 (9): 5403-10.
- Kummrow, M., Meli, M. L., Haessig, M., Goenczi, E., Poland, A., Pedersen, N. C., Hofmann-Lehmann, R. & Lutz, H. (2005). Feline coronavirus serotypes 1 and 2: seroprevalence and association with disease in Switzerland. *Clin Diagn Lab Immunol*, 12 (10): 1209-15.
- Laemmli, U. K. (1970). Cleavage of structural proteins during the assembly of the head of bacteriophage T4. *Nature*, 227 (5259): 680-5.
- Lai, M. & Holmes, K. (2001). Coronaviruses. In Knipe DM, H. P., Griffin DE, Lamb RA, Martin MA, Roizman B, Straus SE (ed.) *Fields virology*, pp. 1163-1185. Philadelphia, USA: Lippincott Williams & Wilkins.
- Lai, M. M. & Stohlman, S. A. (1978). RNA of mouse hepatitis virus. *J Virol*, 26 (2): 236-42.
- Lai, M. M. & Stohlman, S. A. (1981). Comparative analysis of RNA genomes of mouse hepatitis viruses. *J Virol*, 38 (2): 661-70.
- Lai, M. M. & Cavanagh, D. (1997). The molecular biology of coronaviruses. *Adv Virus Res*, 48: 1-100.
- Langereis, M. A., van Vliet, A. L., Boot, W. & de Groot, R. J. (2010). Attachment of mouse hepatitis virus to O-acetylated sialic acid is mediated by hemagglutinin-esterase and not by the spike protein. *J Virol*, 84 (17): 8970-4.

- Langhans, M., Marcote, M. J., Pimpl, P., Virgili-Lopez, G., Robinson, D. G. & Aniento, F. (2008). In vivo trafficking and localization of p24 proteins in plant cells. *Traffic*, 9 (5): 770-85.
- Laude, H. & Masters, P. S. (1995). The coronavirus nucleocapsid protein. In Siddell, S. G. (ed.) *The Coronaviridae.*, pp. 141-163. New York, USA: Plenum Press.
- Lemmermeyer, T., Lamp, B., Schneider, R., Ziebuhr, J., Tekes, G. & Thiel, H.-J. (2016). Characterization of monoclonal antibodies against feline coronavirus accessory protein 7b. *Vet Microbiol*, 184: 11-9.
- Letourneur, F., Gaynor, E. C., Hennecke, S., Demolliere, C., Duden, R., Emr, S. D., Riezman, H. & Cosson, P. (1994). Coatamer is essential for retrieval of dilysine-tagged proteins to the endoplasmic reticulum. *Cell*, 79 (7): 1199-207.
- Li, B. X., Ge, J. W. & Li, Y. J. (2007). Porcine aminopeptidase N is a functional receptor for the PEDV coronavirus. *Virology*, 365 (1): 166-72.
- Li, W., Moore, M. J., Vasilieva, N., Sui, J., Wong, S. K., Berne, M. A., Somasundaran, M., Sullivan, J. L., Luzuriaga, K., Greenough, T. C., et al. (2003). Angiotensin-converting enzyme 2 is a functional receptor for the SARS coronavirus. *Nature*, 426 (6965): 450-4.
- Licitra, B. N., Millet, J. K., Regan, A. D., Hamilton, B. S., Rinaldi, V. D., Duhamel, G. E. & Whittaker, G. R. (2013). Mutation in spike protein cleavage site and pathogenesis of feline coronavirus. *Emerg Infect Dis*, 19 (7): 1066-73.
- Lin, C. N., Chang, R. Y., Su, B. L. & Chueh, L. L. (2013). Full genome analysis of a novel type II feline coronavirus NTU156. *Virus Genes*, 46 (2): 316-22.
- Liu, D. X. & Inglis, S. C. (1991). Association of the infectious bronchitis virus 3c protein with the virion envelope. *Virology*, 185 (2): 911-7.
- Liu, D. X. & Inglis, S. C. (1992a). Identification of two new polypeptides encoded by mRNA5 of the coronavirus infectious bronchitis virus. *Virology*, 186 (1): 342-7.
- Liu, D. X. & Inglis, S. C. (1992b). Internal entry of ribosomes on a tricistronic mRNA encoded by infectious bronchitis virus. *J Virol*, 66 (10): 6143-54.
- Liu, D. X., Fung, T. S., Chong, K. K., Shukla, A. & Hilgenfeld, R. (2014). Accessory proteins of SARS-CoV and other coronaviruses. *Antiviral Res*, 109: 97-109.
- Lodish, H., Berk, A. & Zipursky, S. (2000). Section 17.7, Protein Glycosylation in the ER and Golgi Complex. . In *Molecular Cell Biology. 4th edition*. New York: W. H. Freeman.

- Lomniczi, B. (1977). Biological properties of avian coronavirus RNA. *J Gen Virol*, 36 (3): 531-3.
- Lorusso, A., Decaro, N., Schellen, P., Rottier, P. J., Buonavoglia, C., Haijema, B. J. & de Groot, R. J. (2008). Gain, preservation, and loss of a group 1a coronavirus accessory glycoprotein. *J Virol*, 82 (20): 10312-7.
- Lu, X., Pan, J., Tao, J. & Guo, D. (2011). SARS-CoV nucleocapsid protein antagonizes IFN-beta response by targeting initial step of IFN-beta induction pathway, and its C-terminal region is critical for the antagonism. *Virus Genes*, 42 (1): 37-45.
- Luo, S., Hu, K., He, S., Wang, P., Zhang, M., Huang, X., Du, T., Zheng, C., Liu, Y. & Hu, Q. (2015). Contribution of N-linked glycans on HSV-2 gB to cell-cell fusion and viral entry. *Virology*, 483: 72-82.
- Madhugiri, R., Fricke, M., Marz, M. & Ziebuhr, J. (2014). RNA structure analysis of alphacoronavirus terminal genome regions. *Virus Res*, 194: 76-89.
- Madhugiri, R., Fricke, M., Marz, M. & Ziebuhr, J. (2016). Coronavirus cis-Acting RNA Elements. *Adv Virus Res*, 96: 127-163.
- Marshall, R. D. (1972). Glycoproteins. *Annu Rev Biochem*, 41: 673-702.
- Masters, P. (2007). Genomic cis-acting elements in coronavirus RNA replication. In V, T. (ed.) *Coronaviruses - Molecular and Cellular Biology.*, pp. 65-80. Norfolk, UK: Caister Academic Press.
- Masters, P. S. (2006). The molecular biology of coronaviruses. *Adv Virus Res*, 66: 193-292.
- McBride, C. E. & Machamer, C. E. (2010). Palmitoylation of SARS-CoV S protein is necessary for partitioning into detergent-resistant membranes and cell-cell fusion but not interaction with M protein. *Virology*, 405 (1): 139-48.
- McCoy, W. H., Wang, X. L., Yokoyama, W. M., Hansen, T. H. & Fremont, D. H. (2012). Structural Mechanism of ER Retrieval of MHC Class I by Cowpox. *Plos Biology*, 10 (11).
- McDonald, A. G., Hayes, J. M. & Davey, G. P. (2016). Metabolic flux control in glycosylation. *Curr Opin Struct Biol*, 40: 97-103.
- Mihindukulasuriya, K. A., Wu, G., St Leger, J., Nordhausen, R. W. & Wang, D. (2008). Identification of a novel coronavirus from a beluga whale by using a panviral microarray. *J Virol*, 82 (10): 5084-8.

- Montali, R. J. & Strandberg, J. D. (1972). Extraperitoneal lesions in feline infectious peritonitis. *Vet Pathol*, 9 (2): 109-21.
- Montesinos, J. C., Sturm, S., Langhans, M., Hillmer, S., Marcote, M. J., Robinson, D. G. & Aniento, F. (2012). Coupled transport of Arabidopsis p24 proteins at the ER-Golgi interface. *J Exp Bot*, 63 (11): 4243-61.
- Montesinos, J. C., Langhans, M., Sturm, S., Hillmer, S., Aniento, F., Robinson, D. G. & Marcote, M. J. (2013). Putative p24 complexes in Arabidopsis contain members of the delta and beta subfamilies and cycle in the early secretory pathway. *J Exp Bot*, 64 (11): 3147-67.
- Motokawa, K., Hohdatsu, T., Hashimoto, H. & Koyama, H. (1996). Comparison of the amino acid sequence and phylogenetic analysis of the peplomer, integral membrane and nucleocapsid proteins of feline, canine and porcine coronaviruses. *Microbiol Immunol*, 40 (6): 425-33.
- Munro, S. & Pelham, H. R. (1987). A C-terminal signal prevents secretion of luminal ER proteins. *Cell*, 48 (5): 899-907.
- Munro, S. (1998). Localization of proteins to the Golgi apparatus. *Trends Cell Biol*, 8 (1): 11-5.
- Munson, L., Marker, L., Dubovi, E., Spencer, J. A., Evermann, J. F. & O'Brien, S. J. (2004). Serosurvey of viral infections in free-ranging Namibian cheetahs (*Acinonyx jubatus*). *J Wildl Dis*, 40 (1): 23-31.
- Narayanan, K., Maeda, A., Maeda, J. & Makino, S. (2000). Characterization of the coronavirus M protein and nucleocapsid interaction in infected cells. *J Virol*, 74 (17): 8127-34.
- Narayanan, K., Huang, C. & Makino, S. (2008a). Coronavirus accessory proteins. In Perlman S, Gallagher T & Snijder EJ (eds) *Nidoviruses.*, pp. 235-244. Washington, DC: ASM Press.
- Narayanan, K., Huang, C. & Makino, S. (2008b). SARS coronavirus accessory proteins. *Virus Res*, 133 (1): 113-21.
- Nash, T. C. & Buchmeier, M. J. (1997). Entry of mouse hepatitis virus into cells by endosomal and nonendosomal pathways. *Virology*, 233 (1): 1-8.
- Nelson, M. A., Herrero, L. J., Jeffery, J. A., Hoehn, M., Rudd, P. A., Supramaniam, A., Kay, B. H., Ryan, P. A. & Mahalingam, S. (2016). Role of envelope N-

- linked glycosylation in Ross River virus virulence and transmission. *J Gen Virol*, 97 (5): 1094-106.
- Nilsson, I. & von Heijne, G. (1990). Fine-tuning the topology of a polytopic membrane protein: role of positively and negatively charged amino acids. *Cell*, 62 (6): 1135-41.
- Nilsson, J., Ruetschi, U., Halim, A., Hesse, C., Carlsohn, E., Brinkmalm, G. & Larson, G. (2009). Enrichment of glycopeptides for glycan structure and attachment site identification. *Nat Methods*, 6 (11): 809-11.
- Nilsson, T. & Warren, G. (1994). Retention and retrieval in the endoplasmic reticulum and the Golgi apparatus. *Curr Opin Cell Biol*, 6 (4): 517-21.
- O'Brien, S. J., Roelke, M. E., Marker, L., Newman, A., Winkler, C. A., Meltzer, D., Colly, L., Evermann, J. F., Bush, M. & Wildt, D. E. (1985). Genetic basis for species vulnerability in the cheetah. *Science*, 227 (4693): 1428-34.
- O'Reilly, K. J., Fishman, B. & Hitchcock, L. M. (1979). Feline infectious peritonitis: isolation of a coronavirus. *Vet Rec*, 104 (15): 348.
- Olyslaegers, D. A., Dedeurwaerder, A., Desmarests, L. M., Vermeulen, B. L., Dewerchin, H. L. & Nauwynck, H. J. (2013). Altered expression of adhesion molecules on peripheral blood leukocytes in feline infectious peritonitis. *Vet Microbiol*, 166 (3-4): 438-49.
- Ontiveros, E., Kuo, L., Masters, P. & Perlman, S. (2001). Analysis of nonessential gene function in recombinant MHV-JHM. Gene 4 knockout recombinant virus. *Adv Exp Med Biol*, 494: 83-9.
- Oostra, M., de Haan, C. A., de Groot, R. J. & Rottier, P. J. (2006). Glycosylation of the severe acute respiratory syndrome coronavirus triple-spanning membrane proteins 3a and M. *J Virol*, 80 (5): 2326-36.
- Pasternak, A. O., van den Born, E., Spaan, W. J. & Snijder, E. J. (2001). Sequence requirements for RNA strand transfer during nidovirus discontinuous subgenomic RNA synthesis. *EMBO J*, 20 (24): 7220-8.
- Paul-Murphy, J., Work, T., Hunter, D., McFie, E. & Fjelline, D. (1994). Serologic survey and serum biochemical reference ranges of the free-ranging mountain lion (*Felis concolor*) in California. *J Wildl Dis*, 30 (2): 205-15.

- Pedersen, N. C. (1976). Morphologic and physical characteristics of feline infectious peritonitis virus and its growth in autochthonous peritoneal cell cultures. *Am J Vet Res*, 37 (5): 567-72.
- Pedersen, N. C., Boyle, J. F., Floyd, K., Fudge, A. & Barker, J. (1981). An enteric coronavirus infection of cats and its relationship to feline infectious peritonitis. *Am J Vet Res*, 42 (3): 368-77.
- Pedersen, N. C. & Black, J. W. (1983). Attempted immunization of cats against feline infectious peritonitis, using avirulent live virus or sublethal amounts of virulent virus. *Am J Vet Res*, 44 (2): 229-34.
- Pedersen, N. C. (1984). Pathogenic differences between various feline coronavirus isolates. In Rottier PJ, Zeijst BAM, Spaan WJM & Horzinek, M. C. (eds) *Molecular biology and pathogenesis of coronaviruses*. New York, NY: Plenum Press.
- Pedersen, N. C. (2009). A review of feline infectious peritonitis virus infection: 1963-2008. *J Feline Med Surg*, 11 (4): 225-58.
- Pedersen, N. C., Liu, H., Scarlett, J., Leutenegger, C. M., Golovko, L., Kennedy, H. & Kamal, F. M. (2012). Feline infectious peritonitis: role of the feline coronavirus 3c gene in intestinal tropism and pathogenicity based upon isolates from resident and adopted shelter cats. *Virus Res*, 165 (1): 17-28.
- Pedersen, N. C. (2014). An update on feline infectious peritonitis: virology and immunopathogenesis. *Vet J*, 201 (2): 123-32.
- Pelham, H. R. (1990). The retention signal for soluble proteins of the endoplasmic reticulum. *Trends Biochem Sci*, 15 (12): 483-6.
- Petersen, T. N., Brunak, S., von Heijne, G. & Nielsen, H. (2011). SignalP 4.0: discriminating signal peptides from transmembrane regions. *Nat Methods*, 8 (10): 785-6.
- Poland, A. M., Vennema, H., Foley, J. E. & Pedersen, N. C. (1996). Two related strains of feline infectious peritonitis virus isolated from immunocompromised cats infected with a feline enteric coronavirus. *J Clin Microbiol*, 34 (12): 3180-4.
- Prentice, E., Jerome, W. G., Yoshimori, T., Mizushima, N. & Denison, M. R. (2004). Coronavirus replication complex formation utilizes components of cellular autophagy. *J Biol Chem*, 279 (11): 10136-41.

- Pyrce, K., Jebbink, M. F., Berkhout, B. & van der Hoek, L. (2004). Genome structure and transcriptional regulation of human coronavirus NL63. *Virology*, 1: 7.
- Raman, S., Bouma, P., Williams, G. D. & Brian, D. A. (2003). Stem-loop III in the 5' untranslated region is a cis-acting element in bovine coronavirus defective interfering RNA replication. *J Virol*, 77 (12): 6720-30.
- Raykhel, I., Alanen, H., Salo, K., Jurvansuu, J., Nguyen, V. D., Latva-Ranta, M. & Ruddock, L. (2007). A molecular specificity code for the three mammalian KDEL receptors. *J Cell Biol*, 179 (6): 1193-204.
- Regan, A. D. & Whittaker, G. R. (2008). Utilization of DC-SIGN for entry of feline coronaviruses into host cells. *J Virol*, 82 (23): 11992-6.
- Regan, A. D., Cohen, R. D. & Whittaker, G. R. (2009). Activation of p38 MAPK by feline infectious peritonitis virus regulates pro-inflammatory cytokine production in primary blood-derived feline mononuclear cells. *Virology*, 384 (1): 135-43.
- Regan, A. D., Ousterout, D. G. & Whittaker, G. R. (2010). Feline lectin activity is critical for the cellular entry of feline infectious peritonitis virus. *J Virol*, 84 (15): 7917-21.
- Rizzo, G., Forti, K., Serroni, A., Cagiola, M., Baglivo, S., Scoccia, E. & De Giuseppe, A. (2016). Single N-glycosylation site of bovine leukemia virus SU is involved in conformation and viral escape. *Vet Microbiol*, 197: 21-26.
- Rose, K. M. & Weiss, S. R. (2009). Murine Coronavirus Cell Type Dependent Interaction with the Type I Interferon Response. *Viruses*, 1 (3): 689-712.
- Roth, J. (2002). Protein N-glycosylation along the secretory pathway: relationship to organelle topography and function, protein quality control, and cell interactions. *Chem Rev*, 102 (2): 285-303.
- Rottier, P. (1995). The coronavirus membrane protein. In SG, S. (ed.) *The Coronaviridae.*, pp. 115-139. New York, USA: Plenum Press.
- Rottier, P. J., Nakamura, K., Schellen, P., Volders, H. & Haijema, B. J. (2005). Acquisition of macrophage tropism during the pathogenesis of feline infectious peritonitis is determined by mutations in the feline coronavirus spike protein. *J Virol*, 79 (22): 14122-30.

- Sawicki, S. G. & Sawicki, D. L. (1995). Coronaviruses use discontinuous extension for synthesis of subgenome-length negative strands. *Adv Exp Med Biol*, 380: 499-506.
- Sawicki, S. G., Sawicki, D. L., Younker, D., Meyer, Y., Thiel, V., Stokes, H. & Siddell, S. G. (2005). Functional and genetic analysis of coronavirus replicase-transcriptase proteins. *PLoS Pathog*, 1 (4): e39.
- Schagger, H. & von Jagow, G. (1987). Tricine-sodium dodecyl sulfate-polyacrylamide gel electrophoresis for the separation of proteins in the range from 1 to 100 kDa. *Anal Biochem*, 166 (2): 368-79.
- Schochetman, G., Stevens, R. H. & Simpson, R. W. (1977). Presence of infectious polyadenylated RNA in coronavirus avian bronchitis virus. *Virology*, 77 (2): 772-82.
- Schroder, S., Schimmoller, F., Singer-Kruger, B. & Riezman, H. (1995). The Golgi-localization of yeast Emp47p depends on its di-lysine motif but is not affected by the ret1-1 mutation in alpha-COP. *J Cell Biol*, 131 (4): 895-912.
- Schwarz, F. & Aebi, M. (2011). Mechanisms and principles of N-linked protein glycosylation. *Curr Opin Struct Biol*, 21 (5): 576-82.
- Schwegmann-Wessels, C. & Herrler, G. (2006). Sialic acids as receptor determinants for coronaviruses. *Glycoconj J*, 23 (1-2): 51-8.
- Scobey, T., Yount, B. L., Sims, A. C., Donaldson, E. F., Agnihothram, S. S., Menachery, V. D., Graham, R. L., Swanstrom, J., Bove, P. F., Kim, J. D., et al. (2013). Reverse genetics with a full-length infectious cDNA of the Middle East respiratory syndrome coronavirus. *Proc Natl Acad Sci U S A*, 110 (40): 16157-62.
- Semenza, J. C., Hardwick, K. G., Dean, N. & Pelham, H. R. (1990). ERD2, a yeast gene required for the receptor-mediated retrieval of luminal ER proteins from the secretory pathway. *Cell*, 61 (7): 1349-57.
- Setty, S. R., Strohlic, T. I., Tong, A. H., Boone, C. & Burd, C. G. (2004). Golgi targeting of ARF-like GTPase Arl3p requires its Nalpha-acetylation and the integral membrane protein Sys1p. *Nat Cell Biol*, 6 (5): 414-9.
- Sharif, S., Arshad, S. S., Hair-Bejo, M., Omar, A. R., Zeenathul, N. A., Fong, L. S., Rahman, N. A., Arshad, H., Shamsudin, S. & Isa, M. K. (2010). Descriptive

- distribution and phylogenetic analysis of feline infectious peritonitis virus isolates of Malaysia. *Acta Vet Scand*, 52: 1.
- Shen, S., Wen, Z. L. & Liu, D. X. (2003). Emergence of a coronavirus infectious bronchitis virus mutant with a truncated 3b gene: functional characterization of the 3b protein in pathogenesis and replication. *Virology*, 311 (1): 16-27.
- Siddell, S., Wege, H. & Ter Meulen, V. (1983). The biology of coronaviruses. *J Gen Virol*, 64 (Pt 4): 761-76.
- Siddell, S. G., Ziebuhr, J. & Snijder, E. J. (2005). Coronaviruses, Toroviruses, and Arteriviruses. In BWJ, M. & V, t. M. (eds) *Topley & Wilson's Microbiology and Microbial Infections*, pp. 823-856. Chichester, UK: John Wiley & Sons, Ltd.
- Skehel, J. J., Stevens, D. J., Daniels, R. S., Douglas, A. R., Knossow, M., Wilson, I. A. & Wiley, D. C. (1984). A carbohydrate side chain on hemagglutinins of Hong Kong influenza viruses inhibits recognition by a monoclonal antibody. *Proc Natl Acad Sci U S A*, 81 (6): 1779-83.
- Snijder, E. J., van der Meer, Y., Zevenhoven-Dobbe, J., Onderwater, J. J., van der Meulen, J., Koerten, H. K. & Mommaas, A. M. (2006). Ultrastructure and origin of membrane vesicles associated with the severe acute respiratory syndrome coronavirus replication complex. *J Virol*, 80 (12): 5927-40.
- Snijder, E. J., Decroly, E. & Ziebuhr, J. (2016). The Nonstructural Proteins Directing Coronavirus RNA Synthesis and Processing. *Adv Virus Res*, 96: 59-126.
- Sola, I., Mateos-Gomez, P. A., Almazan, F., Zuniga, S. & Enjuanes, L. (2011). RNA-RNA and RNA-protein interactions in coronavirus replication and transcription. *RNA Biol*, 8 (2): 237-48.
- Spiro, R. G. (2002). Protein glycosylation: nature, distribution, enzymatic formation, and disease implications of glycopeptide bonds. *Glycobiology*, 12 (4): 43R-56R.
- Stanley, P. (2011). Golgi glycosylation. *Cold Spring Harb Perspect Biol*, 3 (4).
- Stern, D. F. & Sefton, B. M. (1982). Coronavirus proteins: structure and function of the oligosaccharides of the avian infectious bronchitis virus glycoproteins. *J Virol*, 44 (3): 804-12.
- Stoddart, C. A. & Scott, F. W. (1989). Intrinsic resistance of feline peritoneal macrophages to coronavirus infection correlates with in vivo virulence. *J Virol*, 63 (1): 436-40.

- Taguchi, F. & Hirai-Yuki, A. (2012). Mouse Hepatitis Virus Receptor as a Determinant of the Mouse Susceptibility to MHV Infection. *Front Microbiol*, 3: 68.
- Takano, T., Ohshima, T., Kokumoto, A., Satoh, R. & Hohdatsu, T. (2011). Vascular endothelial growth factor (VEGF), produced by feline infectious peritonitis (FIP) virus-infected monocytes and macrophages, induces vascular permeability and effusion in cats with FIP. *Virus Res*, 158 (1-2): 161-8.
- Tekes, G. (2008). *Etablierung eines revers – genetischen Systems für feline Coronaviren*. Giessen: Justus Liebig University, Institute of Virology.
- Tekes, G., Hofmann-Lehmann, R., Stallkamp, I., Thiel, V. & Thiel, H.-J. (2008). Genome organization and reverse genetic analysis of a type I feline coronavirus. *J Virol*, 82 (4): 1851-9.
- Tekes, G., Hofmann-Lehmann, R., Bank-Wolf, B., Maier, R., Thiel, H.-J. & Thiel, V. (2010). Chimeric feline coronaviruses that encode type II spike protein on type I genetic background display accelerated viral growth and altered receptor usage. *J Virol*, 84 (3): 1326-33.
- Tekes, G., Spies, D., Bank-Wolf, B., Thiel, V. & Thiel, H.-J. (2012). A reverse genetics approach to study feline infectious peritonitis. *J Virol*, 86 (12): 6994-8.
- Terada, Y., Matsui, N., Noguchi, K., Kuwata, R., Shimoda, H., Soma, T., Mochizuki, M. & Maeda, K. (2014). Emergence of pathogenic coronaviruses in cats by homologous recombination between feline and canine coronaviruses. *PLoS One*, 9 (9): e106534.
- Thiel, V., Herold, J., Schelle, B. & Siddell, S. G. (2001a). Infectious RNA transcribed in vitro from a cDNA copy of the human coronavirus genome cloned in vaccinia virus. *J Gen Virol*, 82 (Pt 6): 1273-81.
- Thiel, V., Herold, J., Schelle, B. & Siddell, S. G. (2001b). Viral replicase gene products suffice for coronavirus discontinuous transcription. *J Virol*, 75 (14): 6676-81.
- Tooze, J., Tooze, S. & Warren, G. (1984). Replication of coronavirus MHV-A59 in sac- cells: determination of the first site of budding of progeny virions. *Eur J Cell Biol*, 33 (2): 281-93.

- Townsley, F. M. & Pelham, H. R. (1994). The KKXX signal mediates retrieval of membrane proteins from the Golgi to the ER in yeast. *Eur J Cell Biol*, 64 (1): 211-6.
- Townsley, S., Li, Y., Kozyrev, Y., Cleveland, B. & Hu, S. L. (2015). Conserved Role of an N-Linked Glycan on the Surface Antigen of Human Immunodeficiency Virus Type 1 Modulating Virus Sensitivity to Broadly Neutralizing Antibodies against the Receptor and Coreceptor Binding Sites. *J Virol*, 90 (2): 829-41.
- Tresnan, D. B., Levis, R. & Holmes, K. V. (1996). Feline aminopeptidase N serves as a receptor for feline, canine, porcine, and human coronaviruses in serogroup I. *J Virol*, 70 (12): 8669-74.
- Trombetta, E. S. (2003). The contribution of N-glycans and their processing in the endoplasmic reticulum to glycoprotein biosynthesis. *Glycobiology*, 13 (9): 77R-91R.
- Tyrrell, D. A., Almeida, J. D., Cunningham, C. H., Dowdle, W. R., Hofstad, M. S., McIntosh, K., Tajima, M., Zakstelskaya, L. Y., Easterday, B. C., Kapikian, A., et al. (1975). Coronaviridae. *Intervirology*, 5 (1-2): 76-82.
- Van Hamme, E., Dewerchin, H. L., Cornelissen, E. & Nauwynck, H. J. (2007). Attachment and internalization of feline infectious peritonitis virus in feline blood monocytes and Crandell feline kidney cells. *J Gen Virol*, 88 (Pt 9): 2527-32.
- Van Hamme, E., Desmarets, L., Dewerchin, H. L. & Nauwynck, H. J. (2011). Intriguing interplay between feline infectious peritonitis virus and its receptors during entry in primary feline monocytes. *Virus Res*, 160 (1-2): 32-9.
- Varki, A., Cummings, R., Esko, J., Freeze, H., Stanley, P., Bertozzi, C., Hart, G. & Etzler, M. (2009). *Essentials of Glycobiology, 2nd edition*. Cold Spring Harbor, NY: Cold Spring Harbor Laboratories Press.
- Vennema, H., Heijnen, L., Rottier, P. J., Horzinek, M. C. & Spaan, W. J. (1992). A novel glycoprotein of feline infectious peritonitis coronavirus contains a KDEL-like endoplasmic reticulum retention signal. *J Virol*, 66 (8): 4951-6.
- Vennema, H., Poland, A., Foley, J. & Pedersen, N. C. (1998). Feline infectious peritonitis viruses arise by mutation from endemic feline enteric coronaviruses. *Virology*, 243 (1): 150-7.

- Vennema, H. (1999). Genetic drift and genetic shift during feline coronavirus evolution. *Vet Microbiol*, 69 (1-2): 139-41.
- Vlasak, R., Luytjes, W., Leider, J., Spaan, W. & Palese, P. (1988). The E3 protein of bovine coronavirus is a receptor-destroying enzyme with acetylcholinesterase activity. *J Virol*, 62 (12): 4686-90.
- Vogel, L., Van der Lubben, M., te Lintelo, E. G., Bekker, C. P., Geerts, T., Schuijff, L. S., Grinwis, G. C., Egberink, H. F. & Rottier, P. J. (2010). Pathogenic characteristics of persistent feline enteric coronavirus infection in cats. *Vet Res*, 41 (5): 71.
- Wang, K., Lu, W., Chen, J., Xie, S., Shi, H., Hsu, H., Yu, W., Xu, K., Bian, C., Fischer, W. B., et al. (2012). PEDV ORF3 encodes an ion channel protein and regulates virus production. *FEBS Lett*, 586 (4): 384-91.
- Ward, J. M. (1970). Morphogenesis of a virus in cats with experimental feline infectious peritonitis. *Virology*, 41 (1): 191-4.
- Wege, H., Muller, A. & ter Meulen, V. (1978). Genomic RNA of the murine coronavirus JHM. *J Gen Virol*, 41 (2): 217-27.
- Weiss, R. C., Vaughn, D. M. & Cox, N. R. (1988). Increased plasma levels of leukotriene B4 and prostaglandin E2 in cats experimentally inoculated with feline infectious peritonitis virus. *Vet Res Commun*, 12 (4-5): 313-23.
- Weiss, S. R. & Navas-Martin, S. (2005). Coronavirus pathogenesis and the emerging pathogen severe acute respiratory syndrome coronavirus. *Microbiol Mol Biol Rev*, 69 (4): 635-64.
- Wilson, D. W., Lewis, M. J. & Pelham, H. R. (1993). pH-dependent binding of KDEL to its receptor in vitro. *J Biol Chem*, 268 (10): 7465-8.
- Woo, P. C., Lau, S. K., Lam, C. S., Lai, K. K., Huang, Y., Lee, P., Luk, G. S., Dyrting, K. C., Chan, K. H. & Yuen, K. Y. (2009). Comparative analysis of complete genome sequences of three avian coronaviruses reveals a novel group 3c coronavirus. *J Virol*, 83 (2): 908-17.
- Woo, P. C., Lau, S. K., Lam, C. S., Lau, C. C., Tsang, A. K., Lau, J. H., Bai, R., Teng, J. L., Tsang, C. C., Wang, M., et al. (2012). Discovery of seven novel mammalian and avian coronaviruses in the genus deltacoronavirus supports bat coronaviruses as the gene source of alphacoronavirus and

- betacoronavirus and avian coronaviruses as the gene source of gammacoronavirus and deltacoronavirus. *J Virol*, 86 (7): 3995-4008.
- Woo, P. C., Lau, S. K., Lam, C. S., Tsang, A. K., Hui, S. W., Fan, R. Y., Martelli, P. & Yuen, K. Y. (2014). Discovery of a novel bottlenose dolphin coronavirus reveals a distinct species of marine mammal coronavirus in Gammacoronavirus. *J Virol*, 88 (2): 1318-31.
- Ye, Y., Hauns, K., Langland, J. O., Jacobs, B. L. & Hogue, B. G. (2007). Mouse hepatitis coronavirus A59 nucleocapsid protein is a type I interferon antagonist. *J Virol*, 81 (6): 2554-63.
- Yeager, C. L., Ashmun, R. A., Williams, R. K., Cardellichio, C. B., Shapiro, L. H., Look, A. T. & Holmes, K. V. (1992). Human aminopeptidase N is a receptor for human coronavirus 229E. *Nature*, 357 (6377): 420-2.
- Yoo, D. W., Parker, M. D. & Babiuk, L. A. (1991). The S2 subunit of the spike glycoprotein of bovine coronavirus mediates membrane fusion in insect cells. *Virology*, 180 (1): 395-9.
- Yount, B., Curtis, K. M. & Baric, R. S. (2000). Strategy for systematic assembly of large RNA and DNA genomes: transmissible gastroenteritis virus model. *J Virol*, 74 (22): 10600-11.
- Yount, B., Denison, M. R., Weiss, S. R. & Baric, R. S. (2002). Systematic assembly of a full-length infectious cDNA of mouse hepatitis virus strain A59. *J Virol*, 76 (21): 11065-78.
- Yount, B., Curtis, K. M., Fritz, E. A., Hensley, L. E., Jahrling, P. B., Prentice, E., Denison, M. R., Geisbert, T. W. & Baric, R. S. (2003). Reverse genetics with a full-length infectious cDNA of severe acute respiratory syndrome coronavirus. *Proc Natl Acad Sci U S A*, 100 (22): 12995-3000.
- Yount, B., Roberts, R. S., Sims, A. C., Deming, D., Frieman, M. B., Sparks, J., Denison, M. R., Davis, N. & Baric, R. S. (2005). Severe acute respiratory syndrome coronavirus group-specific open reading frames encode nonessential functions for replication in cell cultures and mice. *J Virol*, 79 (23): 14909-22.
- Zai, J., Mei, L., Wang, C., Cao, S., Fu, Z. F., Chen, H. & Song, Y. (2013). N-glycosylation of the premembrane protein of Japanese encephalitis virus is

- critical for folding of the envelope protein and assembly of virus-like particles. *Acta Virol*, 57 (1): 27-33.
- Zhang, R., Wang, K., Lv, W., Yu, W., Xie, S., Xu, K., Schwarz, W., Xiong, S. & Sun, B. (2014). The ORF4a protein of human coronavirus 229E functions as a viroporin that regulates viral production. *Biochim Biophys Acta*, 1838 (4): 1088-95.
- Ziebuhr, J., Herold, J. & Siddell, S. G. (1995). Characterization of a human coronavirus (strain 229E) 3C-like proteinase activity. *J Virol*, 69 (7): 4331-8.
- Ziebuhr, J. & Siddell, S. G. (1999). Processing of the human coronavirus 229E replicase polyproteins by the virus-encoded 3C-like proteinase: identification of proteolytic products and cleavage sites common to pp1a and pp1ab. *J Virol*, 73 (1): 177-85.
- Ziebuhr, J., Snijder, E. J. & Gorbalenya, A. E. (2000). Virus-encoded proteinases and proteolytic processing in the Nidovirales. *J Gen Virol*, 81 (Pt 4): 853-79.
- Ziebuhr, J., Thiel, V. & Gorbalenya, A. E. (2001). The autocatalytic release of a putative RNA virus transcription factor from its polyprotein precursor involves two paralogous papain-like proteases that cleave the same peptide bond. *J Biol Chem*, 276 (35): 33220-32.
- Zook, B. C., King, N. W., Robison, R. L. & McCombs, H. L. (1968). Ultrastructural Evidence for Viral Etiology of Feline Infectious Peritonitis. *Pathologia Veterinaria*, 5 (1): 91-&.
- Zust, R., Miller, T. B., Goebel, S. J., Thiel, V. & Masters, P. S. (2008). Genetic interactions between an essential 3' cis-acting RNA pseudoknot, replicase gene products, and the extreme 3' end of the mouse coronavirus genome. *J Virol*, 82 (3): 1214-28.

## Acknowledgments

This study was supported by the Deutsche Forschungsgemeinschaft (DFG) through the Collaborative Research Centre 1021: “RNA viruses: RNA metabolism, host response and pathogenesis” (project B01).

I am extremely grateful to **Prof. Dr. Gergely Tekes, PhD** for giving me the possibility to participate in this exciting project. His guidance and expertise helped me develop many traits important for a successful scientist. I am especially thankful for his active support of my career choice.

I am also thankful to **Prof. Dr. John Ziebuhr** and **Prof. Dr. Heinz-Jürgen Thiel** for guidance and support. Their advice helped in shaping of the whole project.

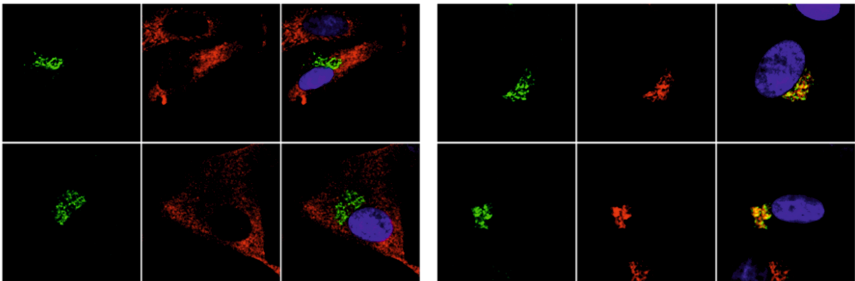
Special thanks to **Dr. Martin Hardt** for giving me the possibility to use the confocal microscope for my studies.

My sincere thanks to all the labmates who helped me on my way to the PhD title. **Rosina Ehmman** for an unending supply of cells and irreplaceable company during lunch breaks. **Claudia Kristen-Burmann** for help in generating viruses and endless patience. **Dr. Tanja Lemmermeyer** for introduction into protein analysis. **Anette Netsch** for technical help and **Giulia Dowgier** for friendly support.

I am also thankful to **GGL** community for help in developing my skills and friendly advice.

I am especially grateful to my partner, **Stephanie** for never ending support and patience. It was thanks to her that I could tackle any obstacle of everyday life with a smile on my face.

Szczególne podziękowania należą się mojej rodzinie – **rodzicom i bratu**. Za wsparcie we wszystkich trudnych chwilach. **Rodzicom** za nieocenione rady, gotowość do pomocy i nieskończone zainteresowanie. **Bratu** za pomoc w przezwyciężeniu wielu trudności. Bez was nie osiągnąłbym tego sukcesu tak sprawnie.



*édition scientifique*  
**VVB LAUFERSWEILER VERLAG**

VVB LAUFERSWEILER VERLAG  
STAUFENBERGRING 15  
D-35396 GIESSEN

Tel: 0641-5599888 Fax: -5599890  
redaktion@doktorverlag.de  
www.doktorverlag.de

ISBN: 978-3-8359-6631-4

